TURUN YLIOPISTON JULKAISUJA
ANNALES UNIVERSITATIS TURKUENSIS

SARJA - SER. A I OSA – TOM. 426
ASTRONOMICA - CHEMICA - PHYSICA - MATHEMATICA

STUDIES ON INTRACHAIN CONJUGATION, HYBRIDIZATION AND INVASION OF OLIGONUCLEOTIDES

by

Anu Kiviniemi

TURUN YLIOPISTO
UNIVERSITY OF TURKU
Turku 2011

From the Department of Chemistry
University of Turku
Turku, Finland

Custos

Professor Harri Lönnberg
Department of Chemistry
University of Turku
Turku, Finland

Reviewers

Professor Frank Seela
Laboratorium für Organische und Bioorganische Chemie
Institut für Chemie
Universität Osnabrück
Osnabrück, Germany

Professor François Morvan
Département des Analogues et Constituants des Acides Nucléiques
Institut des Biomolécules Max Mousseron
Université Montpellier 2
Montpellier, France

Opponent

Professor Jesper Wengel
Nucleic Acid Center
Department of Physics and Chemistry
University of Southern Denmark
Odense, Denmark

ISBN 978-951-29-4724-9 (PRINT)
ISBN 978-951-29-4725-6 (PDF)
ISSN 0082-7002
Uniprint – Suomen Yliopistopaino Oy, Turku, Finland 2011

PREFACE

This thesis is based on experimental work carried out in the Laboratory of Organic Chemistry and Chemical Biology at the Department of Chemistry, University of Turku during the years 2006−2011. The financial support of Graduate School of Organic Chemistry and Chemical Biology and the Academy of Finland are gratefully acknowledged.

First of all I wish to express my deepest gratitude to Professor Harri Lönnberg for giving me the chance to pursue Ph.D studies in the fascinating world of nucleic acids. Optimism is so important in science and I have always found that from his office. His brilliant way of thinking and expressing the science is truly inspiring and I thank him for all the guidance and support. I am also very grateful to my supervisor Doc. Pasi Virta. He is an amazing personality with an endless driving force. His excellent knowledge, innovative ideas and common sense makes him a great scientist. During the years, I have learned a lot under his encouraging and skillful guidance and there has never been a problem that he wouldn´t have resolved in one way or another.

I am grateful to Professor Frank Seela and Professor François Morvan for their careful reviewing of my thesis.

I would also like to thank Doc. Petri Heinonen, who in very beginning was my supervisor. Back in Biocity days, we had many interesting discussions and he taught me great things about oligonucleotide synthesis.

My warm gratitude goes to all present and former co-workers in the Laboratory of Organic Chemistry and Chemical Biology for creating a nice working environment. You have always provided me the help and valuable advices when needed, not to mentioned unforgettable moments in many fun events. I wish to thank: Mrs. Tiina Buss, Dr. Diana Florea-Wang, Mr. Alejandro Gimenez Molina, Mrs. Mia Helkearo, Mrs. Marika Karskela, Mr. Tuomas Karskela, Dr. Johanna Katajisto, Dr. Kaisa Ketomäki, Mrs. Emilia Kiuru, Dr. Niangoran Koissi, Dr. Heidi Korhonen, Mr. Vyacheslav Kungurtsev, Mr. Luigi Lain, Mrs. Maarit Laine, Ms. Anna Leisvuori, Doc. Tuomas Lönnberg, Professor Satu Mikkola, Doc. Helmi Neuvonen, Ms. Teija Niittymäki, Dr. Erkki Nurminen, Doc. Mikko Ora, Dr. Päivi Poijärvi-Virta, Mrs. Outi Rahi, Mrs. Jaana Rosenberg, Mrs. Sharmin Taherpour and Dr. Qi Wang. Especially I would like to thank Emilia and Anna for their friendship and for those many joyful times we have shared in the Lab together. I also express my special gratitude to Kaisa for teaching me HPLC practices and for the good company in many conference journeys. The latter thanks are also devoted to Teija.

The former and present members of the Laboratory of Synthetic Drug Chemistry deserve my sincere thanks for all the warmth and considerations you have shown me during the years. Especially, I am indebted to Doc. Arto Liljeblad, who

patiently guided me to the world of enzymes and chemistry at the very beginning of my master studies.

Other colleagues in Arcanum and in the instrument center are also thanked for all the help and pleasant working company. Mrs. Kirsi Laaksonen has so many times rescued my synthesis with fast chemical orders. The skills of Mr. Kari Loikas and Mr. Mauri Nauma have been invaluable and I have come to a conclusion that there is no machine that they can´t fix. I am also grateful to Ms. Kirsti Wiinamäki and Dr. Olli Martiskainen for carrying out my MS runs and for the instrument support. And to Dr. Petri Ingman, Doc. Jari Sinkkonen, Dr. Henri Kivelä and Mr. Jaakko Hellman for all the advices and help with NMR. I am also thankful for Mrs. Heli Granlund and Mrs. Leena Mattila for all their kind assistance.

My special thanks are reserved for my closest friends Maria and Niina. You are the ones to know me best and are the cornerstones of my life. I want to thank also Marika, Kaisa and Tiina for their long-lasting friendship. With them I have shared everything from student life to motherhood.

Finally, I express my very deep appreciation for my parents Esa and Liisa. You have evoked my curiosity to this world and undoubtedly also to chemistry. I thank you for always being there for me. My sister Pia and her family are also greatly thanked. I will always need my big sister to believe in me and to understand my thoughts even better than myself.

Last but not least I want to thank my family, my husband Matias and my daughter Emilia. You, I always carry in my heart.

Turku, August 2011

CONTENTS

LIST OF ORIGINAL PUBLICATIONS

This thesis is based on the following publications:

I Kiviniemi, A., Virta, P. and Lönnberg, H.: Utilization of intrachain 4´-*C*-azidomethylthymidine for preparation of oligodeoxyribonucleotide conjugates by click chemistry in solution and on a solid support. *Bioconjugate Chem.* **2008**, *19*, 1726-1734.

II Kiviniemi, A., Virta, P. and Lönnberg, H.: Solid-supported synthesis and click conjugation of 4´-*C*-alkyne functionalized oligodeoxyribonucleotides. *Bioconjugate Chem.* **2010**, *21*, 1890-1901.

III Kiviniemi, A., Virta, P., Drenichev, M. S., Mikhailov, S. N. and Lönnberg, H.: Solid-supported 2′-*O*-glycoconjugation of oligonucleotides by azidation and click reactions. *Bioconjugate Chem.* **2011**, *22*, 1249–1255.

IV Kiviniemi, A. and Virta, P.: Characterization of RNA invasion by ^{19}F NMR spectroscopy. *J. Am. Chem. Soc*. **2010**, *132*, 8560–8562.

ABBREVIATIONS

A	adenosine
Ac	acetyl
AcOH	acetic acid
ASO	antisense oligonucleotide
Bz	benzoyl
Bn	benzyl
C	cytidine
CD	circular dichroism
cDNA	complementary DNA
CPG	controlled pore glass
CPP	cell-penetrating peptides
DBU	1,8-diazabicyclo[5.4.0]undec-7-ene
DCA	dichloroacetic acid
DCC	*N*,*N'*-dicyclohexylcarbodiimide
DMAP	4-dimethylaminopyridine
DMF	*N*,*N*-dimethylformamide
DMSO	dimethyl sulfoxide
DMTr	4,4´-dimethoxytrityl
dsRNA	double-stranded RNA
DNA	deoxyribonucleic acid
EDTA	ethylenediamine-*N*,*N*,*N´*,*N´*-tetraacetic acid
ESI-MS	electrospray ionization mass spectroscopy
FDA	Food and Drug Administration (U. S. A)
G	guanosine
HIV	human immunodeficiency virus
HPLC	high-performance liquid chromatography
LNA	locked nucleic acid
MeCN	acetonitrile
MMTr	monomethoxytrityl
mRNA	messenger RNA
miRNA	microRNA
NMR	nuclear magnetic resonance
ON	oligonucleotide
PEG	polyethylene glycol
PMO	morpholino oligonucleotide
PNA	peptide nucleic acid
RISC	RNA-induced silencing complex
RNA	ribonucleic acid
RNAi	RNA interference
RNase	ribonuclease
RP	reversed phase
siRNA	small interfering RNA
T	thymidine
T_m	melting temperature

TAR	*trans*-activating response element
TAT	*trans*-activator protein
TBTA	tris[(1-benzyl-1,2,3-triazol-4-yl)methyl]amine
TBDMS	*tert*-butyldimethylsilyl
TEA	triethylamine
TEAA	triethylammonium acetate
Tf	triflyl (trifluoromethylsulfonyl)
Tfa	trifluoroacetyl
TFA	trifluoroacetic acid
THF	tetrahydrofuran
TMGA	tetramethylguanidinium azide
TOM	triisopropylsilyloxymethyl
Ts	tosyl (*p*-toluenesulfonyl)
UV	ultraviolet

1. INTRODUCTION

The growing understanding of RNA´s functional repertoire has opened a new view to not just life itself, but also for our ability to control gene expression and thus regulate cell processes. Since the discovery of first catalytic RNAs in early 1980s,[1,2] the initial concept of passive RNA responsible only for the transfer of information between DNA and protein synthesis, has greatly changed. Besides the "classic" categories of RNA in the translation process, *i.e*. messenger RNA (mRNA), transfer RNA (tRNA) and ribosomal RNA (rRNA), we now know that various non-protein-coding RNAs participate in cellular regulation at different levels.[3] The diverse RNA family in eukaryotes includes small regulatory RNAs (Section 1.1.1.1), ribozymes (RNAs with enzymatic activity) and even riboswitches (RNA sensors in mRNA that are capable of modulating gene expression in response to internal and external inputs) although the last mentioned are mostly found in prokaryotes.[4] They all interact through a combination of complementary base pairing, protein complexing, and catalysis. It has been estimated that less than 2% of the human genome is translated into protein, yet more than 40% of the genome is thought to be transcribed into RNA.[5]

As RNA's real capacity has started to reveal, drug design based on RNA-targeting has become an attractive alternative to traditional drug discovery focused on protein-targets. Selective gene-silencing offers high therapeutic potential, since in principle any single gene within the genome can be silenced by affecting its mRNA transcript.[6-9] The recognition takes place via Watson-Crick base pairing (Figure 1) and is, hence, sequence-specific. The technology shows considerable opportunities in combating against major human health threats, such as cancer[10-12] and viral infections[13]. For this purpose, the natural cellular mechanism called RNA interference (RNAi) has recently received a vast interest.[14-19] RNAi can be triggered by synthetic double-stranded RNAs, as was described for the first time in 1998 with a nematode *caenorhabditis elegans*.[20] For this achievement, Fire and Mello received a Nobel Prize in 2006. The pioneering work employing synthetic oligonucleotides as therapeutic agents had, however, started already in 1978, when Zamecnik and Stephenson made experiments with single-stranded antisense oligodeoxynucleotides and managed to prevent translation of Rous Sarcoma virus (RSV) RNA *in vitro*.[21,22] This led to early development of an antisense oligonucleotide approach: a novel concept of blocking sequence-specifically disease related genes by introduction of a synthetic complementary strand (the antisense strand) to the cell (Figure 2). Besides nucleic acids, cellular RNA may be targeted by small molecule compounds and peptides and by combining various technologies.[23-25]

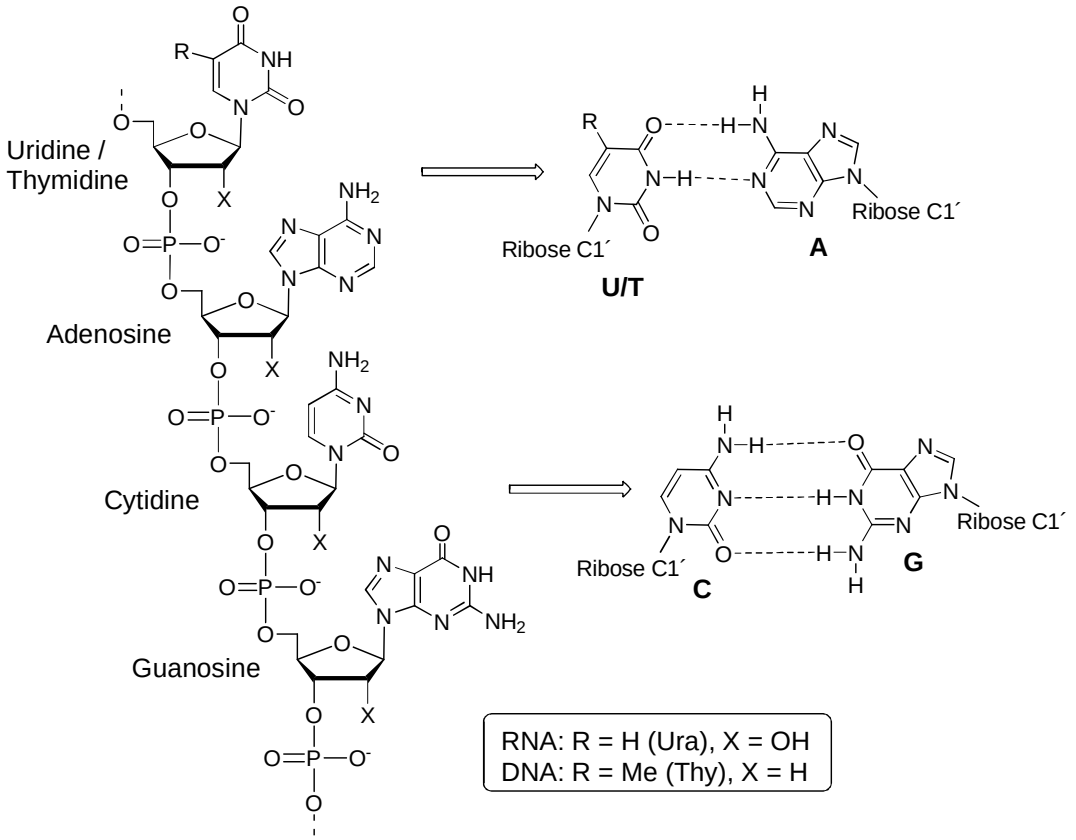

Figure 1. The structure of RNA and DNA and Watson-Crick base pairing upon duplex formation.

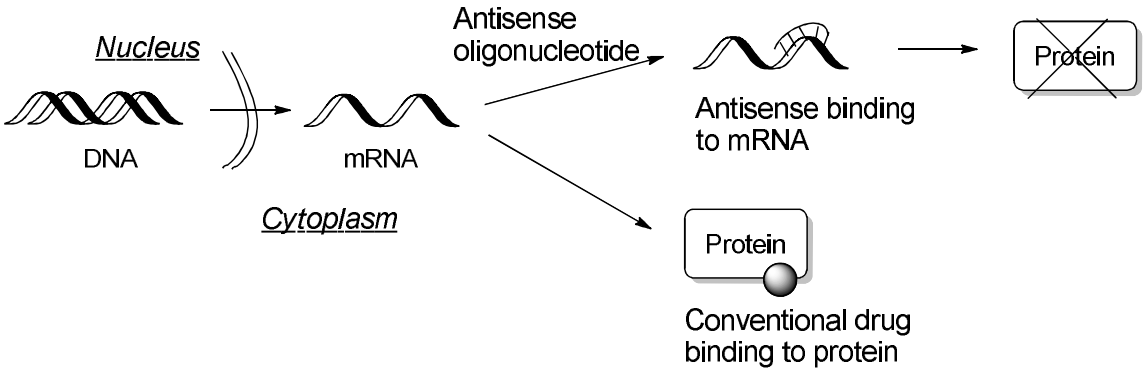

Figure 2. Antisense principle and the action of conventional protein targeting drug.

Currently, only one antisense drug (1998, Vitravene®) and one aptamer oligonucleotide (2004, Macugen®, aptamer = molecule that bind to a specific target molecule such as protein acting frequently like an antibody) have been approved by the FDA.[19] They both are for the treatment of an eye disease as is the first RNAi based human-therapeutics, which entered clinical trials at 2004. High expectations are loaded for development of nucleic acid drugs, but there are still a

number of challenges that the technology needs to overcome. These problems are approached through chemical modifications of the antisense oligonucleotides and exploitation of conjugations to other molecules.[26-32] The modifications are aimed at enhancing hybridization specificity and affinity to the target RNA, to increase stability towards nuclease degradation, to decrease toxicity and finally to improve pharmacokinetics and cellular uptake of the drug.

1.1 Antisense strategies

Strategies that target mRNA and, hence, prevent its translation into protein include the use of single stranded antisense oligonucleotides (Section 1.1.2), nucleic acid enzymes (ribozyme and DNAzyme) and double-stranded small interfering RNA (siRNA or miRNA, Section 1.1.1).[8] In general, post-transcriptional gene silencing (PTGS) means down-regulation of a gene at the RNA level, *i.e.* after transcription without a need to manipulate the host genome. Antisense mechanisms based on PTGS can be divided into two main categories: those that interfere with RNA´s function without promoting RNA degradation and those that induce degradation.[17,31]

1.1.1 RNA interference

1.1.1.1 Small regulatory RNAs

Small RNAs are around 20-30 nucleotide long RNA molecules that are found in almost all eukaryotic organisms.[3,18] Their function is to control endogenous genes and defend the cell against invasive nucleic acids such as viruses, transposons and transgenes. This control is generally inhibitory and often takes place by interfering with mRNA translation. Three main groups of small RNAs are identified: short interfering RNA (siRNA), micro RNA (miRNA) and piwi-interacting RNA (piRNA). From these, siRNA and miRNA are best known and their presence in cells triggers a cellular mechanism called RNA interference (RNAi). RNAi depends on many protein interactions and refers to a natural gene regulatory system, wherein double-stranded RNAs (dsRNA) inhibit the expression of complementary genes.

1.1.1.2 The mechanisms of RNAi

In mammalian cells, the RNA interference is primarily a process of PTGS and the gene expression is suppressed in the cytoplasm by degrading mRNA or directly repressing translation.[19] The importance of RNAi for mammalian transcriptional gene silencing (TGS) at the DNA level by inhibition of transcription in the nucleus has not yet been clearly demonstrated. Figure 3 illustrates the siRNA and miRNA pathways of PTGS.[3,14]

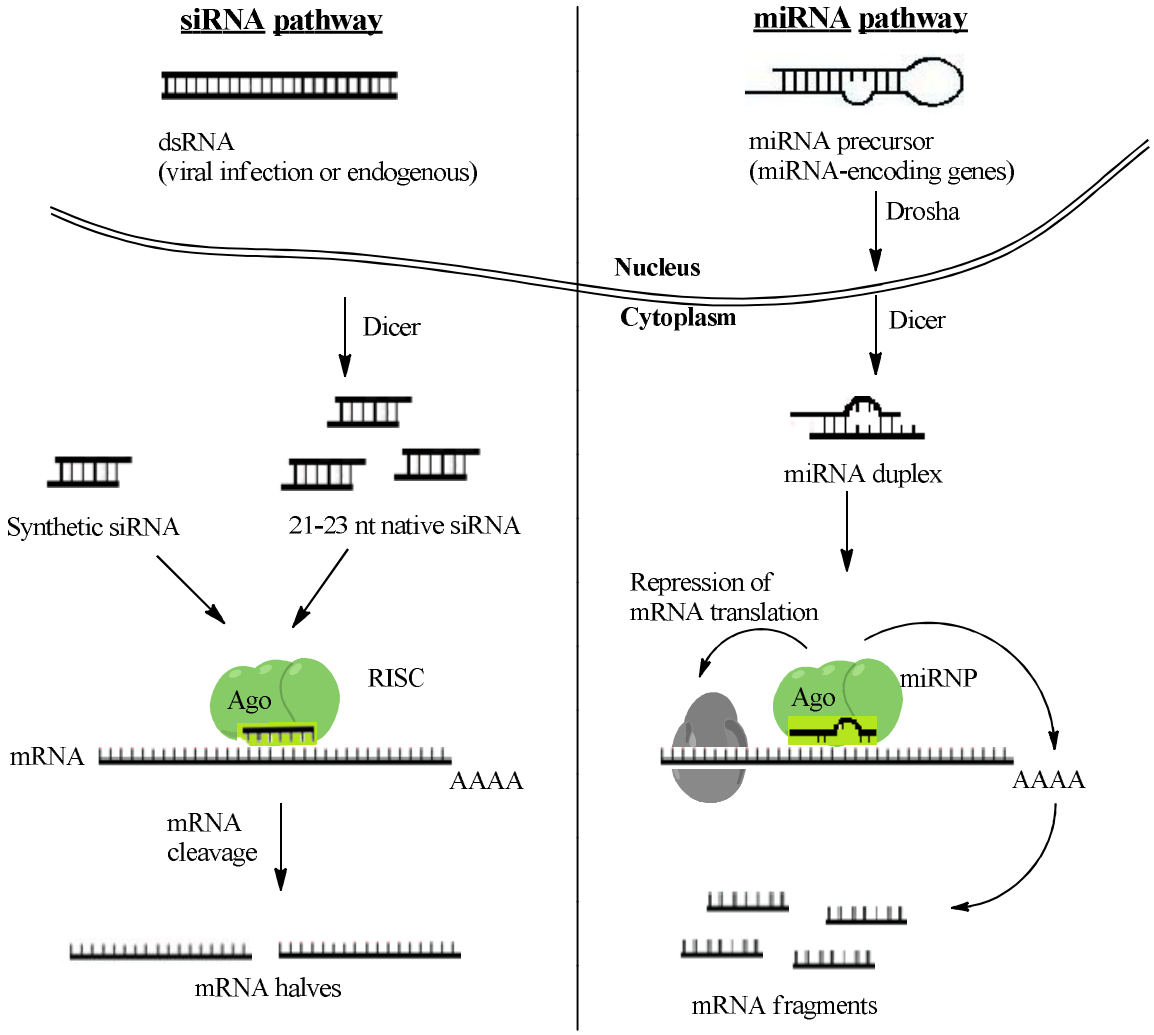

Figure 3. Simplified model for the RNAi mechanism by siRNA and miRNA.[3,14]

siRNAs are approximately 21-23 nucleotide long duplexes having 2-base 3´-overhangs and 5´-phosphate groups.[3,18,19] They are processed by endoribonuclease enzyme called Dicer from larger dsRNA duplexes, which derive either from endogenous sources or are taken up from the environment. Hence, the siRNAs participate in cell´s defend mechanisms and regulate protein-coding genes. The actual effector of the RNAi is a ribonucleoprotein complex RISC (RNA-induced silencing complex), which is guided by the siRNA to the complementary target RNA. In RISC, the strand with a lower binding affinity at its 5´-end becomes the antisense (guide) strand of the siRNA and the sense (passanger) strand is degraded. The remaining single-stranded antisense strand then directs the sequence-specificity of silencing by RISC. The target mRNA is cleaved at a specific site in the center of the duplex, *i.e* 10 nucleotides from the 5´-end of the siRNA strand. The catalytic component of RISC that degrades the target RNA is a protein Argonaut 2 (Ago2) containing an RNase H like domain (see Section 1.1.2).

miRNAs are evolutionarily conserved from plants to animals and encoded by specific genes to regulate many biological processes including development, growth, proliferation and apoptosis.[12] They are assumed to control the activity of

about 30% of all protein-coding genes in mammals.[19] That is why they have emerged as biomarkers of distinct biological states and play an important role in many diseases, such as viral infections and cancer, in which miRNAs are shown to act as either oncogenes (gene that has the potential to cause cancer) or tumor suppressors.[3,12,19] Whereas siRNA pathway requires perfect sequence complementarity to the target RNA, miRNA can bind with mismatches. miRNA precursors contain hairpin structures, often with bulged regions, which are processed by the enzymes Drosha (in the nucleus) and Dicer (in the cytoplasm) into approximately 22 nucleotide long duplexes resembling siRNAs. One strand of the duplex incorporates into a RISC-like miRNA-ribonucleoprotein (miRNP) complex including Ago protein. As with siRNA, the relative thermodynamic stability of the miRNA strands usually determines the guide strand.[18] Preferential recognition of the target sequences by miRNA occurs in the 3´-untranslated region (3´-UTR) of the mRNAs. The degree of miRNA-mRNA complementarity seems to be an important factor as to, whether miRNAs induce mRNA degradation or repress their translation. The precise mechanism is still unclear. Unlike in siRNA pathway, miRNA induced mRNA degradation seems to be initiated by deadenylation, decapping or exonucleolytic digestion.

The biogenesis and mechanisms of siRNA and miRNA pathways clearly overlap.[12,18] One important difference between them concerns their self-silencing ability. As defense molecules, siRNAs typically silence the same DNA or RNA sequence from which they were derived, making their production a continual struggle against themselves. siRNAs are highly specific to individual gene targets, whereas miRNAs can bind to multiple transcripts and each gene target can have multiple miRNA-binding sites. Hence, most miRNAs silence other than their own genes and the demand to bind heterologous targets makes them more constrained and less adaptable for defense purposes.

1.1.2 Antisense oligonucleotides

Before the discovery of natural regulatory RNAs and their function in cell biology, the antisense strategy, exploiting synthetically prepared single-stranded antisense oligonucleotides (ASO), had already evolved.[7-10,33] ASO molecules are typically 12-25 nucleotides long nucleic acid analogs designed to inhibit the function of an RNA target. After passing through the cell membrane and entering the cytoplasm and/or nucleus, an antisense oligonucleotide hybridizes with its target mRNA and interacts by a mechanism depending on its chemical composition and location of the hybridization (Figure 4). Two main cellular mechanisms that contribute to their activity are activation of RNase H leading to mRNA degradation and translational arrest blocking the binding to ribosome. Additional mechanisms include interference with mRNA maturation by inhibition of splicing and destabilization of pre-mRNA in the nucleus.

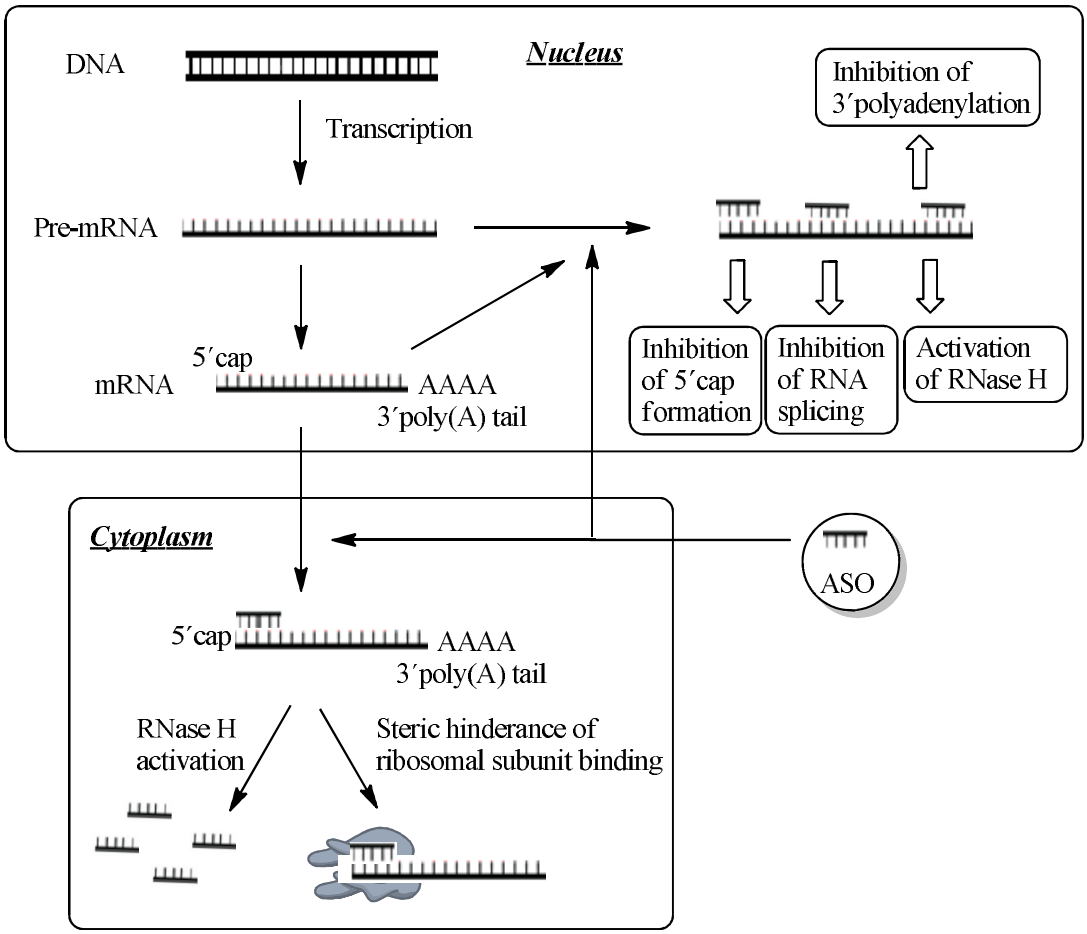

Figure 4. Modes of PTGS action of antisense oligonucleotides.[9]

The most extensively used and best understood ASO mechanism is based on induction of RNase H enzyme.[7,33,34] As a ubiquitous endonuclease (enzyme that cleaves the phosphodiester bond within a polynucleotide chain), it cleaves the RNA strand of an RNA-DNA heteroduplex, usually close to the center of the targeted RNA. The precise recognition elements for RNase H are unknown, but oligonucleotides having DNA-like properties, such as short as tetramers, can result in activation. The normal function of RNase H is to help the removal of RNA primers in DNA replication, but it may play other roles in the cell and although its concentration is thought to be greater in the nucleus, it is also found in the cytoplasm.[33] In addition to RNase H, there are other RNases present in cells that may be exploited in a similar manner.[10]

1.1.3 Comparing antisense approaches

Obviously, the antisense oligonucleotide and siRNA approaches have a lot in common and the methodological development benefits from each other. There is no clear evidence that one antisense mechanism would be superior to another and the true potency of both approaches will be assessed only by real clinical development.[32,35] The following demonstrates a few most notable differences. Although both strategies target mRNA, it is likely that single stranded antisense

oligomers must find their targets unassisted, since there seems to be no evolved cellular mechanism for promoting antisense strand recognition in contrary to RISC incorporating siRNA. On the other hand, siRNAs cannot target nuclear RNAs or introns in contrast to ASOs and, hence, RNAi is restricted to cytoplasm. Some concern has been raised for possible disturbance and toxicity that synthetic siRNAs may have for the native cellular RNAi machinery responsible for many important physiological processes (off-target effect).

1.2 Cell delivery of oligonucleotides

The delivery of oligonucleotides to cells is one of the major challenges for antisense technologies, as far as the systemic (*i.e*. affecting the entire body) delivery *in vivo* is concerned. Oligonucleotide drugs enter the cell most probably via some form of endocytosis, which involves the association of the drug molecule either to the cell membrane (adsorptive endocytosis) or to a membrane-bound receptor (receptor-mediated endocytosis) and results in vesicular uptake.[26,29,36,37] The large size, hydrophilic character and anionic backbone of nucleic acids prevent a direct cellular permeation process at any significant level. After internalization to the cytoplasm, oligonucleotide vesicles enter the endosome-lysosome compartment. Endosomes are membranous organelles that function as intracellular sorting centers. If the oligonucleotide is unable to escape the endosome, as often is the case, it is likely to be degraded by lysosome and fails to reach its site of action in the cytosol or nucleus. Efficient endocytosis requires cooperative action of all the stages of cell delivery: cellular uptake, vesicular trafficking and finally endosomal release (Figure 5).

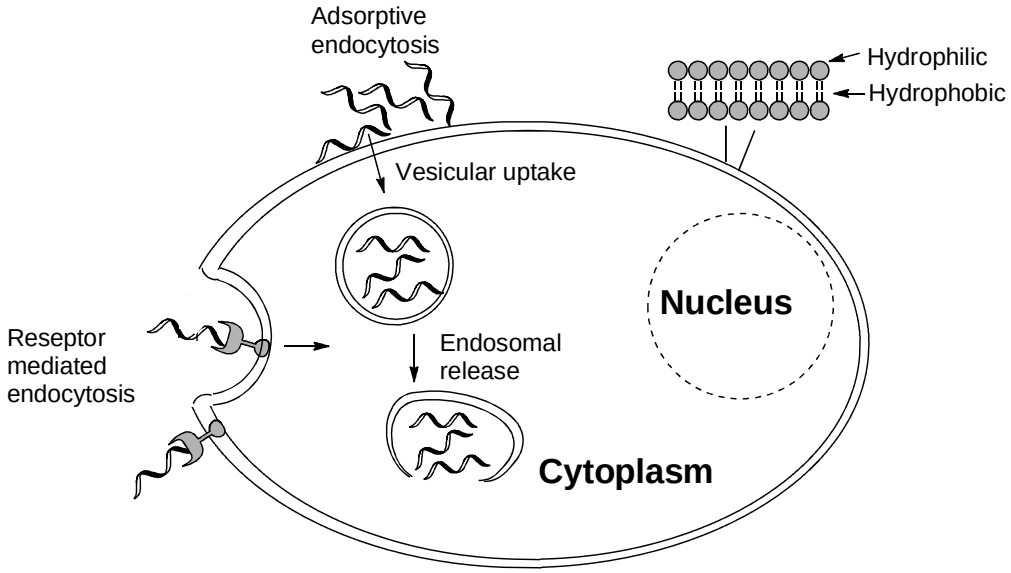

Figure 5. Simplified presentation of the cell delivery.

When unmodified naked oligonucleotides are added to cells, an inefficient cellular uptake is observed.[36] The adsorption to the cell surface is complicated by the negative charges in both oligonucleotide and membrane, causing ionic repulsion. However, simple elimination of the negative charge alone does not improve cellular uptake, as demonstrated by neutral oligonucleotide mimics incorporating methylphosphonate and PNA analogues (see structures in Section 1.3.2.1).[26] In addition, both unmodified and uncharged oligonucleotides tend to have low binding to proteins within blood plasma and are therefore rapidly excreted in the urine reducing delivery to tissues.[31] Consequently, numerous chemical modifications and conjugate groups have been studied for their ability to facilitate cellular uptake and bioavailability *in vivo* (Section 1.3).

Besides being able to improve cellular uptake of the oligonucleotide, the conjugates that allow targeted delivery are highly desirable. Cell-type-specificity would not only minimize the chance of potential adverse effects, but would also reduce the required dose to achieve therapeutic effect.[30] Receptors are proteins that are embedded in the plasma membrane and form a binding site for a specific molecule. Oligonucleotide that is conjugated with a targeting moiety can be recognized by cell-surface receptor and mediate the internalization of nucleic acid through receptor-mediated endocytosis. The employed cell-specific ligands include aptamers, antibodies, sugar molecules (Section 1.3.3.5), vitamins (Section 1.3.3.1) and hormones.

On the other hand, one way to resolve all the problems related to the endocytosis-mediated uptake would be to bypass it.[26,37] Direct penetration through cell membrane would be an energy-independent route but also unspecific for cell- and tissue-type, which can be good or bad. This type of non-endocytic delivery has been pursued with positively charged cell penetrating peptides (Section 1.3.3.2) such as TAT or Penetratin. Although it appears that endocytosis persists to be the main uptake pathway for these peptides, the possibility of direct penetration cannot be excluded. Other non-endocytic delivery techniques include microinjection, permeabilization and electroporation that are not, however, compatible with gene delivery *in vivo* due to their highly invasive nature.[37] In microinjection each cell is injected with the gene using glass capillary pipettes. Permeabilization uses pore-forming agents that are able to induce transmembrane channels or large apertures in the cell membrane, which then allow the entry. Finally, the electroporation technique involves the use of an electric field that opens pores in the cell.

In general, the mechanisms related to cell delivery of oligonucleotides are complex and still not well understood. Compared to cellular uptake, the nuclear entry may not be the rate-limiting step for free oligonucleotides since they are shown to continuously shuttle between the nucleus and cytoplasm.[29]

1.3 Chemical modifications of nucleic acid drugs

Regardless of the immense attractiveness of gene silencing as a therapeutic strategy, the oligonucleotides are not optimal drug-like molecules.[28,29,31] One of the

first biological barriers encountered by siRNAs or antisense oligonucleotides is the nuclease activity in plasma and tissues as natural phosphodiester bonds are rapidly degraded *in vivo*. Even though the double stranded siRNAs are more stable against nuclease attack than their single-stranded counterparts, the protection is needed. The relatively large polyanionic nucleic acids do not easily cross cell membranes and, hence, exhibit inefficient cellular uptake and poor bioavailability. Their cell targeting is unspecific and the distribution in tissues and intracellular media is limited. Moreover, oligonucleotides may have toxic side effects, which are classified as hybridization dependent or hybridization independent.[8,31] The former class can be attributed to exaggerated pharmacological effects and hybridization to non-target RNA instead of the intended mRNA. This hybridization dependent off-targeting can be minimized by careful selection of the target. siRNAs can additionally have unwanted participation in miRNA pathways. Hybridization independent toxicity is related to the chemically modified oligonucleotides but may still exhibit some sequence specificity arising from motifs that define a receptor interaction and trigger an immune response.

A wide variety of chemical modifications and conjugate groups have been introduced into oligonucleotides to overcome the problems discussed above. Section 1.3.2 will summarize some of the most well-known structural modifications used in oligonucleotides and in Section 1.3.3 those covalently attached conjugate groups that are aimed at facilitating the delivery are discussed. In general, conjugation refers to covalent attachment of functional molecules to nucleic acids. All three structural subunits in nucleic acids, *i.e.* ribose sugar, phosphate backbone and base moiety have been modified and functionalized. No single modification covers all the desired properties and, hence, their combinations are common. The ideal oligonucleotide structure appears to be case and application dependent.

1.3.1 General remarks for oligonucleotide design

If the antisense oligonucleotide is intended to utilize the RNase H dependent pathway, the chemical modifications have to support it. The nucleoside conformation is a critical factor for the activity of RNase H, which is destined to degrade the RNA strand in a DNA/RNA hybrid and fails to use RNA/RNA duplex as a substrate.[34] While higher thermal stabilities are achieved using modifications such as the 2´-modified sugars (analogs of RNA) that adopt an RNA-like 3´-*endo* sugar puckering, they shift the A-B-type helical arrangement of the DNA/RNA heteroduplex to the A-type RNA helix and fail to promote RNase H activity. The same is true for many other potential nucleotide analogs. This has led to the development of a chimeric gapmer strategy, in which a central DNA region capable of activating RNase H (often 6-10 nucleotide long) is flanked on the 5´- and 3´-ends by modified sections.[38,39] The modified wings provide antisense efficiency based on e.g. increased affinity and nuclease stability. Much more versatile arrangements are allowed for oligonucleotides using non-RNase H pathways, which are based on mere steric blocking.

When modifications are introduced into siRNA-oligonucleotides, it is worth bearing in mind that care should be exercised while increasing stability towards target mRNA.[19,28] Since the siRNA strand having weaker base paring at its 5´-end is favored as an antisense strand in RISC, the over stabilization may lead to wrong strand selection causing off-targeting and problems in unwinding of siRNA duplex. By contrast, a high-affinity modification, such as LNA, at the 5´-end of the sense strand is often beneficial as also is high-binding affinity at 3´-end of the antisense strand. Besides wrong strand selection, off-targeting can arise from unwanted participation of siRNAs to miRNA-pathways. This can be reduced with modifications at seed region or at 5´-end of the antisense strand. siRNA design demands careful strategic modulation of both strands for maximal efficiency. In general, bulkier modifications and conjugate groups are better tolerated at the terminal positions of the oligonucleotides. The most conventional synthetic siRNA structure mimicking the natural product of the Dicer enzyme is shown in Figure 6. The 3´-overhangs can be modified in various ways and especially the termini of the sense strand accommodates conjugate groups. Chemical phosphorylation of the antisense 5´-end helps to ensure high potency.

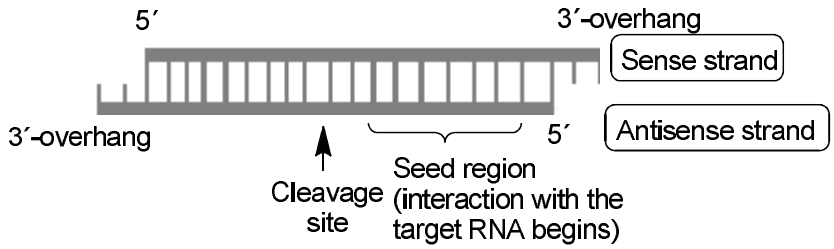

Figure 6. Structure of a siRNA.[19]

Other kinds of duplex architectures and even single-stranded antisense alternatives are also possible for functional siRNAs.[28] For example a siRNA made of three strands, so-called small internally segmented interfering RNA (sisiRNA), has been shown to reduce off-target effects along with increased potency.[40] In sisiRNA, the antisense strand is kept intact and it is hybridized with two 9-13 nucleotides long sense strands. While most of the synthetic duplexes contain 19-21 base pairs, other lengths are also possible as long as dsRNAs do not exceed the length of 30 nucleotides which can trigger the interferon response.[28]

Besides detailed design of ASOs and siRNAs, search of an accessible target sequence within the target RNA plays an important role in efficient gene silencing. This topic is approached in Section 1.5.

1.3.2 Structural analogs

1.3.2.1 Modifications of phosphate linkage and sugar moiety

The phosphodiester internucleosidic linkage has been modified to increase nuclease stability of both antisense oligonucleotides and siRNA (Figure 7).[8,9,19,31] Replacement of the non-bridging oxygen with sulfur (phosphorothioate) is the most widely applied and easily synthesized derivative, which is importantly tolerated by RNase H and the RNAi machinery. Additionally, phosphorothioate modifications in ASO are beneficial for pharmacokinetics as they promote cell delivery by binding to proteins in plasma which prolongs their circulation time. The only ASO drug approved for clinical use is a 21 base pair long phosphorothioate modified oligodeoxynucleotide called Vitravene, which is an anti-viral drug for an eye disease caused by a cytomegalo virus. However, if the phosphorothioate content in oligonucleotide is high, toxic side effects can result from their tendency to interact nonspecifically with cellular proteins and hybridization to mRNA is weakened.

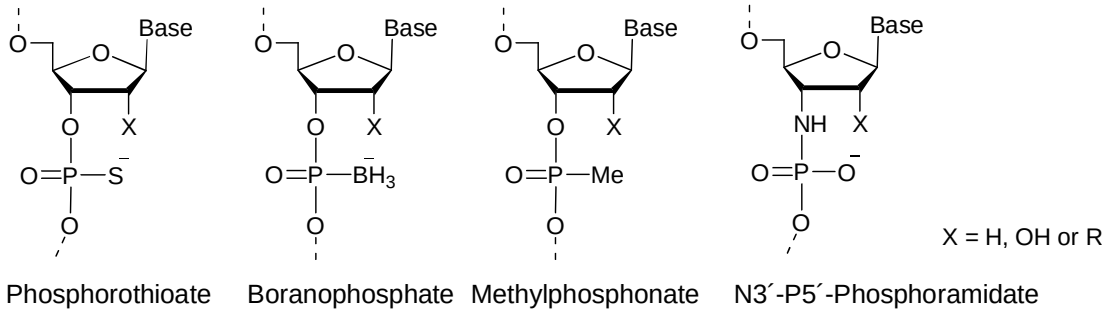

Figure 7. Modifications to the phosphodiester backbone enhancing nuclease stability.

Nuclease resistance is also enhanced using e.g boranophosphates, phosphoramidates and non-ionic methylphosphonate analogues.[27,31] The laborious chemical synthesis limits the use of boron derivatives, although they seem to be compatible with siRNA function and their activity and nuclease resistance was reported to exceed those of the corresponding siRNA having phosphorothioate modifications.[41] N3´-P5´-Phosphoramidates and methylphosphonates are RNase H inactive. Since oligonucleotides, incorporating phosphoramidate linkages, exhibit high-affinity binding properties, they are potential antisense agents for steric blocking mechanism and their efficiency has been demonstrated *in vivo*.[42]

As analogues of oligoribonucleotides, the 2´-position in ribose sugar is synthetically easily accessed. 2´-Modifications, such as 2´-*O*-methyl, 2´-*O*-methoxyethyl (MOE), 2´-*O*-[2-(methylamino)-2-oxoethyl] (NMA) and 2´-fluoro groups, increase the binding affinity and nuclease stability (Figure 8).[31,39,43] Furthermore, 2´-derivatives show improved metabolic stability and increased lipophilicity. However, these 2´-modifications cannot induce RNase H cleavage of the target RNA. To circumvent this, the modifications have been incorporated, as mentioned above, into chimeric oligonucleotides composing a ´gap´ region of

RNase H –resistant nucleotides linked to an unmodified region capable of activating RNase H. Alternatively, the modified oligonucleotides are employed as steric blockers. 2´-*O*-MOE modified ASOs have demonstrated effective inhibition of many viral and cellular gene products both *in vitro* and *in vivo*, and MOE modifications seem to reduce non-specific protein binding, which can diminish toxicity.[10,39,44] Similar effects were obtained with 2´-*O*-NMA derivatives.[43] In the case of siRNA, 2´-position modifications are generally well-tolerated and the 2´-OH is not required for recognition by the RNAi machinery.[45] Whereas heavily 2´-*O*-Me modified oligonucleotides usually decrease RNAi activity, the small 2´-fluoro substituent is rather compatible with siRNA function and partial modifications are tolerated throughout the sense and antisense strands.[27,28,32] Both, 2´-*O*-Me and 2´-fluoro derivatives have been shown to reduce the immunostimulatory effects of siRNA.[46,47] Likewise the 2´-fluoro-*β*-D-arabinonucleotide (FANA) has been shown to be well-tolerated in antisense oligonucleotides and siRNA duplexes, in which especially the sense strand can be modified.[28] Importantly, also DNA nucleosides (2´-H) can be accepted to certain extends within siRNA duplexes.

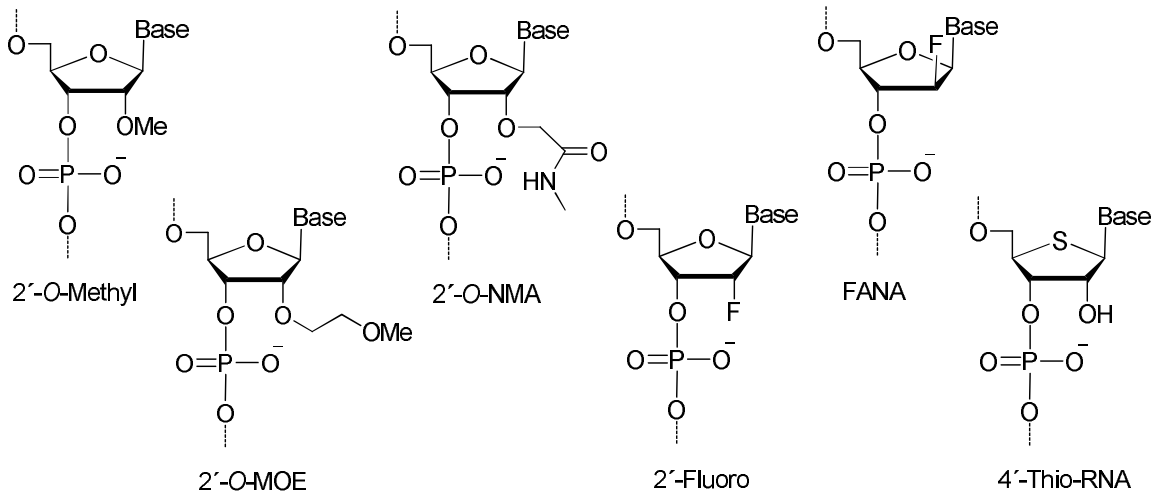

Figure 8. 2´-Modified sugar moiety and 4´-thionucleotide.

4´-Thiolation of RNA and DNA, *i.e.* replacement of the 4´-ring oxygen by sulfur, improves thermal stability and nuclease resistance.[28,48] Furthermore, 4´-thio-modifed siRNAs exhibit potent RNAi activity in particularly when antisense and sense strands are modified at the end of the chains.

Promising conformationally restricted nucleoside analogs that enhance nuclease stability include locked nucleic acid (LNA) and less-strained 2´-*O*,4´-*C*-ethylene-bridged nucleic acid (ENA) (Figure 9).[8,49,50] They contain a methylene or ethylene bridge that connects the 2´-oxygen of the ribose with the 4´-carbon. Their incorporation into oligonucleotides significantly enhances the hybridization affinities (ΔT_m = +3 to +8 °C per monomer) and even though a central positioning prevents RNase H function, the high-binding ability of a chimeric DNA-LNA

gapmer has shown to accelerate RNase H cleavage. Chimeric 2´-*O*-methyl-LNA modified oligonucleotides have been targeted to inhibit HIV-1 gene expression through steric blocking.[51] Although LNA exhibits high potency for ASO, it has been reported to increase the risk of hepatoxicity.[52] In a recent study, this side effect was not detected when the ASO length was reduced (20-mer to 14-mer) and methyl or methoxymethyl group was attached to the methylene bridge in LNA structure.[53] The development of other bridged nucleic acid (BNA) structures, such as 2´-,4´-methyleneoxymethylene BNA (BNA^{COC})[54], 2-*O*,4´-*C*-aminomethylene BNA (BNA^{NC}), 2´,4´-aminooxymethylene BNA and 2´,4´-(*N*-methoxy)aminomethylene BNA has continued and the last three mentioned have appeared potential in animal models.[55] In siRNA duplex, extensive modifications generally lead to decreased activity and the most commonly used sites for LNA nucleotides are the termini of the sense strand and the 3´-overhangs of the antisense strand.[28]

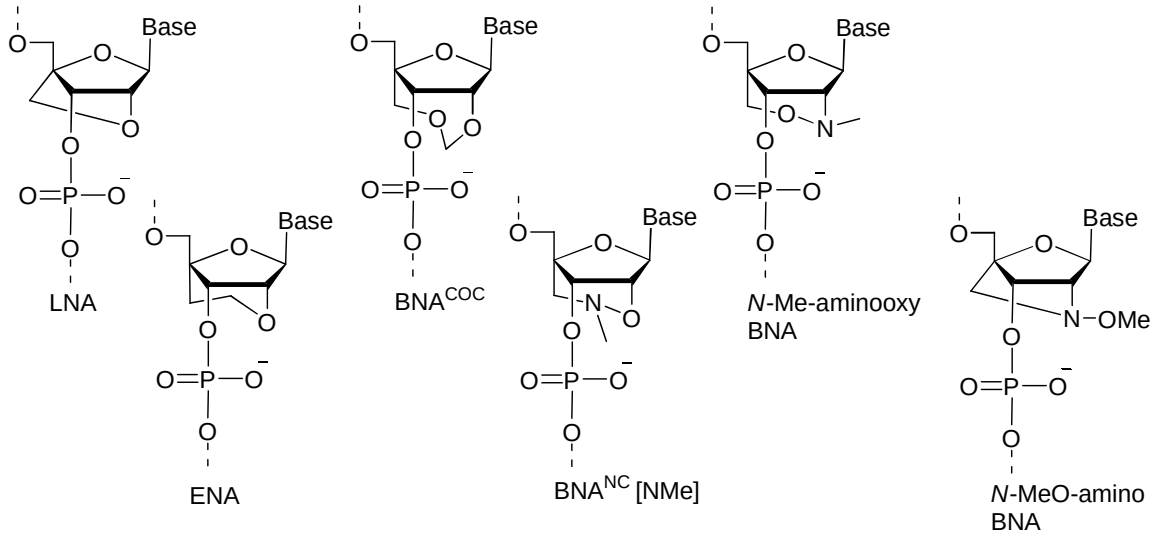

Figure 9. Conformationally constrained sugar modifications.

A number of DNA and RNA analogs, having phosphate or ribose moiety completely replaced with another structure, have been developed. These include peptide nucleic acid (PNA), morpholino oligonucleotides (PMO), hexitol nucleic acid (HNA), altritol nucleic acid (ANA), cyclohexene nucleic acid (CeNA) and tricyclo-DNA (tcDNA) (Figure 10).[8,56-58] In antisense use, all the oligonucleotide analogs comprising these entities have high affinities to mRNA and enhanced nuclease stability, but they do not support cleavage mechanism through RNase H, except for CeNA-RNA duplexes, which have been reported to activate RNase H with a catalytic rate lowered by a 600 fold, compare to unmodified DNA-RNA hybrids.[59]

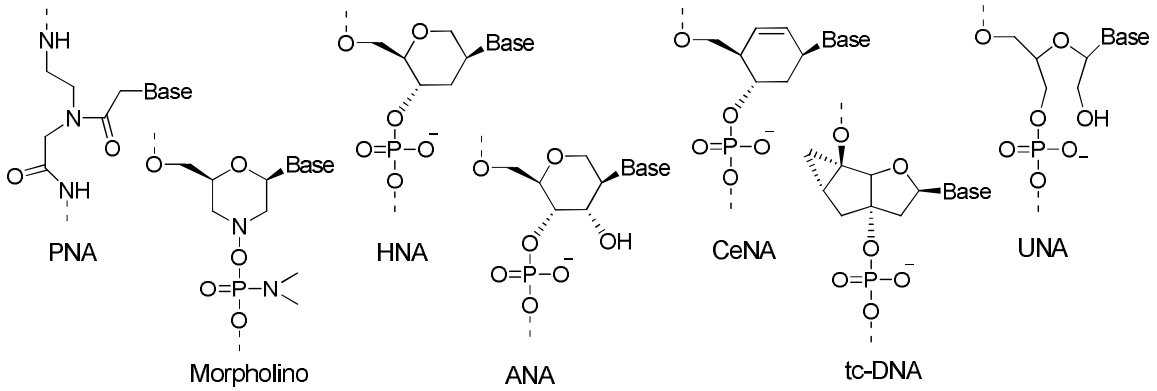

Figure 10. Nucleotide analogs with replaced sugar or phosphate structure.

In PNAs, the sugar-phosphate backbone is replaced with a peptide-related structure.[8,56] Besides being highly nuclease resistant, PNA provides high-affinity binding to complementary RNA or DNA. As uncharged molecules, PNAs seem to be nontoxic owing to their low affinity for proteins. However, their solubility and poor cellular uptake limits their potential as antisense agents. Instead, PNA has been utilized as cell-penetrating peptide (CPP) conjugates (Section 1.3.3.2).[60,61] Similarly CPPs have been used to facilitate the cell delivery of another uncharged oligomer PMO[57], in which the sugar-phosphate structure is placed with a six-membered morpholino ring and phosphoroamidate backbone. PMOs have shown antisense efficacy based on steric blocking *in vivo* and also in human clinical trials.[10,62] Improved performance was recently reported with siRNAs that incorporated morpholino analogues at 3´-end of both strands.[63]

HNA, an analog having six-membered 1,5-anhydrohexitol carbohydrate moiety, hybridizes strongly with RNA (prefer A-form duplex) and its 3´-OH derivative called ANA results in even more increased duplex stabilities.[58] An HNA-gapmer oligonucleotide comprising a central phosphorthioate sequence has been used to target the mRNA of MDR1-gene playing a role in multi-drug resistance of cancer cells.[64] Lipofectamin 2000 was used as a transfection agent. Incorporation of a few HNA nucleotides into siRNAs that target the mRNA of human B-Raf oncogene (critical for growth and survival of melanoma cells) has been reported to improve effectiveness and duration of action of the siRNA.[65] Similar effects have been demonstrated for ANA-modified siRNA targeted against mRNA of MDR1[66] and also for siRNA incorporating one or two ceNA modifications, especially in the middle sections of both the sense and antisense strand.[67] Part of the improved biological activity may be attributed to increased stability towards nucleases, achieved even with minimal number of substitutions. However, no clear correlation between activity and biostability has been detected with siRNAs incorporating conformational constrain and complex tc-DNA analogs.[68] The most active siRNAs (~4-fold increase relative to native siRNA) for silencing of EGFP gene (reporter gene that encodes green fluorescent protein) that contained tc-DNA modifications at 3´-ends and in the middle of both stands, were reported to exhibit very different serum stabilities.

Recently a flexible, acyclic and helix destabilizing RNA mimic called unlocked nucleobase analog (UNA, Figure 10) has been shown to reduce off-target silencing by siRNA without compromising on-target efficiency, when incorporated in the seed region of the antisense strand.[69,70] At the 5´-end of the sense strand, UNA can block the loading of wrong strand into RISC and concomitantly improve antisense strand activity.[70] UNA monomers were also found to be compatible with RNase H activity.[71]

1.3.2.2 Modifications of nucleobases

Nucleobases has been modified (Figure 11) mainly to increase binding affinity to complementary nucleic acids.[8,31] This can be accomplished by enhancing stacking interactions or strengthening the Watson-Crick base-pairing. However, the base-pair recognition must not be disturbed and, hence, the number of heterocyclic base modifications generally is limited. Some base modifications can reduce immune activation.[28,72]

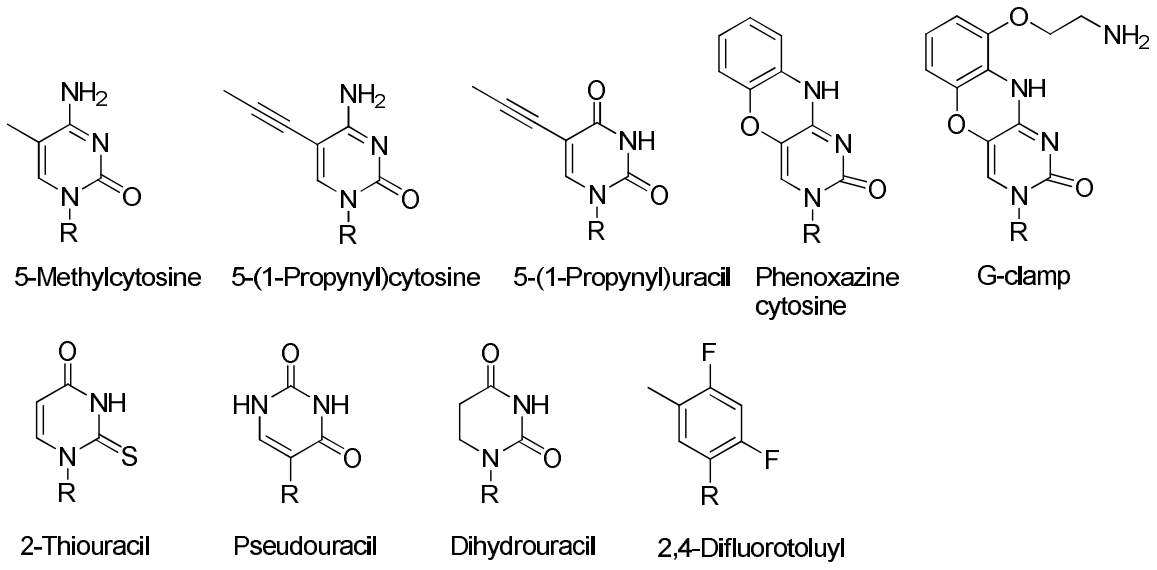

Figure 11. Nucleobase modifications.

With antisense oligomers, the pyrimidine C5 position has commonly been used as the site of modifications, because such substitutions generally improve affinity without affecting the ability to activate RNase H.[31,73] These C5-analogs include 5-methylcytosine and 5-propynyl nucleosides. However, 5-propynyl substituents have been found to be toxic *in vivo*.[74] Tricyclic phenoxazine and G-clamp cytosine derivatives have also been shown to enhance stacking.[73]

With siRNAs, nucleobases, such as 2´-thiouracil and pseudouracil, has been used to enhance potency and specificity.[28,75] The most active duplexes were those having a high-affinity 2´-thiouracil base at the 3´-end of the antisense strand and a low-affinity dihydrouracil base at the 3´-end of the sense strand. In general, bulky or cationic base modifications are not well-tolerated by RNAi. Many other base

substitutions compatible with RNAi have been prepared, including some atypical base structures like 2,4-difluorotoluyl base. Difluorotoluyl ribonucleoside cannot form hydrogen bonds, but it has been shown to improve the nuclease resistance in serum and maintain siRNA activity even at an internal position.[76]

1.3.3 Conjugate groups for cell delivery

Two strategies contribute to the search for chemically enhanced delivery of oligonucleotides.[77] One is design of non-covalently assembled oligonucleotide-complexes, in which cellular uptake is increased by various carriers. These include cationic lipids, dendrimers, polymers, cyclodextrins, and even carbon nanotubes. These applications are not discussed here in more detail.

The second strategy comprises covalently bound oligonucleotide conjugates, such as lipophilic substituents, cell-penetrating peptides and ligands for cell surface receptors. In principle, stoichiometric covalently bound oligonucleotide conjugates can provide higher concentrations of the nucleic acid drugs compared to the non-covalently bound complexes, in which an excess of complexing agent is generally required. In addition, to reach the site of action within the target cell, the nucleic acid needs to stay associated with its carrier during the extracellular delivery, which may not be the case with non-covalently bound complexes.[78] On the other hand, covalent attachment of a bulky conjugate group to the oligonucleotide may influence its intracellular distribution, such as the entry to nucleus, or disturb hybridization to the target.[77] To circumvent this, a cleavable linkage between the oligonucleotide and ligand has been employed.[30] For example, acid labile linkages (e.g. *β*-thiopropionate) are expected to be cleaved in the acidic endosome compartments and reducible bonds (e.g. disulfide) in the reductive cytosolic environment to release the intact oligonucleotide inside the cell.

1.3.3.1 Lipophilic and vitamin conjugates

The internalization of anionic oligonucleotides requires a passage through the hydrophobic interior of the phospholipid bilayer membrane. Therefore, conjugation with lipids has been employed as a possible method to facilitate oligonucleotide uptake.[26,60,79] Besides reducing the hydrophilic nature of oligonucleotides, some hydrophobic ligands, such as cholesterol, can bind to lipoproteins, which are cholesterol carriers in blood. Consequently, cholesterol conjugate becomes recognized by their target cells leading to internalization by lipoprotein-mediated endocytosis. The cholesterol-siRNA conjugate has been shown to induce silencing of the apolipoprotein B mRNA (apoB encodes a protein essential for cholesterol metabolism) in mice liver and jejunum, which was not detected with naked siRNA.[80] Cholesterol was conjugated to the 3´-end of the sense strand in siRNA via pyrrolidine linker.

Other lipophilic siRNAs conjugated with long-chain fatty acids and bile acid (Figure 12) also bind to lipoproteins allowing siRNA uptake and gene silencing *in vivo*.[81] The length of the alkyl chain is critical for the binding to lipoproteins and,

hence, to the gene silencing capability. A novel mechanism for cell entry of lipoprotein-associated cholesterol-siRNA has been suggested. Instead of simple receptor-mediated endocytosis, the conjugated siRNA is argued to pass from the lipoprotein receptor to a separate transmembrane transporter, which mediates the cellular uptake. Such a transmembrane protein is Sid 1 that seems to be required for siRNA uptake.

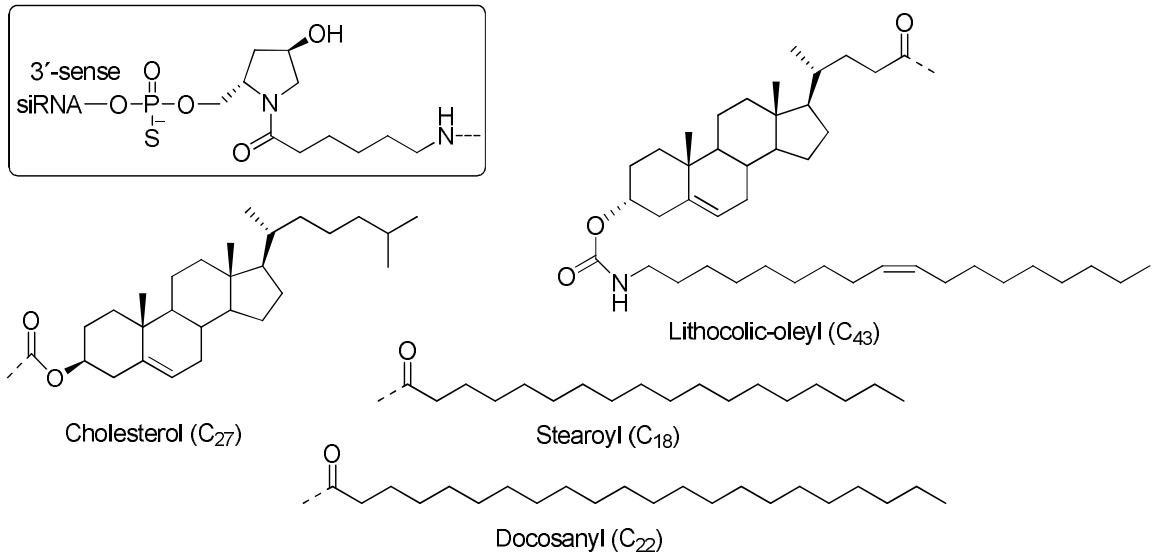

Figure 12. Structures of fatty acid and bile acid siRNA-conjugates.

Cholesterol has also been attached to the 5´-end of siRNA sense strand.[82,83] According to a study on targeting p38 MAP kinase mRNA in mouse lung, cholesterol conjugation may extend but not increase siRNA-mediated knockdown.[83]

Hydrophobic vitamin E has its own physiological transport pathway to most organs and one of its eight natural isomers, *viz.* *α*-tocopherol has been conjugated to the 5´-end of the antisense strand in siRNA (Figure 13a).[84] The *α*-tocopherol moiety was designed to be cleaved by Dicer after entering the cell, producing a mature siRNA against apoB mRNA. Efficient *in vivo* silencing was achieved in liver without induction on interferons or other side effects.

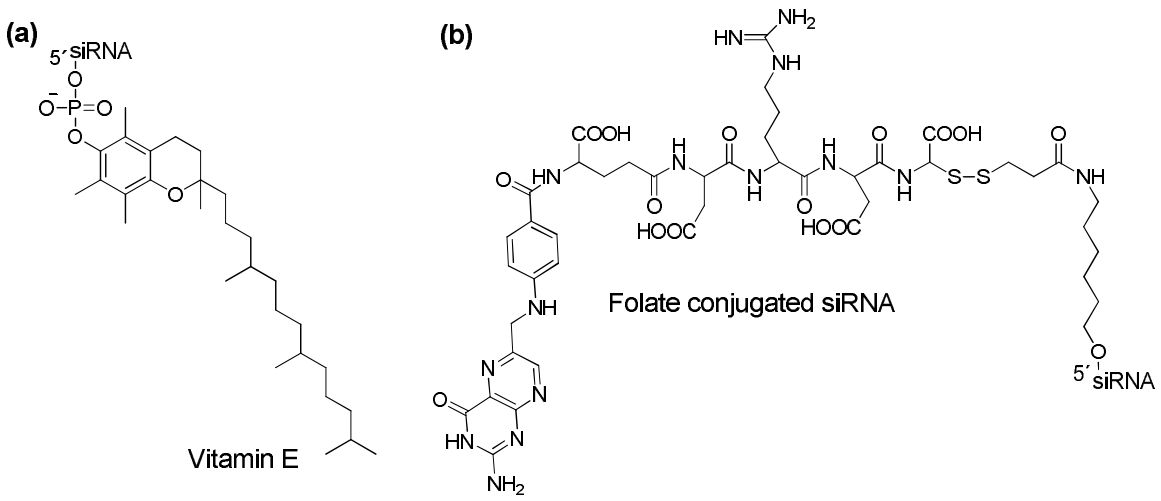

Figure 13. Vitamin conjugates: (a) *α*-tocopherol-bound siRNA, (b) Folate conjugated siRNA.

Other vitamins, including fat-soluble vitamin A (retinol) and folic acid, have also been used as carriers for nucleic acids.[85,86] In general, vitamins are described to be internalized through cell-surface receptors and their recognition often depends on interaction with binding proteins. In the case of vitamin E, binding to lipoproteins or other serum proteins initiates the cellular uptake.[85] By contrast, vitamin A is probably absorbed by cells through the receptor of retinol-binding protein and recently, vitamin A-coupled liposomes has been used for siRNA delivery to hepatic stellate cells.[87] Folic acid conjugations have been applied to various macromolecules to allow their binding to folate receptors.[86] Since folate receptors are overexpressed in many human tumors, they can be exploited in targeted cancer therapies and receptor-mediated *in vivo* delivery to malignant cells and tissues has been reported with folic acid conjugated siRNA (Figure 13b).[88]

1.3.3.2 Cell penetrating peptides

Cell penetrating peptides (CPP) compose a large group of unrelated sequences, which are often positively charged and have a high content of basic amino acids and a length of 10-30 residues.[32,60,61,89] They are able to mediate the cellular uptake of nucleic acids, in most cases probably through endocytosis, although the precise mechanism remains elusive and may depend on the case. Some of the most commonly used CPPs include TAT (trans-activator protein from HIV-1) peptide, Penetratin, Transportan and arginine-rich CPPs (Figure 14a).

(a)

Name	*sequence*
TAT	GRKKRRQRRRPPQ
Penetratin	RQIKIWFQNRRMKWKK
R6Pen	R_6RQIKIWFQNRRMKWKKGGC
Pip	e.g. $(RXR)_3$IdKILFQNdRRMKWHKBC
Transportan	GWTLNSAGYLLGKINLKALAALAKKIL
Oligoarginine	R_8 / R_9
Arginine-rich	e.g. $(RXR)_4XB$
CPPs	and $(RXRRBR)_2XB$

(A = alanine, B = β-alanine, C = cysteine, F = phenylalanine, G = glycine, H = histidine, I = isoleucine, K = lysine (dK = D-lysine), L = leucine, M = methionine, N = asparagine, P = proline, Q = glutamine, R = arginine, S = serine, T = threonine, W = tryptophan, X = 6-aminohexanoic acid, Y = tyrosine)

(b)

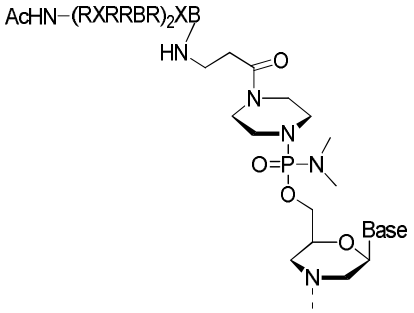

Figure 14. (a) Some commonly used cell penetrating peptides, (b) Example of arginine-rich CPP-PMO conjugate.

In early studies, TAT and Penetratin peptides were shown to improve biological effects when attached to 5´-ends of antisense oligonucleotides via disulfide bond.[60,90] However, it seems that inefficient escape from endocytic vesicles generally limits the function of some antisense CPP-conjugates and most of the endosomolytic agents used *in vitro* studies are too toxic for *in vivo* applications.[89,91] This has led to chemical modification of standard CPPs and few representative examples are shown in Figure 14a from CPP families of Penetratin and poly-arginine.[61] Also strategies such as co-treatment with endosome-disrupting peptides and photochemical internalization have been explored.

CPPs have most extensively been used for the delivery of neutral oligonucleotide analogs such as PMO (morpholino oligonucleotides) and PNA (peptide nucleic acid) showing in several studies good effectiveness in modulation of the RNA splicing processes via steric blocking.[60-62] Recently, hereditary muscle disease (Duchenne muscular dystrophy (DMD)), which is caused by a mutation in the dystrophin gene was approached with PMO conjugate of arginine-rich CPP (*i.e.* $(RXRRBR)_2XB$) linked through a stable amide bond (Figure 14b).[92] Systemic delivery was reported to restore dystrophin protein levels to almost normal in the cardiac and skeletal muscles in mice. In general, incorporation of structures like 6-aminohexanoic acid (X) and β-alanine (B) into oligoarginine peptides has been reported to increase serum stability and to generate higher antisense activities of CPP-PMO, which even exceed those seen with TAT-peptide.[93] It has been hypothesized that although X/B-containing conjugates enter cells less efficiently than oligoarginines, a greater ability to escape from endosomes/lysosomes could count for the good activity of these arginine-rich CPPs.[94] PNA internalizing peptides (Pip) have been derived from Penetratin CPP, and their PNA conjugates have shown enhanced serum-stability and exhibited strong activities for splicing redirection *in vitro* and *in vivo*.[95]

siRNA having TAT peptide conjugated to the 3´-end of the antisense strand via a sulfosuccinimidyl-4-(*p*-maleimidophenyl)-butyrate linker, was reported to show substantial improvement in delivery and downregulation of the target protein.[96] Similarly Penetratin peptide attached via a disulfide linkage to the 5´-terminus of the sense strand showed effects on primary mammalian neuronal cells.[97] In another study, Penetratin and TAT conjugated siRNAs, however, showed only very modest gene-silencing.[83] Penetratin-conjugate also triggered an innate immune response, while unconjugated Penetratin and TAT peptides caused uncharacterized effects upon gene expression. The latter observation emphasizes the importance of the conjugate purity on assessing the siRNA activities.

Besides being covalently bound to CPP, the negatively-charged molecules ASO and siRNA may benefit from non-covalent strategies (not covered here), being able to interact with positively charged CPPs and, hence, forming complexes with a positive net charge.[61]

1.3.3.3 PEG conjugates

Polyethylene glycols (PEG, Figure 15a) are amphipathic and non-ionic polymers, which has been conjugated to oligonucleotides to serve as ligands themselves or as linkers for other conjugate groups.[26,79] PEG-oligonucleotide conjugates are expected to facilitate transport and they have been reported to improve nuclease stability and pharmacokinetics. PEG conjugates are often complexed with cationic polymers or peptides to form colloidal nanoparticles, so-called polyelectrolyte complex micelles (PEC micelles, Figure 15b) useful as delivery vehicles.[30] The main route of cellular entry is believed to be absorptive endocytosis, unless specific ligands that facilitate receptor-mediated endocytosis are present. *In vivo*, targeted delivery to tumor cells has been demonstrated with PEC micelles consisting of polyethylenimine (PEI) and pegylated oligonucleotide conjugates of folic acid[98] or PEG-siRNA conjugates of LHRH (LHRH = luteinizing hormone-releasing hormone peptide)[99].

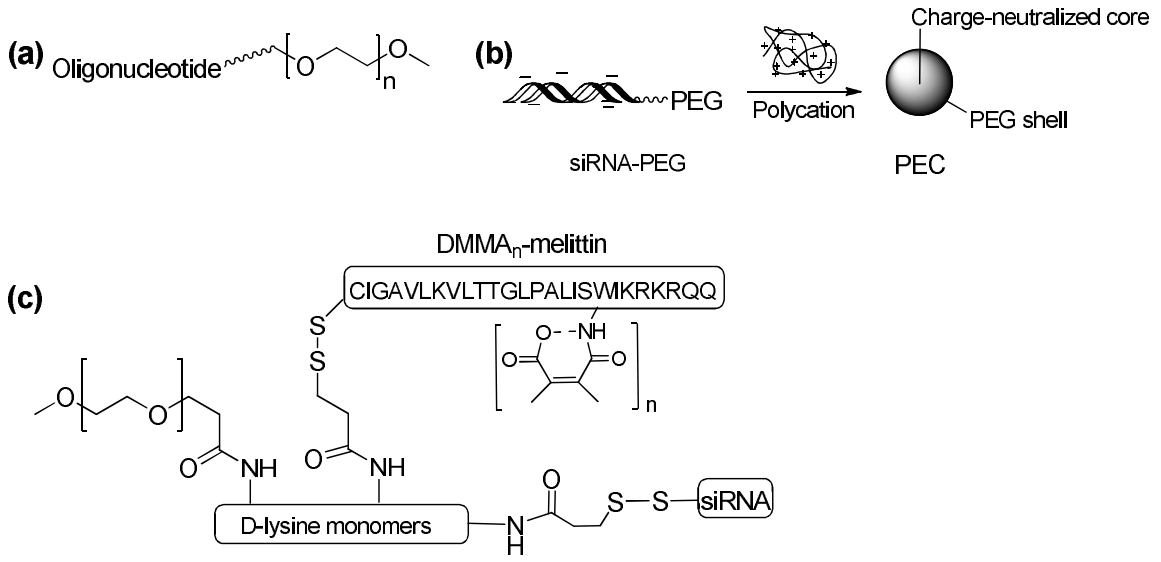

Figure 15. (a) Structure of PEG-oligonucleotide, (b) formation of PEC micelles and (c) PEG-PLL(DMMA$_n$)-Mel-siRNA conjugate. (See abbreviations for amino acids in Figure 14)

Recently, siRNA was covalently incorporated into a pH- and redox-responsive polymer via a disulfide bond (Figure 15 c).[100] Covalent binding was used to overcome the risk of complex dissociation in extracellular environment. The polymer was attached to the 5´- end of the sense strand. It consisted of three different moieties: polylysine (PLL) for binding and protection of RNA, PEG for increasing solubility and improving pharmacokinetics, and the lytic peptide melittin for endosomal release. Melittin was masked with dimethylmaleic anhydride (DMMA) and exposed upon endolysosomal acidification. This siRNA conjugate was reported to exhibit high biocompatibility and efficient gene silencing *in vitro*, but toxicity studies revealed problems *in vivo*.

1.3.3.4 Cationic and polyamine conjugates

Introduction of positive charges into oligonucleotides favors hybridization with nucleic acid targets and possibly enhances cellular permeation, because of reduced electrostatic repulsion.[26,77] Bearing this in mind, many covalently-linked polyamine and cationic oligonucleotide conjugates have been prepared but their effects on cellular uptake have not been broadly assessed. One potential cationic group is guanidinium function, which is adopted from arginine residue and has been shown to improve cellular uptake while introduced on the nucleobases or on the backbone (Figure 16). As guanidinium group is highly basic (pK_a 12.5), the modified oligonucleotides should remain protonated under a wider range of pH than their amino analogues. Fully or partially modified guanidine PNAs were reported to be taken up by several cell lines by a mechanism that referred to direct translocation.[101,102] However, other studies with DNA analogues incorporating 5-[(6-guanidinohexylcarbamoyl)methyl]-2´-deoxyuridine nucleosides[103] or 3´-guanidinobutyl phosphoramidate nucleoside units[104], support an endocytotic

mechanism. *In vivo* splice-correction efficiency has been demonstrated with guanidinium dendritic scaffold covalently-linked to a PMO.[105]

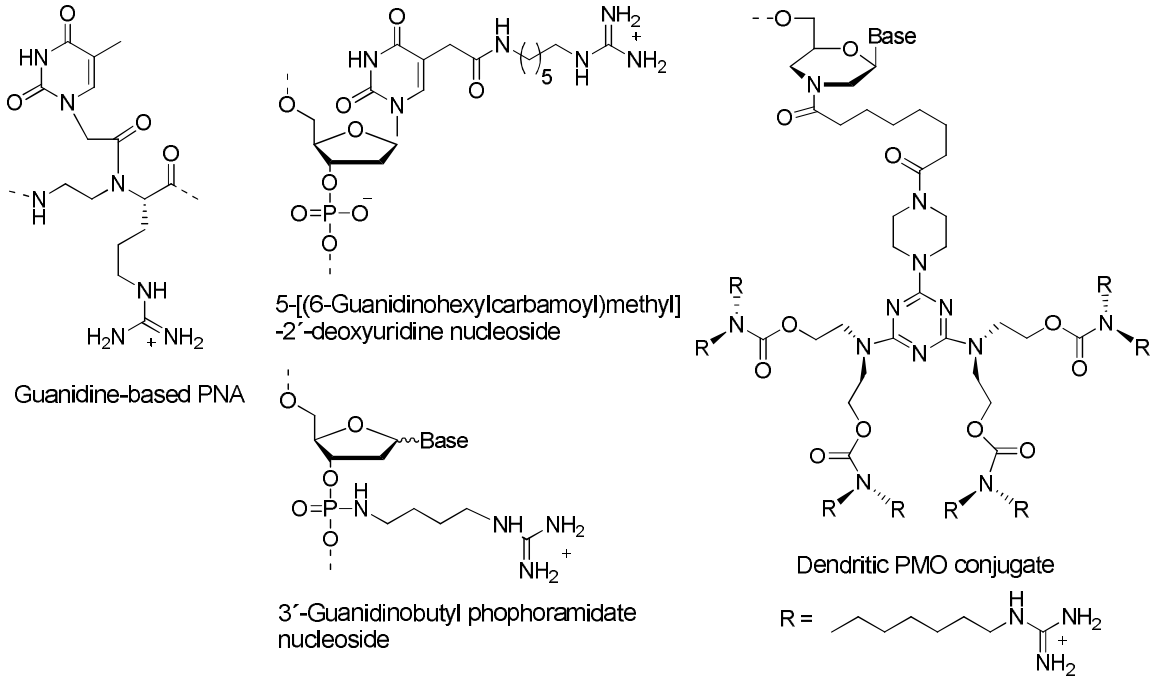

Figure 16. Guanidino oligonucleotide analogues.

Spermine conjugated siRNAs (Figure 17a) were shown to enter human cells and result in gene silencing in submicromolar concentration range.[106] Altogether 30 spermines were conjugated to the 5´-end of the siRNA sense strand to achieve the desired charge ratio. In other studies, 2´-polyamine modified nucleotides (Figure 17b), bearing either a lysylaminohexyl group, a succinyl-linked spermine ligand or its longer pentaamine version, were incorporated into oligonucleotides and reported to have positive antisense effects *in vitro* along with increased duplex stabilities.[107,108]

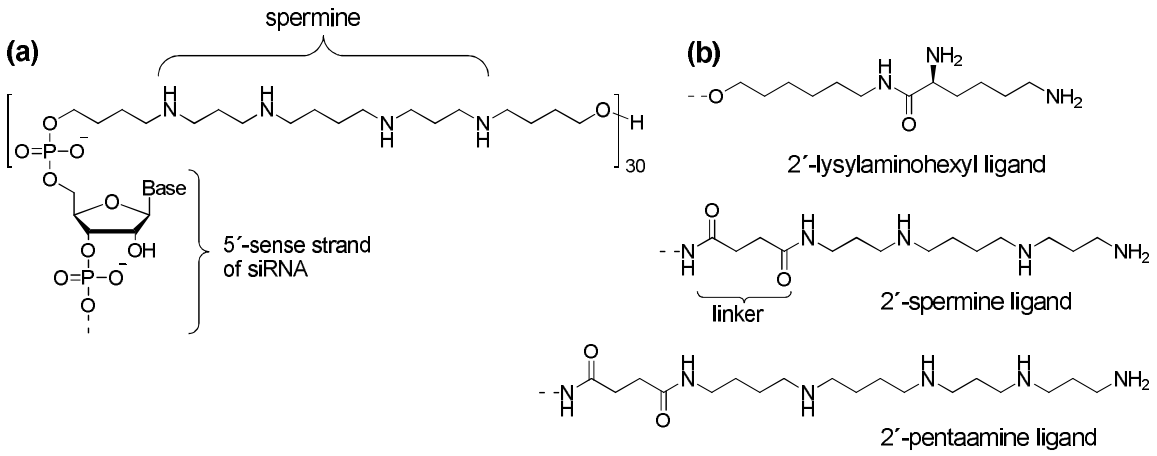

Figure 17. (a) The structure of spermine-siRNA and (b) polyamine conjugations to 2´-position in ribose.

Aminoglycosides (examples in Figure 18) comprise a very versatile and unique group of cationic ligands possessing characteristics exploitable in antisense approaches.[23,109-112] They contain hydrophilic amino-modified sugars and due to their polycationic nature under physiological conditions, they show considerable affinity to nucleic acids. The well-known activity of aminoglycosides as antibiotics is based on inhibition of the bacterial protein synthesis by binding to the ribosomal RNA. Besides ability to bind RNA and inhibit its function, aminoglycosides show potential for chemical cleavage of RNA. Their conjugation to oligonucleotides can also enhance the cellular uptake and neomycin has been shown to assist the cationic lipid-mediated delivery of oligonucleotides.[113] Enhanced uptake has also been observed with neamine conjugated PNA targeting HIV-1 TAR RNA (see Section 1.5.1).[110] Neutral carbohydrate ligands exploited for enhancement of delivery are presented in next section 1.3.3.5.

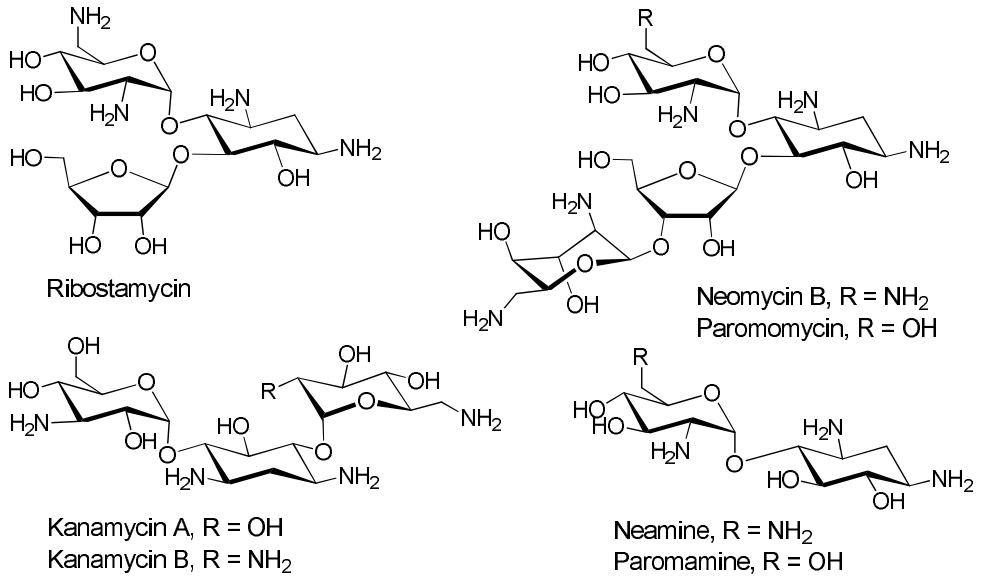

Figure 18. Structures of some aminoglycosides.

1.3.3.5 Glycoconjugates

Both carbohydrate-protein and carbohydrate-carbohydrate interactions play a central role in cellular recognition.[114-116] This is allowed by the wide structural diversity of carbohydrates and can be utilized in targeted delivery of nucleic acid drugs decorated with sugars. Lectins are carbohydrate binding proteins that exist in most living organisms and interact with sugars in a highly specific manner. Extracellular lectins recognize carbohydrate epitopes of other cells and pathogens whereas intracellular lectins take part in processing of glycoconjugates and quality control.[116] The broad range of different kind of lectins can be grouped in families characterized by similar sequences and structural organization.[117]

According to the basic idea of glycotargeting, cell-membrane anchored lectin can recognize the carbohydrate residue of an oligonucleotide drug and induce the internalization by receptor-mediated endocytosis.[118] Since the binding of a single monosaccharide to a lectin is usually rather weak (affinities in millimolar range),

high-affinity binding requires multiple simultaneous interactions with sugars.[117,119] This phenomenon is known as a "cluster glycoside effect", *i.e.* the presence of multivalent ligands is able to enhance binding beyond what could be expected due to the increase in local sugar concentration alone. In nature, the multivalency is often employed to ensure high specificity and thus, to ensure the correct functioning of cells. Consequently, an efficient glycotargeting strategy depends on the development of multivalent glycoconjugates having proper spatial arrangements.[118,120] Along with this, it has been recognized that the length of the spacer, separating the carbohydrate moieties and nucleic acid, needs to be sufficient for optimal binding affinity to lectins. Many synthetic approaches for covalently bound oligonucleotide conjugates have already been reported but only a few have been tested for their biological activity.

Most extensively investigated target for oligonucleotide glycoconjugates is the galactose-specific asialoglycoprotein receptor, which belongs to the so-called C-type lectin family and is located on hepatocytes (cells of the main liver tissue).[117,118] Trivalent *N*-acetylgalactosamine residue (Figure 19a) has been conjugated to methylphosphonate and phosphorotioate oligonucleotides showing enhanced cellular uptake to the animal (mice) liver *in vivo* experiments.[121,122] Similarly, tetravalent galactoside cluster (Figure 19b) markedly improved the hepatic uptake (from 19 % to 77 % of the injected dose in rats) after derivatization and specific accumulation of the antisense oligonucleotide into parenchymal liver cells was reported to increase almost 60-fold.[123]

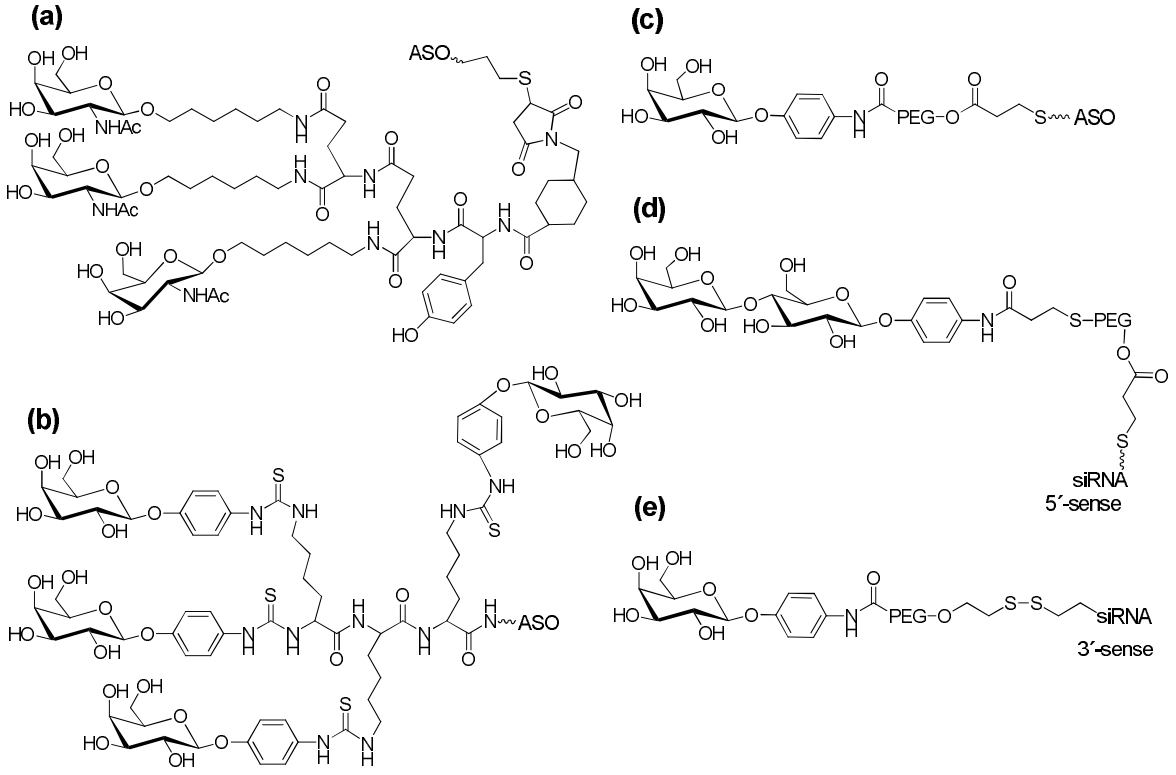

Figure 19. Glycoconjugates for asialoglycoprotein receptor-mediated delivery: (a) trivalent *N*-acetylgalactosamine residue, (b) tetravalent galactoside cluster, (c) galactosylated PEG-ASO conjugate, (d) lactosylated PEG-siRNA conjugate, (e) galactosylated PEG-siRNA conjugate.

The asialoglycoprotein receptor has also been targeted with galactosylated PEG-conjugate attached to the 3´-end of an oligonucleotide phosphorothioate (Figure 19c).[124] Enhanced delivery to hepatocytes was reported *in vivo* via receptor-mediated endocytosis, although this conjugate carried only one sugar residue. In another study, the 5´-end of the sense strand in siRNA was conjugated with lactosylated PEG moiety (Figure 19d) and complexed with poly(L-lysine) to form PEC micelles.[125,126] These micelles, entrapping targeting siRNA for RecQL1 helicase (ReQ helicase family is involved in maintaining genomic stability), showed significant and prolonged growth inhibition of the spheroids formed from human hepatocarcinoma cells.[126] Both sugar-PEG residues (Figure 19c,d) were attached to the oligonucleotides using a *β*-thiopropionate linker, which is expected to be cleaved in the acidic environment of the endosomal compartment. siRNA has also been conjugated through the 3´-end of the sense strand with galactose- or (mannose-6-phosphate)-PEG ligand via a cleavable disulfide bond (Figure 19e).[127] The conjugates were used for targeted delivery to hepatocytes and hepatic stellate cells, respectively, and they resulted in gene silencing *in vitro*.

The structure-function relationship of the glycoside clusters has been evaluated by measuring their affinities towards carbohydrate-binding proteins.[128-130] For example, the affinities of galactose clusters with linear, calixarene or antenna type structures towards the lectins PA-IL (*Pseudomonas aeruginosa* lectin) and RCA 120 (*Ricinus communis* agglutinin) were assessed by using microarray techniques.[130] It was concluded that the spatial arrangement was more important than the number of galactose moieties: a linear trivalent residue showed better binding affinities than antenna and calixarene presentations with ten, four or eight galactose moieties, respectively (Figure 20). This behavior was more pronounced with PA-IL-lectin than with less selective RCA 120.

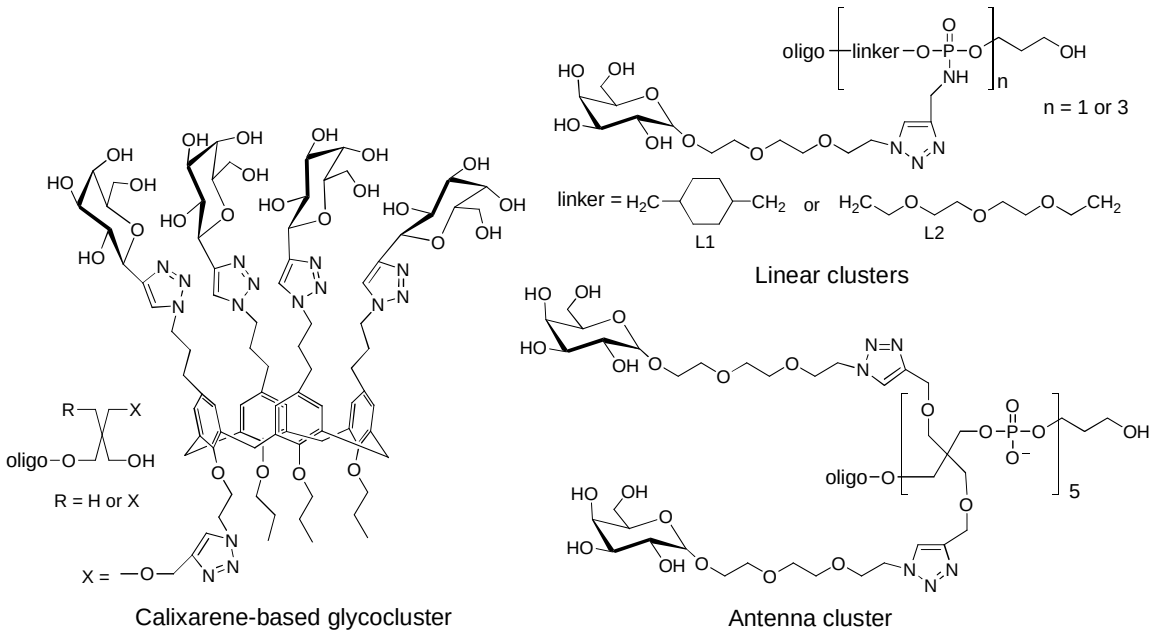

Figure 20. Presentations of different galactose glycoclusters.

Facilitation of cellular surface absorption and uptake through GLUT receptor-mediated endocytosis has been studied with 5´-terminal glucose-DNA conjugates (most potent ones are shown in Figure 21).[131] Glucose is an essential substrate for cell metabolism and glucose transporter proteins are found in most mammalian cell membranes. Conjugates having longer spacers (15-18 atom distances) for the glucose moiety were reported to be internalized better than those having a short linker (4 atom distance). However, the high multivalency seemed to hinder the cellular uptake as the conjugates with a tetravalent glucose presentation did not show improved delivery.

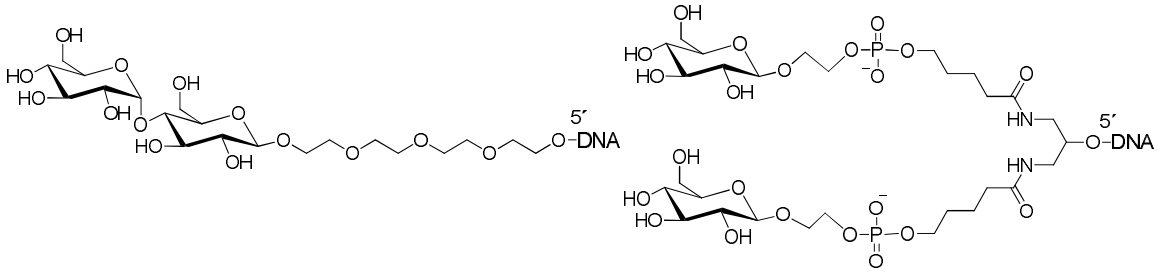

Figure 21. Glucose-DNA conjugates.

1.4 Oligonucleotide conjugation chemistry

1.4.1 Automated oligonucleotide chain assembly

The chemical synthesis of DNA/RNA oligomers is usually carried out on a solid support using an automated synthesizer (Figure 22).[132] According to the basic principle, the 3´-hydroxy group of the 3´-terminal nucleoside residue is covalently attached to a solid support via a cleavable linker, *i.e.* most often via a succinyl linker to amino-modified CPG (Controlled Pore Glass) support. This is followed by a stepwise addition of nucleotide residues to the 5'-terminus of the growing chain by appropriate coupling chemistry. Phosphoramidite coupling promoted by a tetrazole-based activator is the most commonly applied strategy. *H*-Phosphonate chemistry, using e.g. pivaloyl chloride as an activator, is another useful method for oligonucleotide synthesis. In both approaches, the cycle starts with the removal of the acid-labile 5´-*O*-(4,4´-dimethoxytrityl) protecting group from the support-bound nucleoside. The exposed 5´-hydroxy function is then coupled with the incoming monomeric nucleotide bearing a 3´-(2-cyanoethyl-*N*,*N*-diisopropylphosphoramidite) or 3´-(*H*-phophonate) group. The principal difference between the two coupling protocols is that in phosphoramidite strategy, the oxidation step to produce phosphate from the initially formed phosphite is repeated in every cycle, whereas the *H*-phosphonates are oxidized in a single step after completion of the chain assembly. Capping step is required to terminate chain elongation in the case of failed coupling and, thus, to prevent the formation of oligomers with an internal base deletion. The nucleobase moieties are usually protected with base-labile acyl groups that are stable during oligonucleotide synthesis, but are removed during the final ammonolytic treatment. Along with the base protections, also phosphate moieties (in the case of phosphoramidite) become deprotected and the chain is cleaved from the support by ammonolysis.

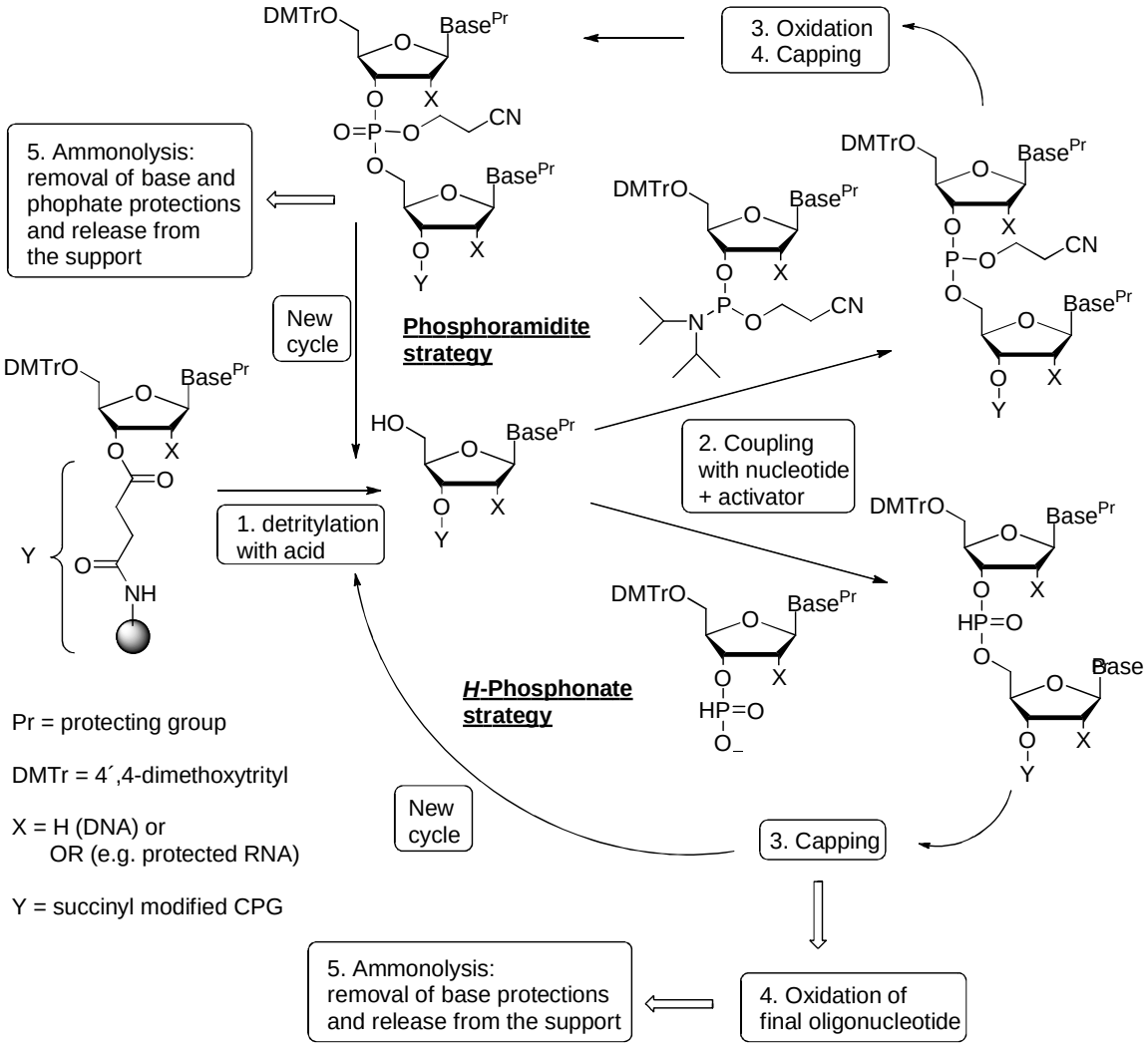

Figure 22. The principle of solid-supported oligonucleotide synthesis by the phosphoramidite and the *H*-phosphonate strategy.

In addition to natural nucleosidic building blocks, it is likewise possible to insert modified monomers into the chain by phosphoramidite or *H*-phosphonate coupling. These include nucleosidic derivatives having modified sugar, base or phosphate moieties as well as non-nucleosidic analogues and many illustrative examples are presented in section 1.3.

1.4.2 Conjugation strategies

Oligonucleotides can be conjugated either at the termini or inside the sequence.[132-134] Since the oligonucleotide is usually assembled in the 3´ → 5´ direction, the conjugation to the 5´-end is quite straightforward on using a phosphoramidite or *H*-phosphonate derived from the conjugate group. However, other type of functionalities can be attached as well via the 5´-hydroxy group. Conjugation to 3´-end is accomplished using modified supports. Another possibility is to assemble the oligonucleotide chain in an inverse manner from the 5´-end to the 3´-end, in which case the 5´-hydroxy group is bound to the support. For intrachain conjugations, the

building block needs to have an exposable hydroxyl group for chain elongation in addition to the phosphoramidite or *H*-phosphonate functionality.

In general, the conjugate groups can be attached to the oligonucleotide either directly using pre-fabricated building blocks or through a reactive moiety that is kept protected during the chain assembly and after exposure subjected to post-synthetic conjugation (Figure 23).[134] There are multiple reasons that make the post-synthetic approach practical and universal. First of all, the preparation of ready-made building blocks with all required functional moieties at one molecule can be a complex task and each compound must be separately phosphitylated. The stepwise character of the post-synthetic method simplifies the synthetic routes and enhances flexibility. Less variable chemical conditions that may complicate protecting group strategies during the oligonucleotide synthesis are needed. Finally, the conjugate groups tend to be rather bulky and their presence at the coupling step can hamper the coupling.

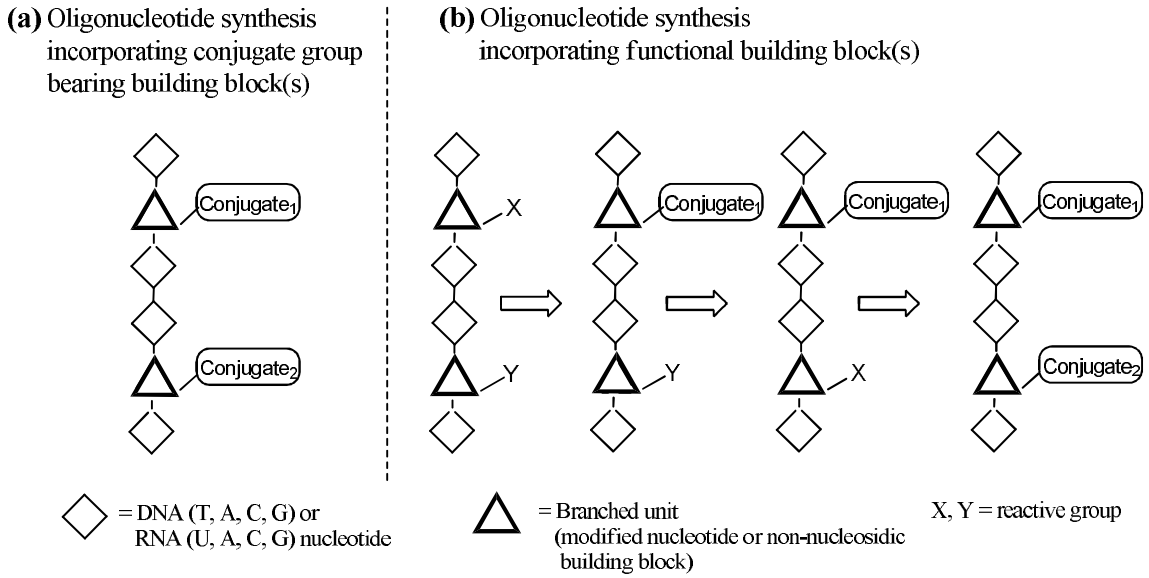

Figure 23. Schematic representation of conjugation strategies applied to attach two different ligands at intrachain positions: (a) ready-made building blocks are used and after chain assembly, the oligonucleotide conjugate is ready without further derivatization or (b) building blocks bear functional groups that are post-synthetically conjugated. In the example illustrated here, the same conjugation chemistry is applied for both conjugate groups and therefore reactive group Y is converted to X prior the second functionalization.

The post-synthetic introduction of the conjugate groups into oligonucleotides falls in two main categories: solution- and solid-phase conjugation.[79,132] The major advantage of solid-phase methods compared to the conjugation in solution is easier purification. The insoluble carrier enables the removal of reagents and unbound side products by simple filtration and washing. Consequently, reagents can be used in a large excess, which helps to drive the reactions to completion. Conjugations made in solution usually require chromatographic purifications before and after each conjugation step, whereas the solid-supported oligomer product is purified only after its release from the carrier. However, most of the conjugations have been

made in solution and the solution-phase approach can really be a method of choice in many instances.[133] For example, if the conjugate group is not stable during ammonolytic treatment or is otherwise incompatible with the applied strategy, it can be introduced to the oligonucleotide in a final solution-made step.

1.4.3 Covalent linkages for conjugate groups

Different kinds of reactive functionalities have been introduced into oligonucleotides enabling a wide variety of chemistry. In principle, many of these post-synthetic conjugation methods can be applied both on a solid support and in solution. A brief overview is given to some of the most commonly used approaches and covalent linkages (Figure 24).[134]

A) Amide:

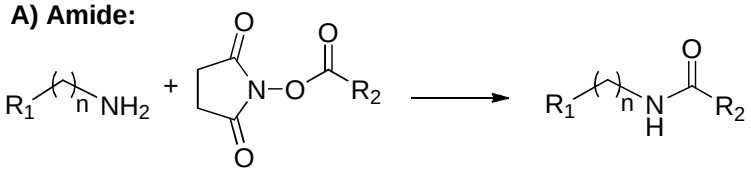

B) Thiourea:

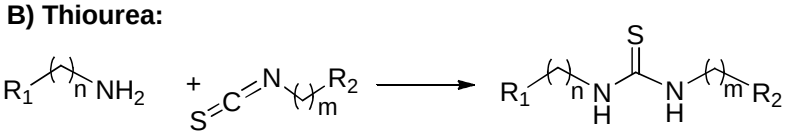

C) Reductive amination:

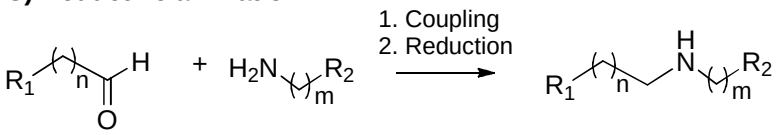

D) Hydrazone:

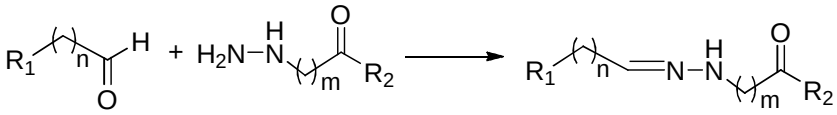

E) Oxime:

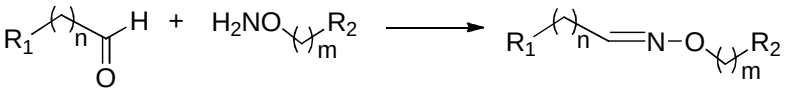

F) Glyoxylic-oxime:

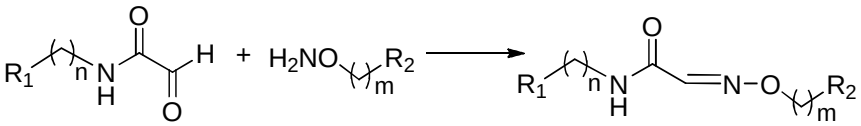

G) Disulfide:

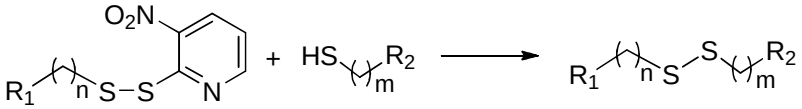

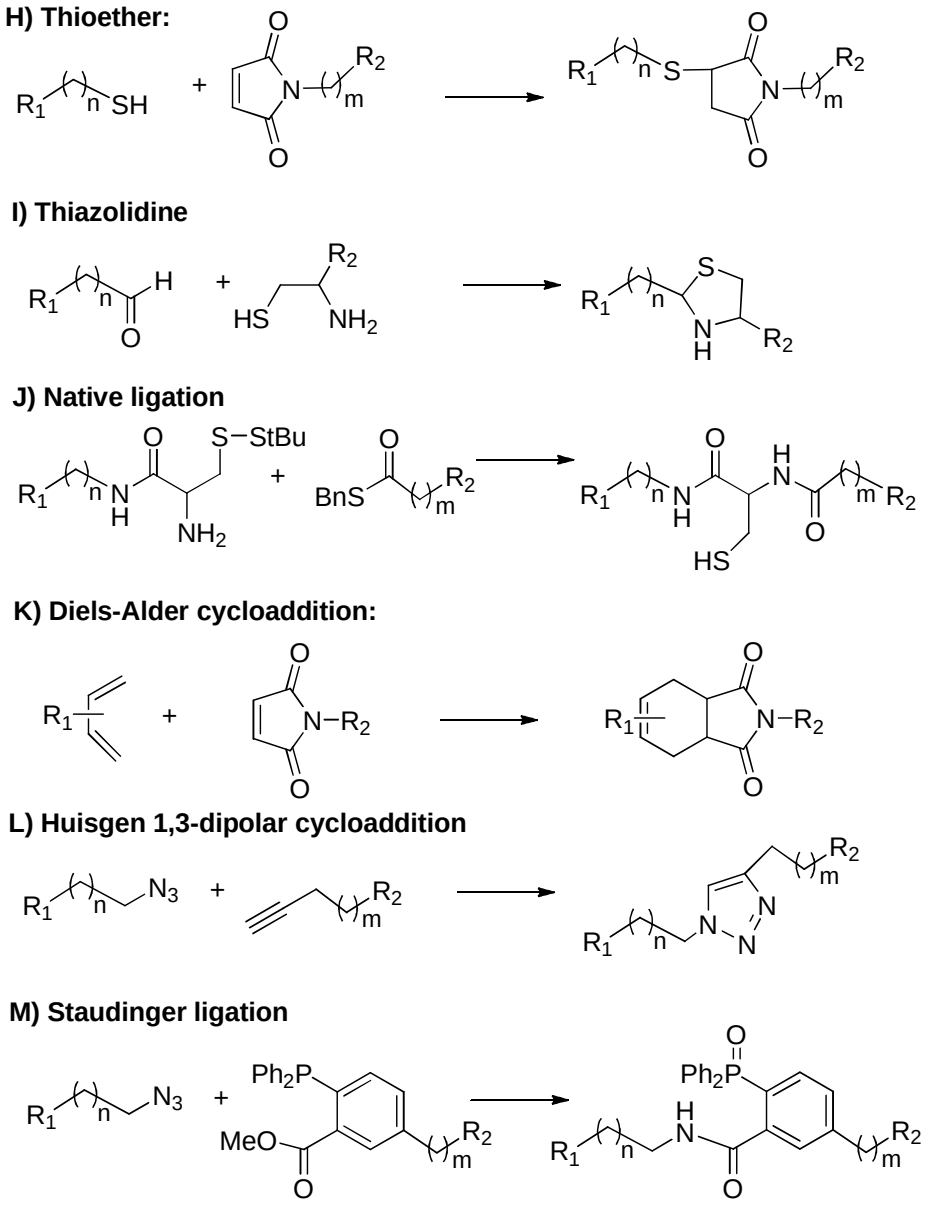

Figure 24. Commonly used conjugation chemistries and covalent linkages.[134] Residues R_1 and R_2 refer to either oligonucleotide or conjugate group side.

Amino groups have been used to form amide (A) or thiourea (B) bonds by a reaction with an activated carboxylic and isothiocyanate groups, respectively. Aldehyde function can be derivatized with an amino, hydrazine and aminooxy groups to produce imine, hydrazine (D) and oxime (E, F) linkages, among which the imine is further reduced to amine bond (C).

The reaction of thiol group with an active thiol (G), maleimide (H) or 1,2-aminothiol (I) group has also been exploited in oligonucleotide conjugations. Especially, the disulfide bond has been used in antisense approaches, because it is unstable in the cytosol due to the reducing environment of intracellular compartments and it, hence, enables the release of oligomer after cellular uptake. An acid-labile *β*-thiopropionate linkage, which is a *β*-substituted thioether, has also been used to liberate a free nucleic acid to cytoplasm as the bond is expected to be

hydrolyzed under acidic conditions present at endosome compartments.[124-126] A biodegradable bond between oligonucleotide and ligand group can be particularly advantageous in the case of very large conjugates such as those creating PEC-nanoparticles (Section 1.3.3.3). Among the sulfur containing linkages, also the thiazolidine is prone to hydrolysis at acidic pH.[134] Finally, the so-called native ligation (J) is another sulfur-based method, which involves the coupling reaction between an activated thioester and an α-aminothiol.

Recently the "click chemistry" has received a vast interest in oligonucleotide conjugations. The concept of click chemistry refers to modular reactions that show high efficiency, yield and stereospecificity.[135] The examples include Diels-Alder (K), Huisgen dipolar cycloadditions (L) and Staudinger ligations (M). The Huisgen 1,3-dipolar cycloaddition reaction has particularly found wide scope in synthetic applications and will be discussed in more detail in the Result and Discussion part.

1.5 Antisense targeting of RNA secondary structures

RNA folds through base pairing interactions into secondary structures composed of duplexes and intramolecular stem-loop regions (hairpin).[33,136-138] These secondary structures (Figure 25) are induced by mismatched and unpaired bases, which cause a perturbation of the fully complementary A-form RNA·RNA helix. In hierarchical pathway, the primary sequence dictates the type of secondary structure formed, which in turn leads to formation of possible tertiary structure. In cell biology, the folding process provides stability for RNA and structural motifs, which are recognized by a number of ligands including proteins, nucleic acids and ribonucleoproteins that participate in the intermediary metabolism and activities of RNA species.

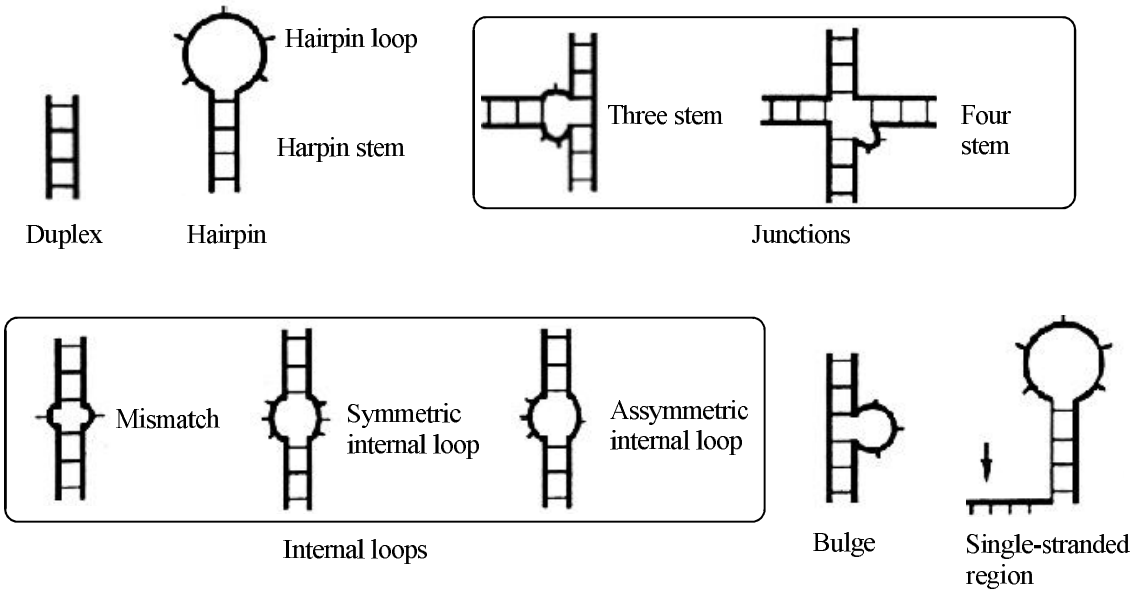

Figure 25. The general classes of RNA secondary structure.[137]

Since the RNA duplex is not a viable target for antisense binding, an effective antisense oligonucleotide design depends on identification of local single-stranded

RNA segments within mRNA accessible for hybridization.[9,33] These sites locate usually at the terminal end, internal loops, joint sequences, hairpins and bulges. Similarly efficient siRNA silencing is influenced by local characteristics of the target RNA and a correspondence between the accessibility for antisense oligonucleotides and siRNAs has been demonstrated.[19,139] Ultimately, it is a question about how well an exterior antisense molecule can invade to the target RNA region and reorganize the secondary structure. The formation of a ligand-RNA complex can be described by equilibrium:

$$RNA + ligand \rightleftharpoons RNA\text{-}ligand\ (complex)$$

Here, the RNA-ligand (complex) refers to all conformations that may result from the binding. The corresponding dissociation constant K_d describes quantitatively the affinity between a ligand and a target RNA and is defined:[140]

$$K_d = \frac{[RNA][ligand]}{[RNA\text{-}ligand]}$$

However, the development of any truly reliable algorithm for computational prediction of a single secondary structure of RNA is problematic due to RNA´s adaptive behavior.[9,136] It is likely that RNA conformation alters significantly as it bounds to various ligands and thus accessibility to a particular RNA site can be changed. There are several experimental methods which are employed for evaluation of ligand-RNA binding, at least as long as small molecule ligands are concerned.[23] These include approaches such as mass-spectrometry-assisted screening, fluorescence spectroscopy using fluorescently labeled RNAs or ligands and gel shift assay, which fractionalizes molecules on the basis of different mobilities through the gel medium. Also UV-denaturation profiles (Section 3.1.4) or CD spectra can be used to assess hybridization affinities of oligonucleotides. Finally, NMR-spectroscopy has been established as a reliable method for structural determinations.[141,142] From the methods listed above, NMR is an exceptional technique to follow invasion process of the antisense oligonucleotide ligand to the folded RNA as it allows detection and quantification of dynamic equilibria between coexisting nucleic acid structures. Especially ^{19}F-NMR employing ^{19}F-labeled oligonucleotides[143-148] has many advantages for such analysis and will be introduced and explored more detailed in Results and Discussion (Section 3.2).

1.5.1 Case study – Antisense approaches targeting HIV TAR

Human immunodeficiency virus (HIV) possesses a remarkable ability to adapt and evade both host immune responses and suppression by antiviral drugs, because of its rapid genetic diversity and the capability to undergo mutations.[149] Thus, despite of the current drugs, the need for new HIV therapies that are less prone to the generation of resistant viral strains persist. For the purpose, several antisense-based approaches have been studied.

One attractive antisense target is the highly conserved *trans*-activating response element TAR (Figure 26), which is a specific bulged RNA hairpin loop located at the 5´-end of all HIV mRNAs.[150] TAR region is recognized by the HIV *trans*-activator protein TAT, which binding to the TAR-element is essential for efficient viral transcription and replication. Thus, inhibition of the TAT-TAR interaction by targeting the TAR-element has been explored as a potential anti-HIV strategy.

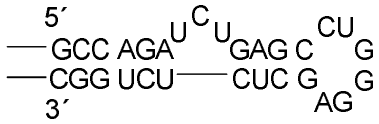

Figure 26. Secondary structure of HIV-1 TAR-element.

A steric block mechanism has been evaluated with modified antisense oligonucleotides incorporating 2´-*O*-methyl, N3´-P5´-phosphoramidate and PNA analogues and also with chimeric oligomers containing 2´-*O*-Me/LNA units.[51,151,152] Targeting the stem-loop region, these 16 or 12 long oligomers were reported *in vitro* to efficiently and sequence-specifically inhibit the reverse transcription (the process by which the RNA-virus can reverse-transcribe their RNA genomes into DNA, which is then integrated into the host genome and replicated along with it). Compared to the solely 2´-*O*-methyl modified oligomers, the addition of LNA units (optimally 40-50 %) was shown to enhance cellular uptake using cationic agents as well as nuclear uptake and increase binding to the target RNA.[51] Shorter than 12 mer OMe/LNA oligonucleotides were inactive.

The cell delivery issues of anti-TAR oligomers have been addressed with cell-penetrating peptides including Transportan, Penetratin, R_6-Penetratin and TAT-peptide.[153-155] Promising results in cell internalization and inhibition of HIV-1 replication were reported with 16mer disulfide-linked PNA-CPP conjugates (Figure 27).[154] Cellular uptake of the PNA-Penetratin conjugate was most efficient, while inhibition ability was highest for PNA-Transportan-27. In addition to antiviral activity, the conjugates with Penetratin, Transportan-21 (more than Transportan-27) and TAT-peptide were importantly shown to act as an anti-HIV virucidal-agents capable of inactivating or destroying viruses, which could essentially have ability to block HIV infections.

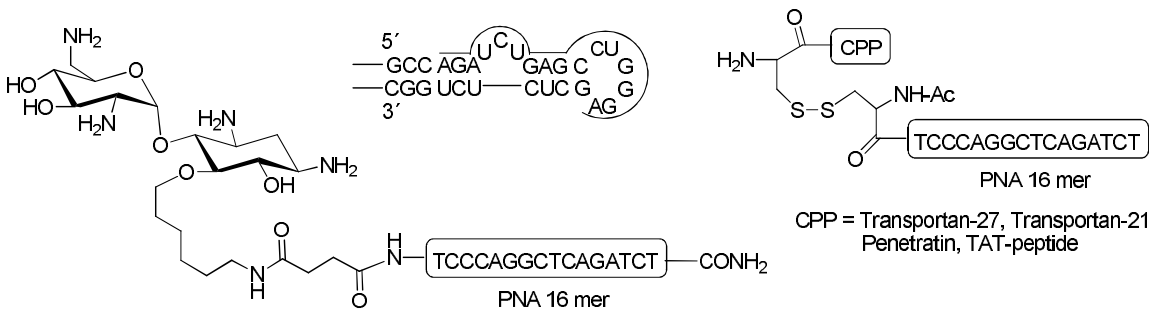

Figure 27. PNA binding site on TAR and the structure of CPP-PNA conjugates.

The cellular uptake of anti-TAR PNA has also been improved by conjugation with neamine (Figure 27) which is a constituent of aminoglycoside antibiotics such as neomycin B (see Section 1.3.3.4) and enhances the solubility of PNA.[110] In addition to the inhibition of HIV-1 replication *in vitro*, neamine-PNA conjugate was shown to exhibit RNA cleavage activity for its target site in TAR.

Targeting of the TAR regions with RNAi-based mechanism has met a mixed success.[150] While some inhibition of HIV replication was observed using 21-mer siRNA duplex in cell culture,[156] it has been suggested that the siRNA activities are affected by too tight secondary structure of TAR.[157] Recently, it was reported that RNAi directed against TAR can inhibit HIV replication, but resistant viral strains were recovered in long term cell cultures.[149] However, none of the altered strains carried a mutation at the target site consistent with a view of TAR as a conserved sequence. Instead, evidence was given that several strains had promoter mutations that indirectly compensated for the RNAi by upregulating viral transcription. Consequently, combinatorial RNAi against various RNA targets of the HIV has been suggested.[158] Modified siRNA containing conformationally locked 2´,4´-carbocyclic *ribo*-thymidine (jcLNA) monomers at both ends of the antisense strand (Figure 28) was reported to have enhance siRNA efficiency in addition to increased serum stability.[159] These properties exceeded those of the LNA counterpart.

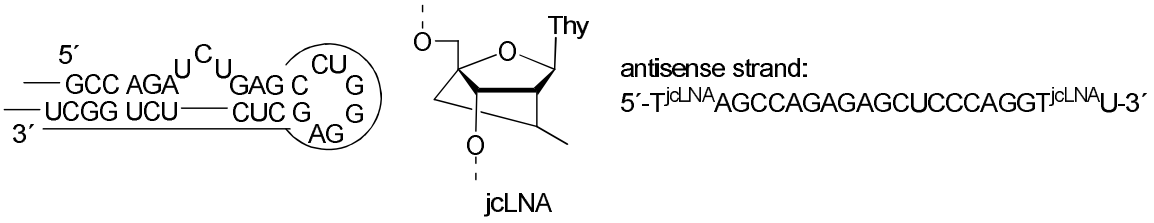

Figure 28. Structure of jcLNA modification and the targeted region within TAR.

2. AIMS OF THE THESIS

Antisense technology holds a tremendous potential for drug discovery based on selective gene-silencing. However, nucleic acids are not optimal drug-like molecules and both single-stranded antisense oligonucleotides and double-stranded siRNAs encounter many biological barriers before they can reach the target RNA in the cell cytoplasm or nucleus. To overcome these barriers, oligonucleotides are chemically modified and conjugated in various ways. The aim of the present thesis is to provide an efficient conjugation strategy for oligonucleotides based on click chemistry. The concept of generality is on high importance for synthesis strategy since the applicable conjugations comprise a vast repertoire of chemically different residues. This criterion is well met with the orthogonal-nature of click reaction referring to the Cu(I)-catalyzed Huisgen 1,3-dipolar cycloaddition between azide and alkyne.

As particularly poor cell delivery limits the development of antisense therapeutics, oligonucleotide conjugations that allow efficient cellular uptake and provide cell-type organ specificity are desired. One such approach is to decorate oligonucleotides with carbohydrates playing role in cell recognition. The sense strand of siRNA can serve as a scaffold to which the lecting binding sugar ligands are tethered at appropriate distances. For this purpose, the present study demonstrates the preparation of several oligonucleotides having glycoconjugates at their intrachain positions. A prerequisite for this approach is that the siRNA duplex formation is not severely retarded.

Finally, the thesis approaches a fundamental RNA invasion process by which the antisense oligonucleotide is able to bind its target and reorganize the secondary structure of the folded mRNA. As the strand invasion process itself is well known, the means through which to follow its progress in detail are rather limited. ^{19}F-NMR spectroscopy offers a novel tool to study RNA conformations and the methodology for monitoring of invasion of short oligonucleotides to the RNA secondary structure model is described.

In more detail the aims of the thesis may be summarized as follows:

- Preparation of the branched building blocks applicable for the click conjugation strategy and for the attachment of residues at intrachain positions.
- Assembly of the modified oligonucleotides and their post-synthetic click-conjugation on a solid support or in solution with different kind of ligands including carbohydrates.
- Assessment of the hybridization properties concerning the conjugates and thus, evaluation of their feasibility for antisense use.
- Characterization of RNA invasion by ^{19}F-NMR spectroscopy.

3. RESULTS AND DISCUSSION

3.1 Click conjugation of oligonucleotides

3.1.1 Nucleosidic building blocks for click conjugations

The concept of click chemistry was evolved to provide simple methods to join together organic molecules in high yields under mild conditions and in the presence of a diverse range of functional groups.[135,160] Sharpless and co-workers have identified a number of reactions that meet the criteria for click chemistry, but especially the Cu(I)-catalyzed Huisgen 1,3-dipolar cycloaddition between azide and alkyne[161,162] has emerged as a most widely applied approach (Figure 29). This particular click reaction has many potential features for the conjugation of nucleic acids.[160,163] The presence of azides or alkynes does not usually disturb the biophysical properties of nucleic acids and they are almost entirely unreactive towards the functional groups normally encountered in nature. Thus they react only with each other forming a triazole unit, which is extremely stable and non-toxic. However, the efficiency of the reaction along with the regioselectivity to produce solely the 1,4-regioisomer (and not 1,5-regioisomer) requires the use of copper(I) catalysis, which can cause radical induced damage within the oligonucleotide chain. To overcome this problem, copper(I)-stabilizing ligands such as TBTA (tris[(1-benzyl-1,2,3-triazol-4-yl)methyl]amine) can be used.[164]

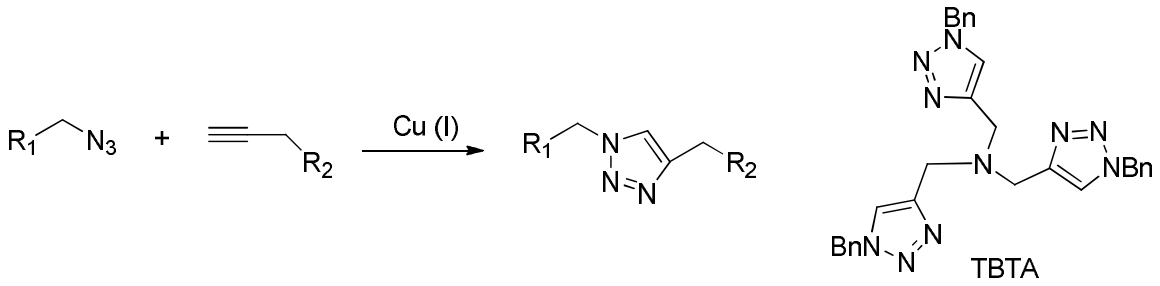

Figure 29. The Cu(I)-catalyzed Huisgen 1,3-dipolar cycloaddition to produce a 1,4-triazole and the structure of copper(I)-stabilizing TBTA-ligand.

To apply a post-synthetic click conjugation strategy on oligonucleotides, four different 4´- and 2´-modified building blocks **1**-**4** bearing azido or alkynyl moiety are introduced by the present study (Figure 30).[I-III] These monomers can be incorporated into oligonucleotide chain using either phosphoramidite or *H*-phosphonate coupling chemistry on an automated DNA/RNA synthesizer (Section 1.4.1). Together these modified nucleotides, *i.e.* 4´-*C*-azidomethylthymidine 3´-(*H*-phosphonate) (**1**), 4´-*C*-[*N*,*N*-di(4-pentyn-1-yl)aminomethyl]thymidine 3´-phosphoramidite (**2**), 4´-*C*-[*N*-methyl-*N*-(4-pentyn-1-yl)aminomethyl]thymidine 3´-phosphoramidite (**3**) and 2´-*O*-[(2-azidoethoxy)methyl]cytidine 3´-(*H*-phosphonate) (**4**) enable the exploitation of the click conjugation on both ways, in other words to have azido function present either on the oligonucleotide or ligand side. Nucleoside **2** bearing two 4-pentyn-1-yl groups is designed for high density functionalization of modified oligonucleotides whereas nucleosides **1**, **3** and **4** allow one-armed conjugations.

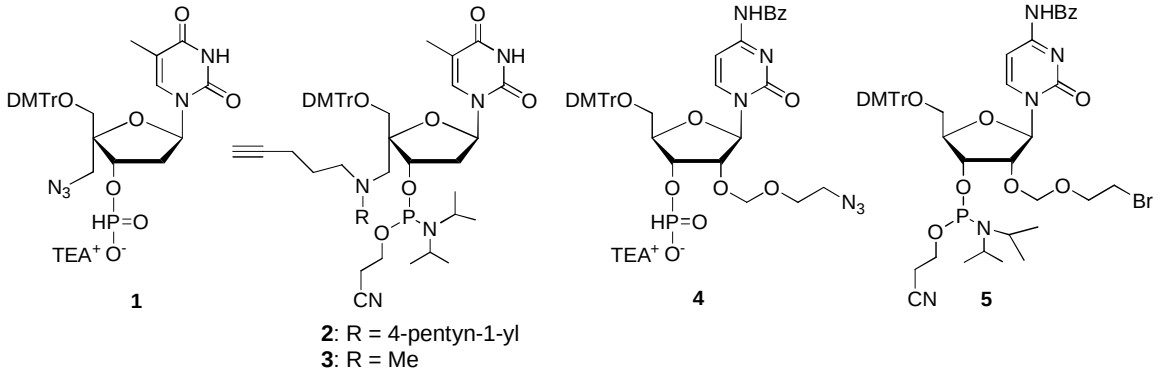

Figure 30. Monomers for oligonucleotide click-conjugation.

Previous studies have shown that ribose 2´- and 4´-positions facing the minor groove upon hybridization are potential for modifications.[39,49,165-173] Oligonucleotides incorporating 2´- or 4´-modified nucleosides have been reported to form rather stable double helices with unmodified complementary sequences and they are less prone to enzymatic degradation than their unmodified counterparts. In addition, 4´-modified nucleosides have shown compatibility with RNase H activity.[169,174] In contrast, 2´-modified nucleosides, which adopt A-type helical geometry do not support RNase H mechanism (Section 1.3.2.1).[39]

Monomers **1** and **4** were incorporated into the oligonucleotide by the *H*-phosphonate chemistry since intramolecular Staudinger reaction between the azido and phosphoramidite group makes the phosphoramidite building block highly unstable. We attempted the oligonucleotide synthesis using 4´-*C*-azidomethylthymidine 3´-phosphoramidite but although the building block could still be isolated with fast work-up, it was not stable enough for chain assembly. Sekine et al. has previously reported that the reaction of 2-azido-2´-deoxyadenosine (**6**) with diethyl-*N*,*N*-diisopropylphosphoramidite gave phosphazide intermediate (**7**) of the Staudinger reaction, which was then converted into final iminophosphorane product **8** (Scheme 1).[175] Nevertheless, as shown by the present study,[I] the presence of an azido group in the growing solid-supported oligonucleotide chain does not disturb the phosphoramidite coupling of subsequent monomers and, hence, the Staudinger reaction seems to interfere with only by a genuinely intramolecular mechanism.

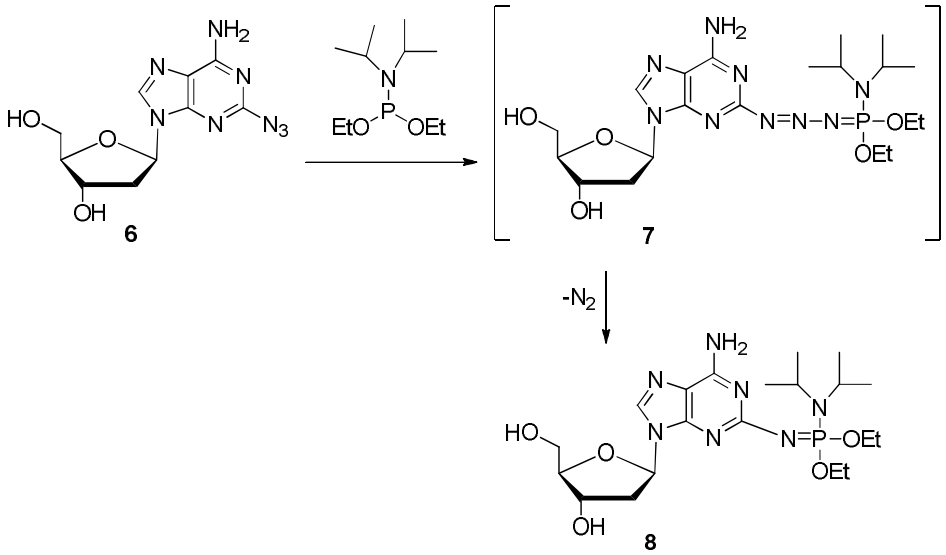

Scheme 1. Staudinger reaction between azido group and phosphoramidite derivative.[175]

Phosphoramidite approach is the most applied method for oligonucleotide synthesis on solid support but *H*-phosphonate methodology is also a viable alternative.[176] On the basis of this work, however, it seemed that structural changes to the standard nucleosides were less tolerated by the *H*-phosphonate protocol which resulted in decreased coupling yields with monomers **1** and **4** (Section 3.1.3.1) while coupling efficiency was well retained on using phosphoramidite monomers **2**, **3** and **5**.[I-III] Although protocol adjustments may partly restore the coupling efficiency, it was concluded that the phosphoramidite approach is preferred when available.

Besides having azido group present at a building block itself, it can be introduced post-synthetically to the oligonucleotide. For this purpose, 2´-*O*-[(2-bromoethoxy)methyl]cytidine 3´-phosphoramidite (**5**) monomer was synthesized and used as a precursor for the corresponding azido derivative. The feasibility of the displacement reaction from bromo to azido group on a solid support has been established in recent studies[177,178] and the method avoids the usage of nucleoside *H*-phosphonate. Importantly, when bromo and azido group bearing monomers are both used in the oligonucleotide synthesis, they allow an attachment of two different ligands to the oligomer. This type of conjugation strategy is outlined in Section 1.4.2 (Figure 23) and demonstrated with 2´-modified monomers **4** and **5**.[III]

3.1.1.1 Synthesis of 4´-*C*-azido and alkynyl modified thymidine monomers

Previously, a synthesis route for 4´-*C*-hydroxymethylthymidine has been developed starting from thymidine.[168,179,180] Accordingly, the 5´-hydroxyl group of 3´-protected thymidine is oxidized to aldehyde and the 4´-*C*-hydroxymethyl moiety is obtained by aldol condensation with formaldehyde followed by Cannizzaro reduction. In the present study, 3´-*O*-(4,4´-dimethoxytrityl)-4´-*C*-hydroxymethylthymidine (**11**) was synthesized in overall yield of 74% (For synthesis procedures see Experimental).[I] Prior to the introduction of the 4´-branch,

5´-OH of the thymidine (**9**) was temporarily protected by benzoyl group, which was removed after completion of 3´-*O*-(4,4´-dimethoxytrityl) protection (→**10**). Noteworthy, the employment of 3´-*O*-4,4´-dimethoxytrityl protection[168] being fully stable under alkaline conditions of aldol-cannizaro step is recommended over 3´-*O*-TBDMS protection, which has also been previously applied for the purpose.[167]

4´-*C*-Azidomethylthymidine has also been previously synthesized,[181] but only in low yield via mesylation of 4´-*C*-hydroxymethyl-3´-*O*-TBDMS-thymidine and subsequent treatment of the mixture of the mono- and di-mesylated products with LiN_3. Since this route includes tricky chromatographic separations of regioisomers, the method that exploits O^2,5´-anhydronucleoside formation[182] in making a difference between the two primary hydroxyl functions seemed more feasible. Accordingly,[I] the primary hydroxyl groups of compound **11** were converted to their triflates to obtain **12**. Deprotonation of the thymine base resulted in cyclization to O^2,5´-anhydro nucleoside, from which the remaining triflate group could be displaced with an azide ion, giving the desired 4´-*C*-azidomethyl group (**13**). The O^2,5´-anhydro linkage was hydrolyzed with sodium hydroxide and the resulting nucleoside 4´-*C*-azidomethyl-3´-*O*-DMTr-thymidine (**14**) was converted to its 5´-*O*-DMTr-isomer (**15**) and finally to the corresponding 3´-(*H*-phosphonate) (**1**). Altogether, the synthesis of building block **1** is efficient and the overall yield from thymidine is 42 %.

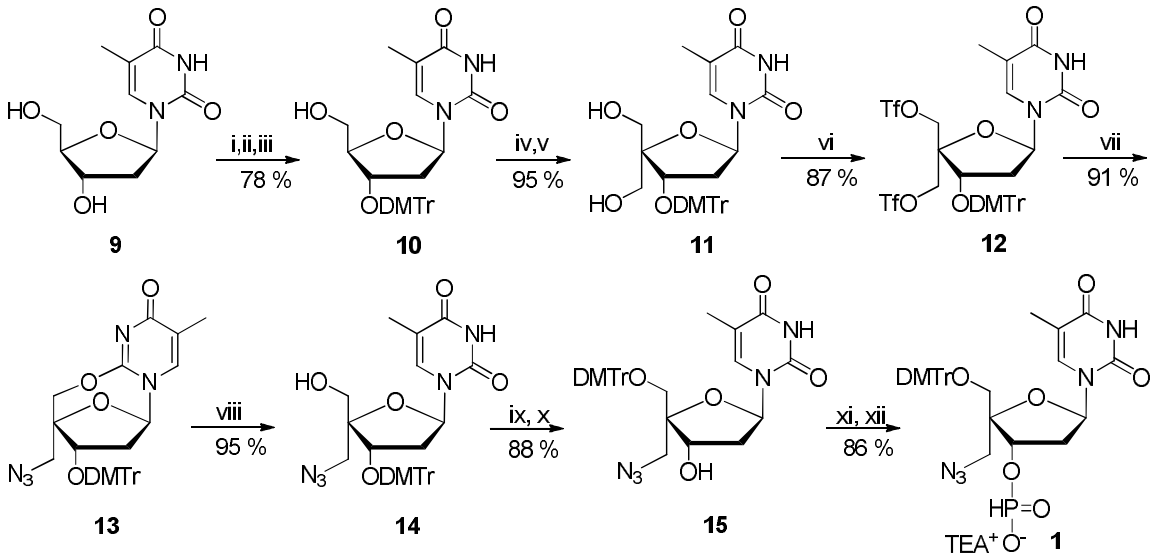

Scheme 2. Reagents: (i) BzCl, pyridine; (ii) DMTrCl, pyridine; (iii) NaOMe, MeOH; (iv) DCC, TFA, pyridine, DMSO; (v) CH_2O, aq NaOH (2.0 mol L^{-1}), 1,4-dioxane; (vi) Tf_2O, CH_2Cl_2, pyridine; (vii) NaH, NaN_3, DMF, pyridine; (viii) aq NaOH (2.0 mol L^{-1}), 1,4-dioxane; (ix) 80 % AcOH; (x) DMTrCl, pyridine; (xi) diphenyl *H*-phosphonate, pyridine; (xii) Et_3N, H_2O.

Because the azido group can be easily converted to amino group by Staudinger reaction, it allows further functionalization and a route to 4´-*C*-alkyne derivatives. Accordingly,[II] 4´-*C*-aminomethyl-3´-*O*-(4,4´-dimethoxytrityl)thymidine (**16**) was obtained by the reaction of compound **14** with triphenylphosphine and water (Scheme 3). Compound **16** was then subjected to reductive alkylation in the

presence of $NaBH_3CN$ under acidic conditions. On using 2 equiv of 4-pentynal, 4´-*C*-[*N*,*N*-di(4-pentyn-1-yl)aminomethyl]thymidine (**17**) was obtained. 4´-*C*-[*N*-Methyl-*N*-(4-pentyn-1-yl)aminomethyl]thymidine (**19**) was, in turn, prepared by two consecutive alkylation steps. Reaction with 1 equiv of 4-pentynal gave 4´-*C*-[*N*-(4-pentyn-1-yl)aminomethyl]thymidine (**18**), which was then *N*-methylated with paraformaldehyde. After the reductive alkylations, the 3´-*O*-4,4´-dimethoxytrityl group was removed with 80% acetic acid. Compounds **17** and **19** were then converted to 5´-*O*-(4,4´-dimethoxytrityl) ethers (**20**, **21**) and phosphitylated to phosphoramidites **2** and **3**.

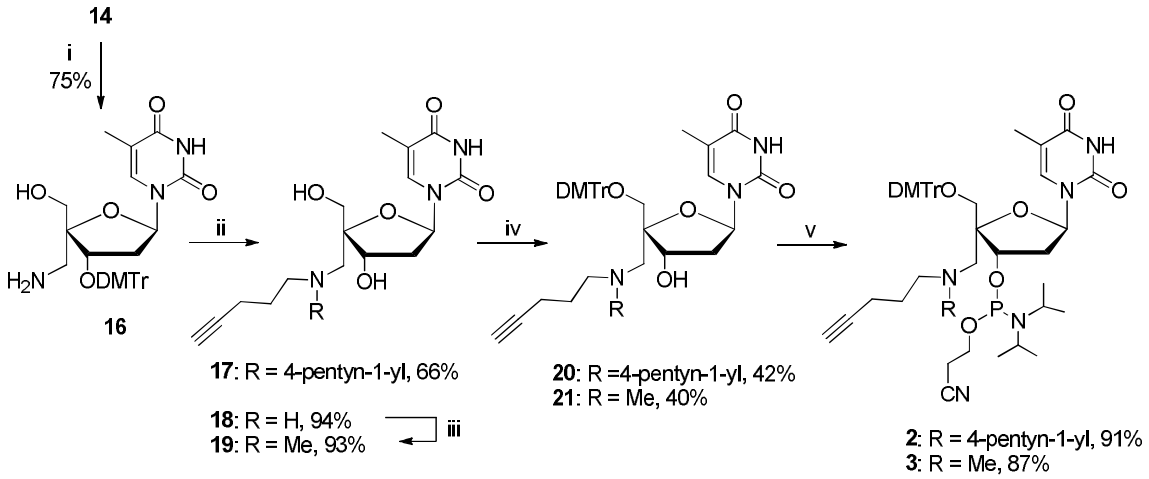

Scheme 3. Reagents: (i) PPh_3, H_2O, NH_3 (aq), THF; (ii) 4-pentynal (1 or 2 eq), $NaBH_3CN$, AcOH, MeOH; (iii) paraformaldehyde, $NaBH_3CN$, AcOH, MeOH; (iv) DMTrCl, pyridine; (v) 2-cyanoethyl *N*,*N*-diisopropylphosphoramidochloridite, Et_3N, CH_2Cl_2.

There are some general observations concerning the synthesis of 4´-*C*-derivatives that should be noted.[I] First of all, the 3´-hydroxy group must be masked before conversion of the hydroxyl function in 4´-*C*-hydroxymethyl group into a better leaving group. The carbon atom of this group is surprisingly prone to nucleophilic attack of a neighboring hydroxyl group: a four-membered ring is easily formed by an attack of either the 5´- or 3´-OH. For example, the oxetane product **23** was the only product obtained when displacement of the tosyl group from 5´-*O*-(4,4´-dimethotrityl)-4´-*C*-tosyloxymethylthymidine (**22**) with azide ion was attempted (Scheme 4, see Experimental). In addition, the efforts to prepare 4´-*C*-propargyloxymethyl or 4´-*C*-pentenyloxymethyl compounds were unsuccessful as O^2,5´-anhydro nucleosides bearing 4´-*C*-propargyloxymethyl (**24**) or 4´-*C*-pentenyloxymethyl (**25**) group resulted in oxetane product **26** when treated with NaOH solution.

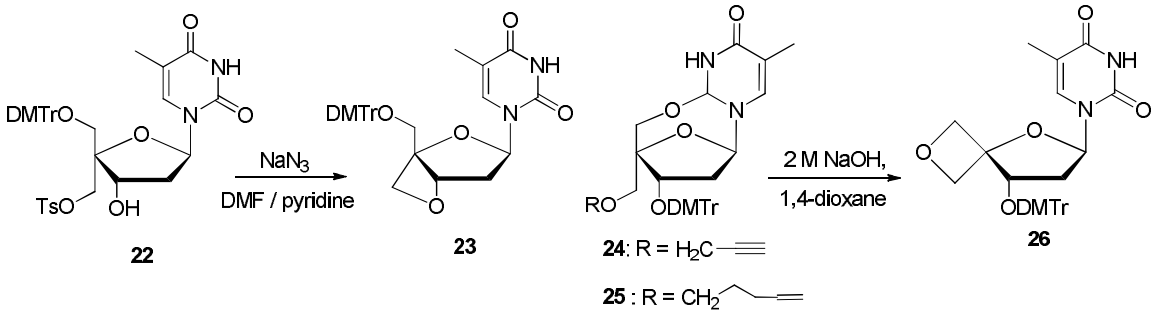

Scheme 4. Easy formation of an oxetane by-product.

3.1.1.2 Synthesis of 2´-*O*-modified cytidine monomers

The synthesis of 2´-*O*-(2-bromoethoxy)methyl (**27a**) and 2´-*O*-(2-azidoethoxy)methyl (**27b**) substituted cytidine nucleosides bearing 3´,5´-*O*-(1,1,3,3-tetraisopropyldisiloxane-1,3-diyl) protections has been described earlier.[183-186] According to an "*O*-glycosylation method", 3´,5´-*O*-(1,1,3,3-tetraisopropyldisiloxane-1,3-diyl)-N^4-benzoylcytidine was treated with (2-bromoethoxy)methyl acetate in the presence of tin tetrachloride at -12°C. Nucleoside **27a** was isolated in 88% yield and conversion to the corresponding 2´-*O*-(2-azidoethoxy)methyl derivative (**27b**) by displacement of the bromo substituent with NaN_3 in DMF was virtually quantitative. To carry on the synthesis of 2´-modified building blocks (**27a**,**b**) bearing azido or bromo functions, the 3',5'-cyclic silyl protecting group was removed with Bu_4NF in THF and the 5´-OH of the deprotected nucleosides (**28a**,**b**) was protected with a 4,4´-dimethoxytrityl to obtain **29a**,**b** (Scheme 5).[III] Finally, **29a** and **29b** were converted to 3´-(2-cyanoethyl-*N*,*N*-diisopropylphosphoramidite) (**5**) and 3´-(*H*-phosphonate) (**4**), respectively.

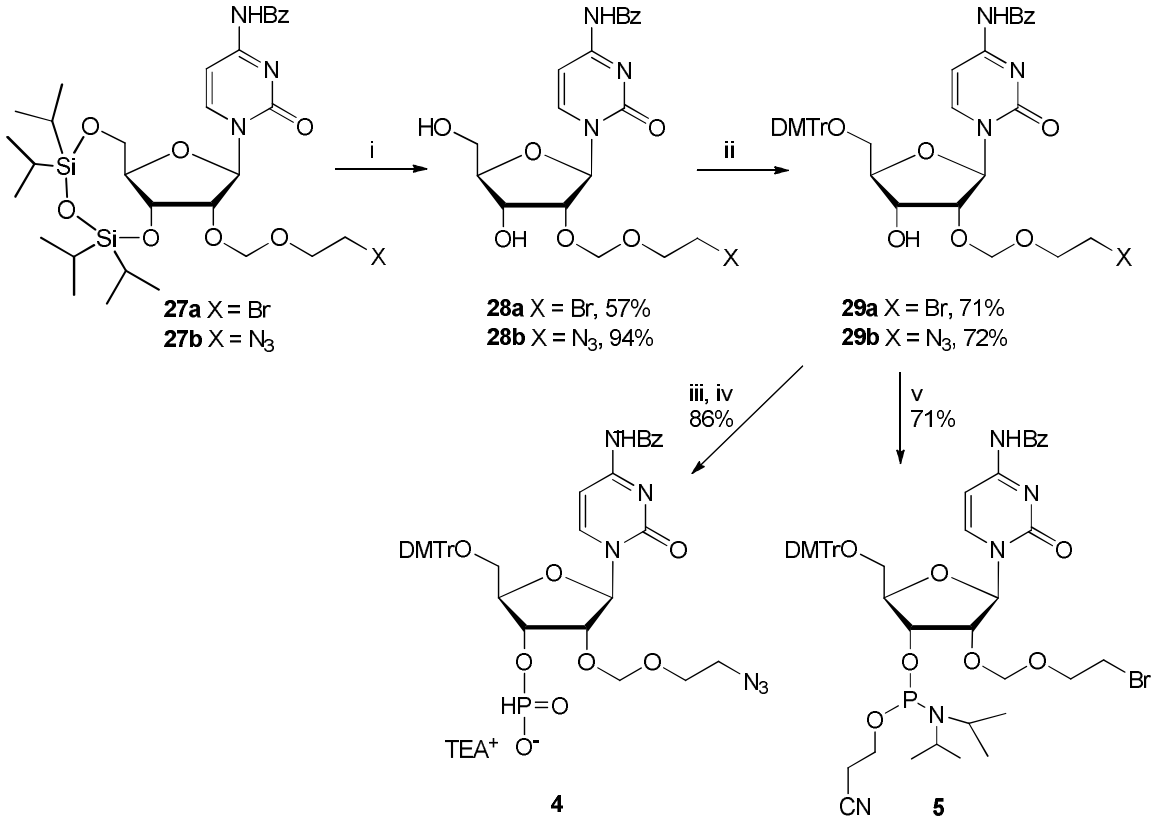

Scheme 5. Reagents: (i) Bu_4NF, THF; (ii) DMTrCl, pyridine; (iii) diphenyl *H*-phosphonate, pyridine; (iv) Et_3N, H_2O; (v) 2-cyanoethyl *N*,*N*-diisopropylphosphoramidochloridite, Et_3N, CH_2Cl_2.

3.1.2 Conjugate groups for click conjugations

For the click conjugations of the oligonucleotides, alkynyl and azido functionalized ligands were synthesized (Figure 31).[I-III] They included derivatives of mannose (**30**, **31**), galactose (**32**), *p*-aminomethylbenzene (**33**, **34**) and aminoglycosides (**35**-**37**).

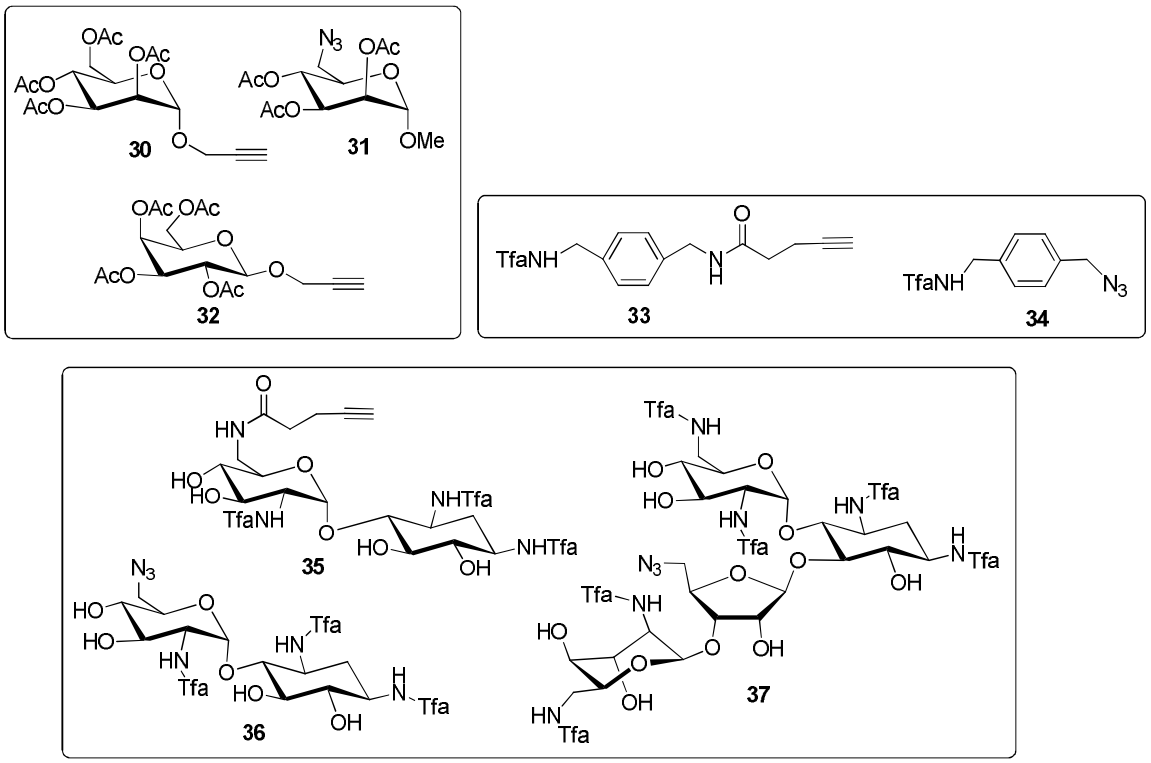

Figure 31. Prepared alkynyl and azido functionalized ligands.

3.1.2.1 Synthesis of alkynyl bearing ligands

The alkynyl-derivatized ligands (**30**, **32**, **33**, **35**) were synthesized as outlined in Scheme 6.[I,III] Fully acetylated propargyl α-D-mannopyranoside (**30**)[I] and β-D-galactopyranose (**32**)[187] were prepared from the commercially available peracetylated α-D-mannopyranose (**38**) and β-D-galactopyranose (**39**) by boron trifluoride etherate promoted glycosidation[188] with propargyl alcohol.

Trifluoroacetylated *N*-[4-(aminomethyl)benzyl]-4-pentynamide (**33**) was synthesized starting from the commercially available 1,4-phenylenedimethanamine (**40**).[I] One of the two amino groups was protected with a 4-monomethoxytrityl group and the other one was acylated with 4-pentynoic acid by DCC activation. The acid-labile trityl protection was finally changed to a base-labile trifluoroacetyl protection, removable by the conventional ammonolysis used for release and deprotection of the oligonucleotide conjugate.

Neamine tetrahydrochloride (**43**) was obtained by methanolysis of commercially available neomycin B trisulfate.[189] The primary 6´-amino group of neamine (**43**)

was selectively acylated with succinimidyl 4-pentynoate.[I] To make this neamine derivative easier to handle and purify, the amino groups were trifluoroacetylated and the hydroxyl groups acetylated, and the product was purified at this stage. Owing to exceptionally difficult acetylation of the 5-hydroxy of neamine, a mixture of compounds **44** and **45** was obtained. Product **35** was received after removal of acetyl-protecting groups with methoxide ion catalyzed transesterification in MeOH under which conditions Tfa-amides are stable. The acetyl groups were removed at this stage to prevent O→N-acyl migration when the amino groups are exposed during the final deprotection of an oligonucleotide conjugate.

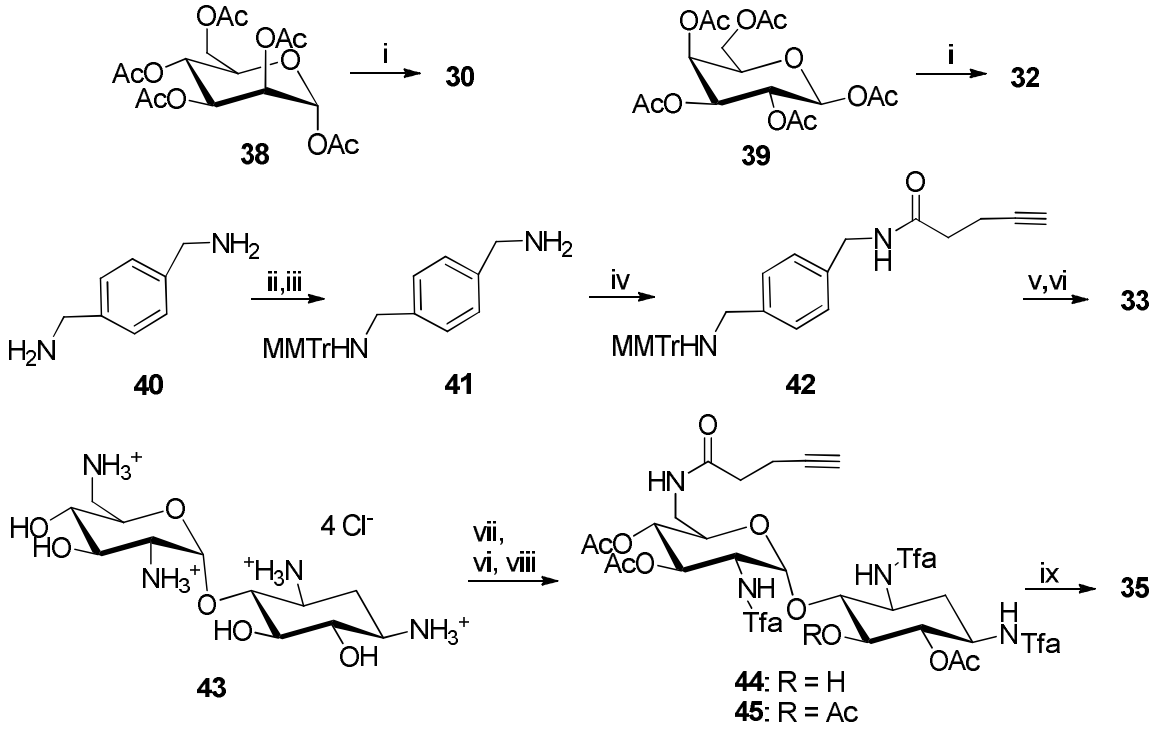

Scheme 6. Reagents: (i) propargyl alcohol, $BF_3 \cdot Et_2O$, CH_2Cl_2; (ii) MMTrCl, dioxane, (iii) aq NaOH (10 % *m/v*); (iv) 4-pentynoic anhydride (from: 4-pentynoic acid, DCC, dioxane), pyridine, DMAP; (v) TFA, CH_2Cl_2, MeOH; (vi) TfaOMe, MeOH, Et_3N; (vii) succinimidyl 4-pentynoate (from: 4-pentynoic acid, *N*-hydroxysuccinimide, DCC, dioxane), water, dioxane, Et_3N; (viii) Ac_2O, pyridine; (ix) NaOMe, MeOH.

3.1.2.2 Synthesis of azido bearing ligands

The azido-functionalized ligands (**31**, **34**, **36**, **37**) used in the click conjugation were synthesized as outlined in Scheme 7.[II] The preparation of mannose-derived ligand, methyl 2,3,4-tri-*O*-acetyl-6-azido-6-deoxy-*α*-D-mannopyranoside (**31**) has been reported previously.[190] Accordingly, the overall yield of 67% was received after tosylation and azidation of the 6´-hydroxy group of methyl *α*-D-mannopyranoside (**46**) and consecutive acetylation to the product **31**.

N-[4-(Azidomethyl)benzyl]-2,2,2-trifluoroacetamide (**34**) was synthesized starting from *N*-(4-methoxytrityl)-1,4-phenylenedimethanamine (**41**), which can be

azidated by the Cu^{2+}-catalyzed diazo transfer reaction described in literature[191]. The acid-labile trityl protection of the product (**47**) was changed to a base-labile trifluoroacetyl protection, removable by the conventional ammonolysis used for the release and deprotection of support-bound oligonucleotides.[II]

Paromamine trihydrochloride (**48**) was obtained by acidic hydrolysis of commercially available paromomycin sulfate.[192] After trifluoroacetylation of the amino groups, the primary 6´-hydroxyl group was protected as a 4,4´-dimethoxytrityl ether (**50**) and the remaining hydroxyl functions were acetylated.[II] The 6´-position was then detritylated, sulfonylated and subjected to azidation. Since the azidation gave poor yields on using mesyl esters as a starting material, conversion of the 6´-hydroxyl group to a triflate was attempted. The conventional treatment with triflic anhydride in the presence of pyridine, however, yielded a 6´-pyridinium salt instead of the desired product. Replacement of pyridine by less nucleophilic DBU then provided the desired triflate, which was azidated to product **53** in 52% overall yield. This was finally deacetylated by methoxide ion catalyzed transesterification in methanol to obtain product **36**, applicable to postsynthetic conjugation of the alkynylated oligonucleotides. 5´´-Azido-1,3,2´,6´,2´´´,6´´´-hexa-*N*-trifluoroacetylneomycin (**37**) was synthesized starting from neomycin trisulfate (**54**) according to the same protocol as described for the paromamine derivative **36** above.

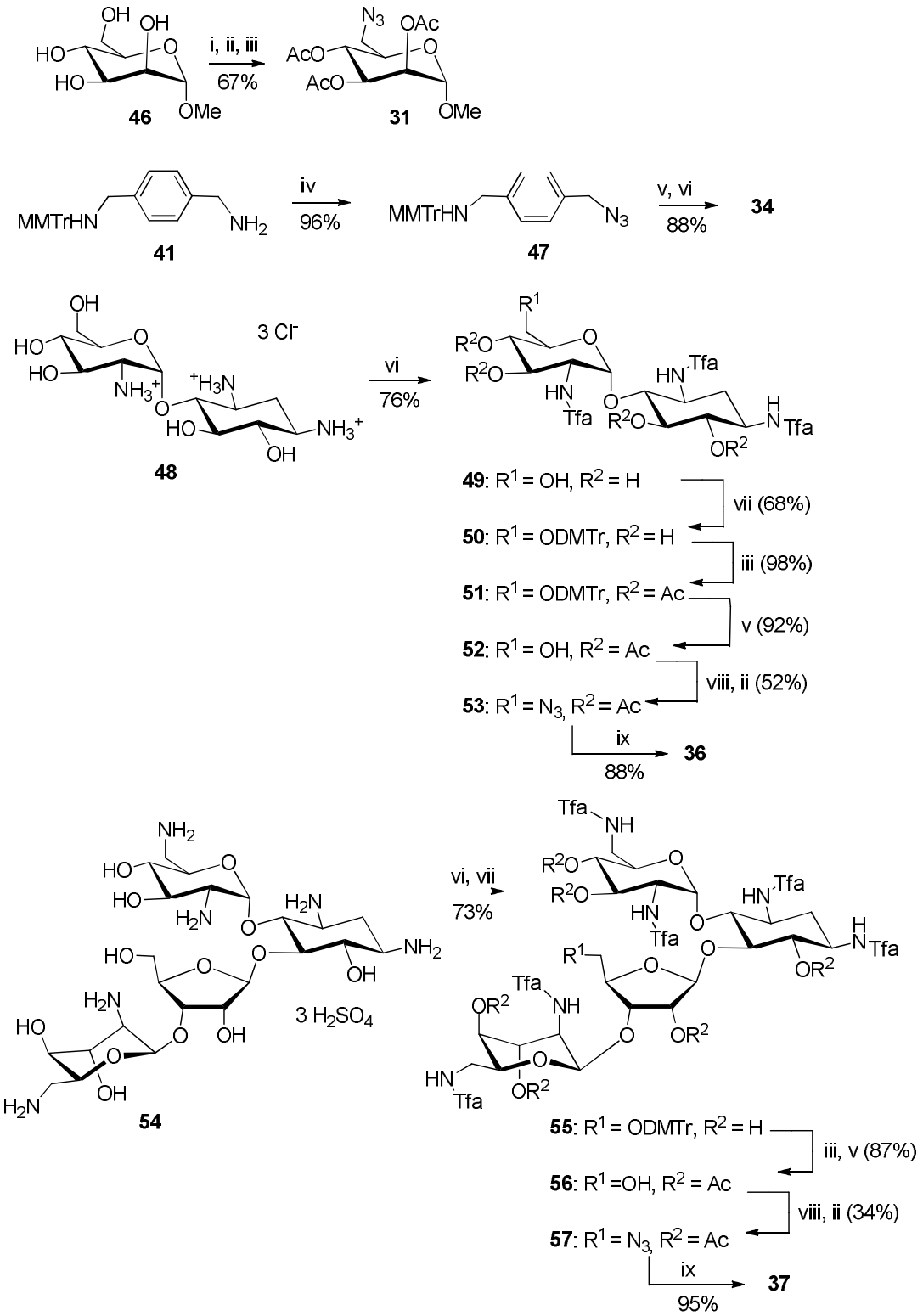

Scheme 7. Reagents: (i) TsCl, pyridine; (ii) NaN_3, DMF; (iii) Ac_2O, DMAP, pyridine; (iv) TfN_3, K_2CO_3, $CuSO_4$, H_2O, MeOH, CH_2Cl_2; (v) 3% DCA, CH_2Cl_2, MeOH; (vi) TfaOMe, Et_3N, MeOH; (vii) DMTrCl, pyridine; (viii) Tf_2O, 10% DBU in MeCN, CH_2Cl_2; (ix) NaOMe, MeOH.

3.1.3 Oligonucleotide synthesis and click conjugation

3.1.3.1 Oligonucleotide assembly

One to three modified nucleosidic units (**1**-**5**) were incorporated into the middle section of a 15-mer oligonucleotide on an automated DNA/RNA synthesizer.[I-III] Conventional phosphoramidite chemistry was applied for the chain assembly, except for the introduction of the azido-functionalized building blocks (**1**, **4**) that had to be coupled as *H*-phosphonates. Thus, a combined protocol including both the phosphoramidite and *H*-phosphonate couplings was generated for the synthesizer. The oligomers were assembled on a CPG-succinyl-nucleoside support apart from oligonucleotides **60**-**63** containing 4´-*C*-alkynyl modified monomers in which case a Q-linker loaded CPG support was used. 4´-*C*-Alkynyl modified oligonucleotides did not withstand solid-supported click conjugation as long as their phosphate groups were 2-cyanoethyl protected, but a chain cleavage took place at a site of the modified monomer. Q-Linker modified CPG support enabled the removal of the cyanoethyl protections by DBU promoted *β*-elimination on a solid support (Section 3.1.3.2.2). Table 1 summarizes the prepared oligonucleotides (**58**-**65**). 4´-*C*-Modified monomers (**1**-**3**) substituted thymidines in 5´-d(CAT CTG GTT CTA CGA)-3´ and 2´-*O*-modified monomers (**4**, **5**) replaced cytidines in otherwise fully 2´-*O*-methyl modified oligoribonucleotides 5´-$r_{2´\text{-}O\text{-}Me}$(CAU CUG GUU CUA CGA)-3´.

Table 1. Prepared oligonucleotides incorporation modified monomer **1**-**5**.

Used monomer	***Prepared oligonucleotide***
1	5´-d(CAT CTG GT**T**[1]CTA CGA)-3´ (**58**) 5´-d(CAT C **T**[1]G GT **T**[1] C **T**[1]A CGA)-3´ (**59**)
2	5´-d(CAT CTG GT **T**[2] CTA CGA)-3´ (**60**) 5´-d(CAT C **T**[2]G GTT C **T**[2]A CGA)-3´ (**61**)
3	5´-d(CAT CTG GT **T**[3] CTA CGA)-3´ (**62**) 5´-d(CAT C **T**[3]G GTT C **T**[3]A CGA)-3´ (**63**)
4 and **5**	5´-$r_{2´\text{-}O\text{-}Me}$(CAU **T**[4]UG GUU **T**[5]UA CGA)-3´ (**64**) 5´-$r_{2´\text{-}O\text{-}Me}$(CAU **T**[5]UG GUU **T**[4]UA **T**[5]GA)-3´ (**65**)

For phosphoramidite building blocks, *i.e.* 4´-*C*-[*N*,*N*-di(4-pentyn-1-yl)aminomethyl]- thymidine (**2**), 4´-*C*-[*N*-methyl-*N*-(4-pentyn-1-yl)aminomethyl]thymidine (**3**) and 2´-*O*-[(2-bromoethoxy)methyl]cytidine (**5**) 3´-phosphoramidite, standard phosphoramidite coupling chemistry with benzylthiotetratzole activator was applied, except that a prolonged coupling time of 10 min (typical for RNA) and an extra detritylation step for monomer **5** was used. All modified monomers were used at the concentration of 0.13 mol L^{-1} in dry MeCN. On the basis of DMTr-cation assay, the coupling yields for the 4´-*C*-modified nucleotides were 97% and for the 2´-*O*-modified nucleotide 99%.

In the case of *H*-phosphonate building blocks, *i.e.* 4´-*C*-azidomethylthymidine (**1**) and 2´-*O*-[(2-azidoethoxy)methyl]cytidine (**4**) 3´-(*H*-phosphonate), the coupling yields were 90% and 85%, respectively. The *H*-phosphonate coupling protocol for the synthesizer was generated on the basis of previous reports.[193,194] A prolonged coupling time (550-750 s) provided some improvements in efficiency. Pivaloyl chloride and adamantane carbonyl chloride were both tested as a condensing agent giving similar results. Both of them were dissolved in a 1:1 mixture of MeCN and pyridine to obtain a concentration of 100 mmol L^{-1}. Nucleoside 3´-(*H*-phosphonates) (**1**, **4**, TEA salts) were used as a 35 mmol L^{-1} solution (MeCN/pyridine (1:1, *v/v*)). Since a mixed *H*-phosphonate and phosphoramidite method could be applied instead of mere *H*-phosphonate coupling, unmodified and commercially available 2´-deoxy or 2´-*O*-methyl A, G, C and T / U monomers were coupled as phosphoramidites. After the oligonucleotide assembly, the support-bound material was removed from the synthesizer and oxidized with iodine (0.1 mol L^{-1}) in wet pyridine (98:2, *v/v*) at room temperature for 1 h because the oxidation step used in phosphoramidite couplings is inefficient to oxidise *H*-phosphonates.

3.1.3.2 Click conjugations

All the click conjugations between modified oligonucleotides and ligands were performed using a mixture of copper (II) sulfate and sodium ascorbate as the reducing agent in the presence of Cu(I)-stabilizing TBTA.[I-III] The reactions on a solid support and in solution followed the same protocol: The ligands were used as a 50 mmol L^{-1} solution in MeOH (except 25 mmol L^{-1} solution was used for the less soluble aminoglycoside ligand **35**) and added to the oligonucleotides in amounts of 10-15 equiv per azido or alkynyl group. After that, $CuSO_4$ and TBTA-ligand were added as a 25 mmol L^{-1} solution in a 12:3:1 (*v/v/v*) mixture of water, DMSO and 2-butanol using 5-7.5 equiv per azido or alkynyl group. Finally, sodium ascorbate (10-15 equiv / azido or alkynyl group) as 0.1 mol L^{-1} aqueous solution was added. A reaction time of 5 h at room temperature was adequate. All the click reactions proceeded virtually quantitatively, as also reported previously for click derivatization on a solid-support or in solution.[160,195,196]

3.1.3.2.1 Conjugation of 4´-*C*-azido modified oligonucleotides

After chain assembly, oligodeoxyribonucleotides **58** and **59** were conjugated with alkyne-derivatized ligands **30**, **33** and **35** by click chemistry.[I] Conjugations were performed either on the CPG-support or in solution. Scheme 8 outlines the procedure in the solution. Essentially the same chemistry was applied on a solid support.

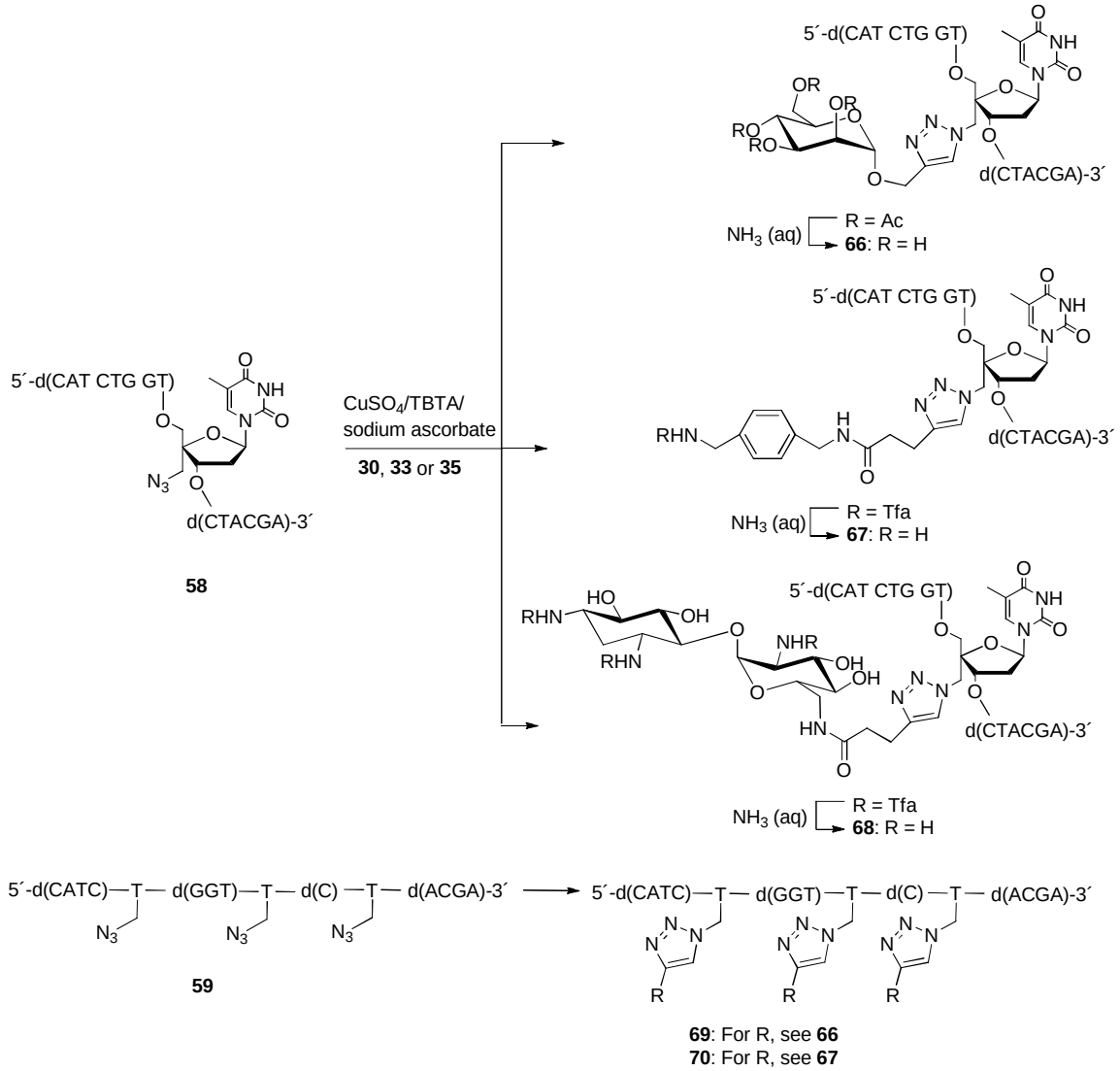

Scheme 8. Derivatization of oligonucleotides **58** and **59** by click chemistry.

Standard ammonolysis (33 % aq NH_3, 55 ºC, overnight) was carried out to release oligonucleotides from the support and to remove the protections from base moieties, phosphodiester linkages and conjugate groups. The advantage of the solid-supported synthesis is that only one ammonolytic treatment is required. By contrast, when the conjugation is carried out in the solution, the deprotection of the conjugate groups introduced requires a second ammonolysis after the click reaction. In principle, unprotected conjugate groups could have been used for conjugation, but in particular with amino groups containing ligands, it is safer to use protections to minimize the interactions with copper ion. The conjugates (**66-70**) were then purified by RP-HPLC and their identity was verified by ESI-MS.
The purity of the oligonucleotide conjugates was additionally checked by capillary electrophoresis. These studies quite unexpectedly revealed that when the click conjugations were performed on a solid support using amino group containing ligands, the conjugates obtained after RP-HPLC purification still gave two peaks in electropherograms. In addition, their melting temperature curves were slightly biphasic, lending further support for the occurrence of the conjugates as two

isomers that had the same molecular mass (in ESI-MS only one set of signals, *m*/*z*, was detected) and could not be separated by HPLC. This problem was not encountered in solid supported conjugation with mannose ligand. Furthermore, when the conjugations were carried out in solution and the products were precipitated with EtOH, this anomality in behavior disappeared: the product was elecrophoretically homogeneous and exhibited normal sigmoid melting curves. Accordingly, some caution seems to be needed on applying click conjugation to ligands that offer good coordination sites, such as amino groups, for copper ions, in spite of the fact that the groups are kept protected during the actual cycloaddition reaction.

Another peculiarity concerning the electropherograms of the crude conjugate products is also worth mentioning. Albeit the solid support was thoroughly washed after the click reaction, the capillary electrophoretic studies of the crude mixtures revealed existence of an additional complex that was not seen by RP-HPLC. This species appeared as a wide peak after the signal of the desired conjugate. Possibly the oligonucleotide conjugate remained partly associated with the TBTA ligand or its Cu(I) complex. Although this marked impurity could not be detected in RP-HPLC purification, it entirely removed it, verified by electropherogram. When the click reaction was carried out in solution, the elctropherogram of the crude product showed only the broad signal of the unidentified associate discussed above. After precipitation of the oligonucleotide conjugate with EtOH, the signals of both the desired conjugate (**67** in Figure 32) and the unidentified associate appeared, but again RP HPLC purification was needed to obtain a pure conjugate.

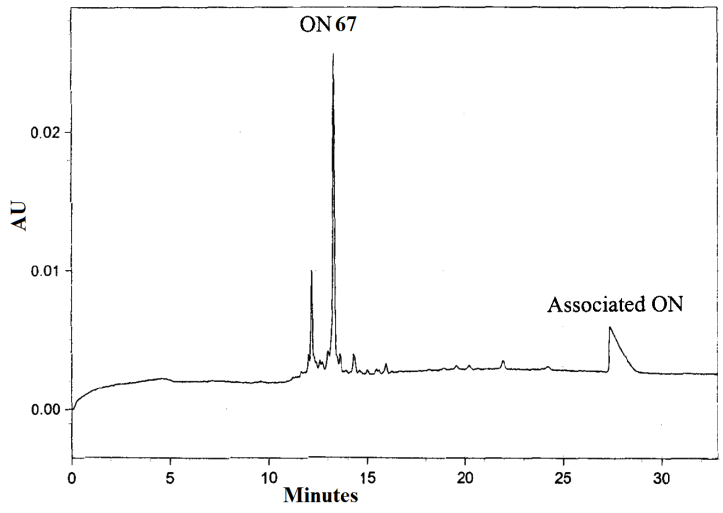

Figure 32. Electropherogram of the crude product (**67**) of the click reaction of oligonucleotide **58** with ligand **33** in solution.

3.1.3.2.2 Conjugation of 4´-*C*-alkynyl modified oligonucleotides

Click chemistry was applied to attach azido-derivatized ligands **31**, **34**, **36** and **37** to the oligodeoxyribonucleotide backbone of **60**-**63**.[II] However, it was noticed that these 4´-*C*-alkynyl modified oligonucleotides did not withstand solid-supported

click conjugation as long as their phosphate groups were 2-cyanoethyl protected, but a chain cleavage took place leaving the modified monomer attached to the 5´-terminus of the support-bound oligonucleotide. By contrast, the 4-pentyn-1-yl functionalized oligonucleotides that had not been subjected to the conditions of click reaction could be isolated in intact form by conventional ammonolysis.

To carry out the click reaction on a solid-support, the 2-cyanoethyl groups had to be removed prior to the click reaction, which was achieved by treatment with 10% DBU in MeCN (5-8 min). Since the succinyl linker is not fully compatible with the DBU treatment, but undergoes a premature cleavage via succinimide formation[197], all the conjugate syntheses were carried out on a commercially available Q-linker loaded CPG support[198]. After exposure of the internucleosidic linkages as phosphodiesters, the azido-functionalized ligands **31**, **34**, **36** and **37** were attached by the click reaction and the conjugates were deprotected and released from the support by ammonolysis (Scheme 9).

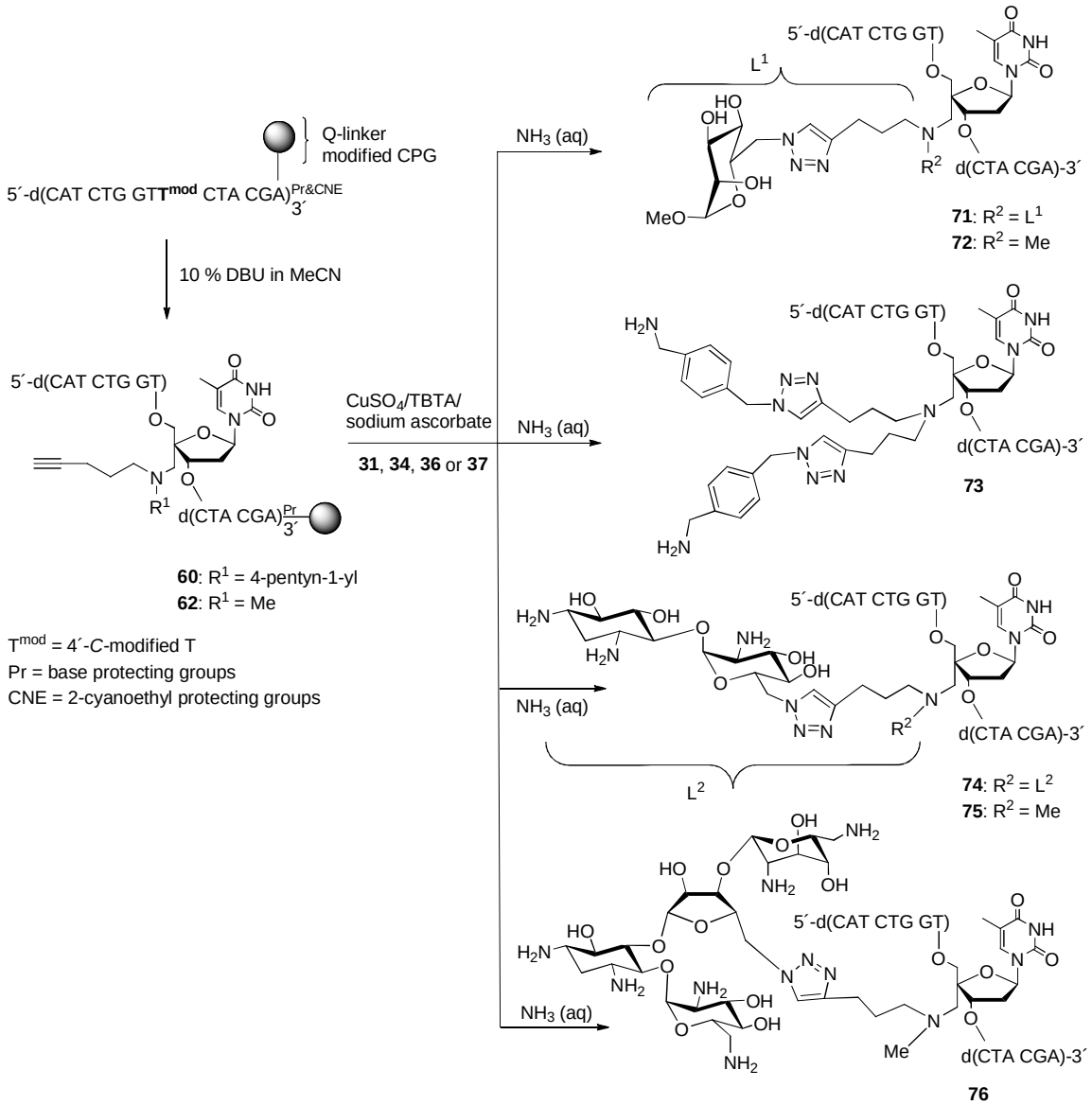

Scheme 9. Synthesis of the conjugated oligodeoxyribonucleotides containing one 4´-*C*-modified monomer.

The crude products (**71**-**80**, see Table 3) were purified by RP-HPLC and their identity was verified by ESI-MS. Figure 33 shows representative examples of the RP-HPLC traces of the crude oligonucleotides **76** (1ˣneomycin ligand), **77** (4ˣmannose ligand) and **80** (2ˣparomamine ligand) and the homogeneous products after purification. In each case the desired conjugate was clearly the main product.

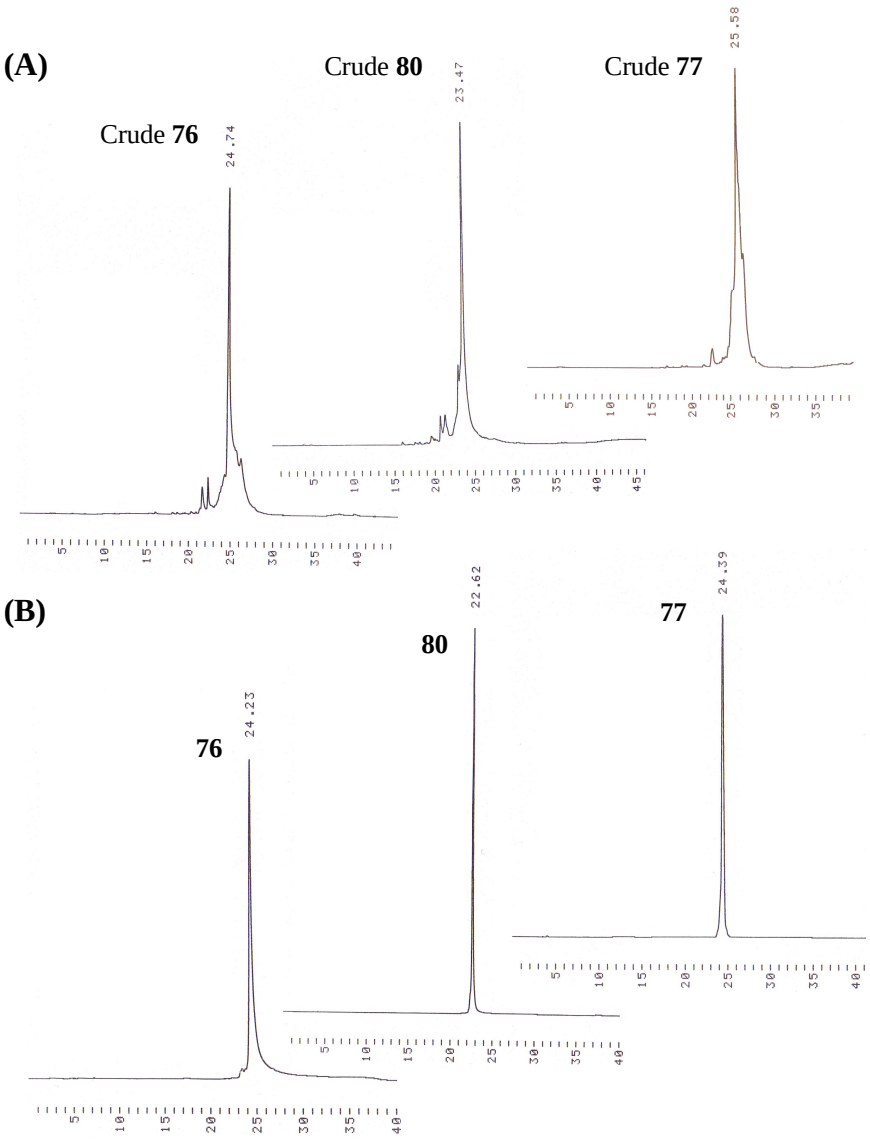

Figure 33. RP HPLC traces of the crude (A) and purified (B) oligonucleotide conjugates **76**, **77** and **80**. (Conditions: 0% to 50% MeCN in 0.1 mol L^{-1} TEAA (aq) buffer over 60 min, flow rate 1 mL min^{-1})

With 4´-*C*-[*N*,*N*-di(4-pentyn-1-yl)aminomethyl]thymidine and 4´-*C*-[*N*-methyl-*N*-(4-pentyn-1-yl)aminomethyl]thymidine monomers (**2**, **3**), capillary electrophoresis, HPLC and ESI-MS data all indicated the presence of only one pure conjugate for each oligonucleotide. Accordingly, all conjugations could be conveniently made on a solid support without complications unlike what was seen in the case of solid-supported click conjugation of oligonucleotides containing the 4´-*C*-azidomethylthymidine monomers.

3.1.3.2.3 Conjugation of 2´-*O*-azidoalkyl and bromoalkyl modified oligonucleotides

2´-*O*-Methyl oligoribonucleotides **64** and **65** containing both bromo and azido functionalities within their chain were applied in a conjugation strategy that enabled the attachment of two different ligands to the oligomers.[III] Accordingly, the support-bound oligonucleotides were subjected to two consecutive conjugations with alkynyl-derivatized monosaccharides. The first sugar was introduced by the Cu(I) promoted click reaction with mannose-ligand **30** and the second by azidation of the 2-bromoethoxy group of monomer **5** followed by another click reaction, this time with galactose derivative **32** (Scheme 10). Both tetramethylguanidinium azide[199] (TMGA/NaI/DMF, 65 °C) or less soluble NaN_3 (NaN_3/NaI/DMF, 65 °C) could be used as a source of azide ion as also previously demonstrated.[177,178]

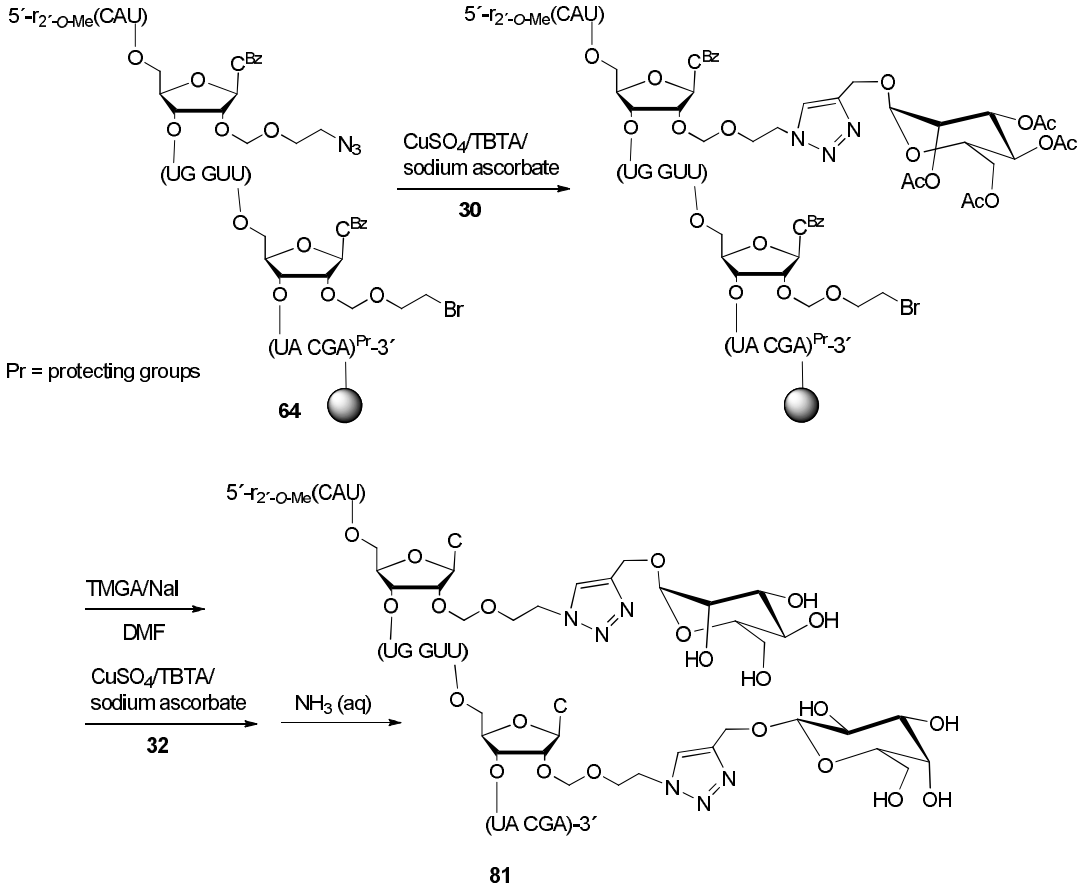

Scheme 10. Solid-supported introduction of two different sugar ligands into 2´-positions within a 2´-*O*-Me-oligoribonucleotide (**81**).

The oligonucleotide conjugates obtained (**81** and **82**) were deprotected and released from the support by standard ammonolysis (33% aq NH_3, 55 °C, overnight). The crude products were purified by RP-HPLC and their identity was verified by ESI-MS. Figure 34 shows the HPLC traces of the crude conjugates and the homogeneity of the products after purification.

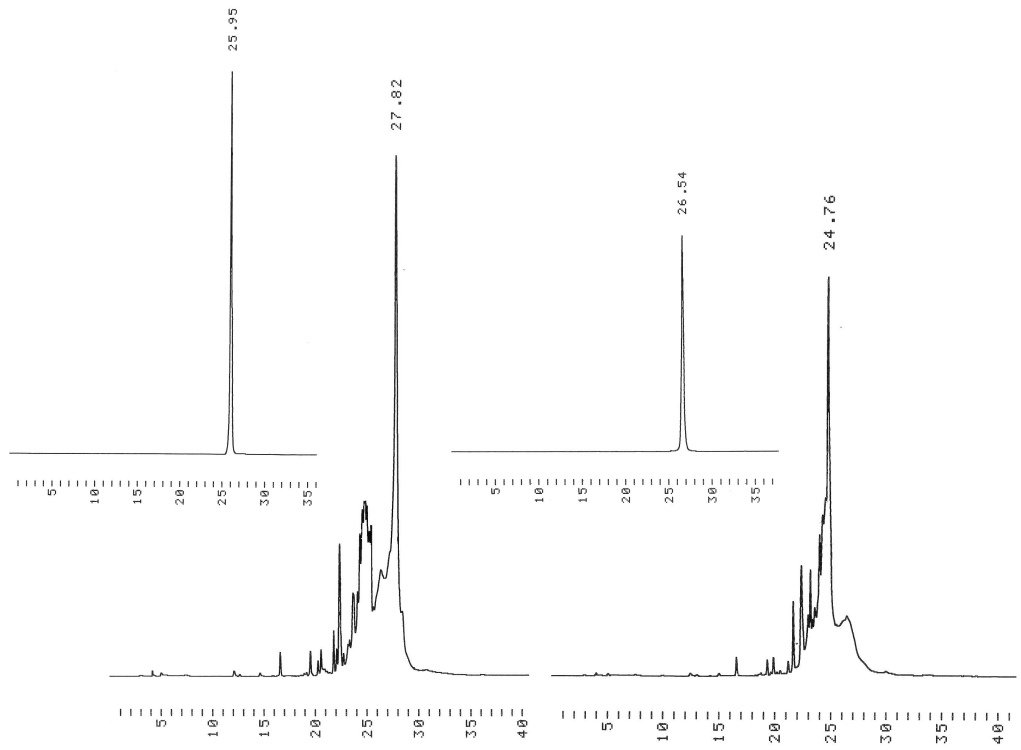

Figure 34. RP HPLC traces of the crude and purified oligonucleotide glycoconjugates **81** and **82**, respectively. (Conditions: 0 to 50 % MeCN in 0.1 mol L^{-1} TEAA buffer over 60 min, flow rate 1 mL min^{-1})

3.1.4 Melting temperature studies of the oligonucleotide conjugates

The introduction of conjugate groups in an oligonucleotide may more or less alter its hybridization properties compared to the unmodified sequence. These changes in binding affinity are assessed by melting temperature (T_m) studies.[200] The T_m value based on the thermal denaturation of the oligonucleotide duplex, refers to the temperature at which a half of the nucleic acid double helix has dissociated into single strands (Figure 35). The process can be monitored by UV-spectroscopy, since the UV-absorbance increases upon the denaturation of double-stranded molecule; a phenomenon known as hypochromic effect. When the absorbance is plotted against temperature, a sigmoidal melting curve is obtained and the T_m of the duplex can be read from its inflection point.

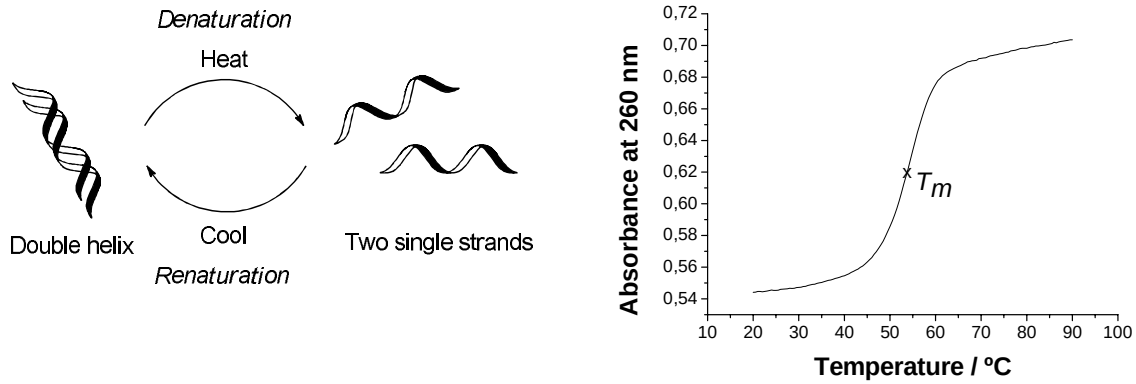

Figure 35. Thermal denaturation of nucleic acids followed by UV- spectroscopy.

In the present study, the influence of the 2´- and 4´-conjugations on the duplex stability was evaluated with three different ligand-types, including neutral carbohydrate ligands (mannose and galactose), a *p*-aminomethylbenzene-derived ligand and aminoglycoside ligands.[I-III] The melting temperatures of the oligonucleotide conjugates **66**-**82** with their complementary DNA or 2´-*O*-methyl RNA sequences were measured at pH 7 at the ionic strength of 0.1 and 1.0 mol L^{-1}. The lower salt concentration represents the physiological conditions and the high salt content was used to elucidate the significance of electrostatic interactions induced by the conjugate groups. At a high ionic strength, the electrostatic repulsion between negatively charged sugar-phosphate backbones is diminished and consequently, the influence resulting from charged functional groups of ligands becomes less prominent. Amino groups, for example, are usually positively charged at neutral pH and their neutralizing effect can often be seen as an increased duplex stability, which is more profound at a low ionic strength.

Mannose and galactose ligands were chosen to test the feasibility of the 2´- and 4´-glycoconjugations since the carbohydrates offer a possible way to improve the delivery and targeting of siRNA and antisense oligonucleotides (Section 1.3.3.5). Previously, the main attention has been paid to preparation of oligonucleotide conjugates bearing a multi-armed glycocluster at either terminus of the chain.[130,177,178,201-204] However, as far as glycotargeting of siRNA is concerned, another approach appears possible, *viz*. decoration of the sense strand with sugars. A prerequisite for this approach is that the sugar ligands do not markedly destabilize the duplex. In other words, the sense strand is aimed at serving as a scaffold to which the lectin-binding sugar ligands are tethered at appropriate distances throughout the molecule. Since the carrier is simultaneously able to hybridize with the antisense strand, the latter becomes enriched at the cell surface and, hence, internalizated by receptor-mediated endocytosis.

3.1.4.1 Hybridization properties of 4´-*C*-conjugates

According to previous studies,[166-171] oligonucleotides containing 4´-*C*-modified DNA monomers generally prefer hybridization towards complementary DNA over RNA. 4´-*C*-Acylthymidines,[205] for example, adopt a *C*(2´)-endo-like conformation found typically in B-type DNA-DNA duplex. In the present study,[I,II] the amino-group bearing conjugates (**67**, **68**, **70**, **73**-**76**, **78**-**80**) were found to have a similar preference for the complementary DNA. However, an opposite behavior was detected with oligonucleotides containing mannose groups (**66**, **69**, **71**, **72**, **77**). The melting temperature values for oligodeoxyribonucleotides **58**-**63** and their conjugates **66**-**80** with the complementary DNA and 2´-*O*-methyl RNA sequences are shown in tables 2 and 3. The results referring to the T_m values of 4´-*C*-azido and 4´-*C*-alkynyl derived oligonucleotides are presented separately because the original studies were made on two different instruments using dissimilar temperature detection (see Experimental). Nevertheless, the temperature shifts are still comparable.

Table 2. Melting experiments of the 4´-*C*-azido-derived oligonucleotide conjugates and their complementary DNA or 2´-*O*-Methyl-RNA sequences[a]

	Compl. DNA T_m / ºC and (ΔT_m / ºC)		Compl. 2´-*O*-methyl RNA T_m / ºC and (ΔT_m / ºC)	
	0.1 mol L^{-1} NaCl	1.0 mol L^{-1} NaCl	0.1 mol L^{-1} NaCl	1.0 mol L^{-1} NaCl
5´-CAT CTG GTT CTA CGA	55.4	65.0	57.0	68.0
5´-CAT CTG GT***B***CTA CGA (**58**)	53.8 (-1.6)	63.3 (-1.7)	56.5 (-0.5)	67.4 (-0.6)
5´-CAT C***B***G GT***B*** C***B***A CGA (**59**)	51.5 (-3.9)	62.3(-2.7)	55.8 (-1.2)	67.4 (-0.6)
5´-CAT CTG GT***D*** CTA CGA (**66**)	53.0 (-2.4)	63.0 (-2.0)	56.8 (-0.2)	68.0 (0)
5´-CAT C***D***G GT***D*** C***D***A CGA (**69**)	50.3 (-5.1)	61.3 (-3.7)	56.2 (-0.8)	69.5 (+1.5)
5´-CAT CTG GT***E*** CTA CGA (**67**)	55.6 (+0.2)	64.7 (-0.3)	56.2 (-0.8)	67.6 (-0.4)
5´-CAT C***E***G GT***E*** C***E***A CGA (**70**)	56.4 (+1.0)	63.9 (-1.1)	55.6 (-1.4)	n. m.
5´-CAT CTG GT***F*** CTA CGA (**68**)	55.8 (+0.4)	63.8 (-1.2)	55.3 (-1.7)	67.3 (-0.7)

[a]In 10 mmol L^{-1} potassium phosphate buffer (pH 7) containing 0.1 mol L^{-1} or 1.0 mol L^{-1} NaCl. The oligonucleotide conjugates and their cDNA or 2´-*O*-methyl RNA targets were used at a concentration of 2 μmol L^{-1}. n.m. = not measured

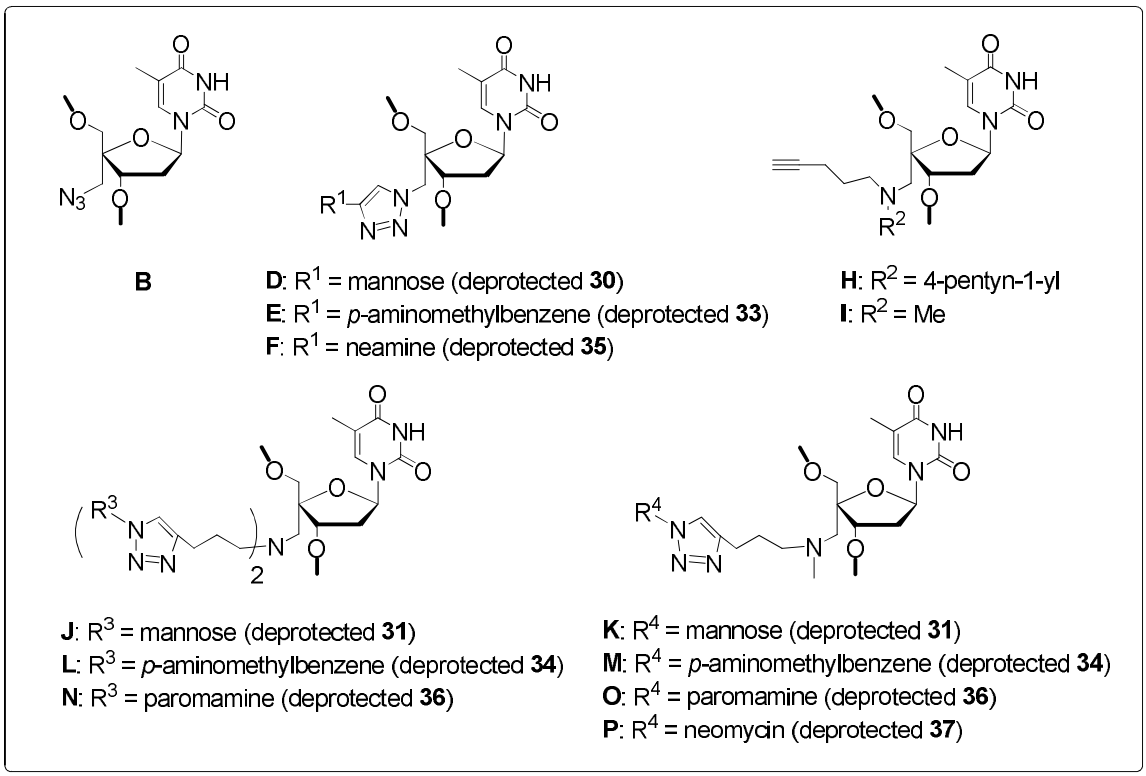

Table 3. Melting experiments of the 4´-*C*-alkynyl-derived oligonucleotide conjugates and their complementary DNA or 2´-*O*-Methyl-RNA sequences[a]

	Compl. DNA T_m / ºC and (ΔT_m / ºC)		Compl. 2´-*O*-methyl RNA T_m / ºC and (ΔT_m / ºC)	
	0.1 mol L^{-1} NaCl	1.0 mol L^{-1} NaCl	0.1 mol L^{-1} NaCl	1.0 mol L^{-1} NaCl
5´-CAT CTG GTT CTA CGA	52.8	61.9	54.1	65.0
5´-CAT CTG GT***H*** CTA CGA (**60**)	54.5 (+1.7)	61.3 (-0.6)	54.7 (+0.6)	65.1 (+0.1)
5´-CAT C***H***G GTT C***H***A CGA (**61**)	52.5 (-0.3)	59.7 (-2.2)	53.0 (-1.1)	65.4 (+0.4)
5´-CAT CTG GT***I*** CTA CGA (**62**)	54.6 (+1.8)	62.5 (+0.6)	55.7 (+1.6)	66.4 (+1.4)
5´-CAT C***I***G GTT C***I***A CGA (**63**)	53.5 (+0.7)	61.6 (-0.3)	52.4 (-1.7)	64.7 (-0.3)
5´-CAT CTG GT***J*** CTA CGA (**71**)	53.8 (+1.0)	62.1 (+0.2)	54.3 (+0.2)	65.5 (+0.5)
5´- CAT C***J***G GTT C***J***A CGA (**77**)	51.3 (-1.5)	59.6 (-2.3)	53.8 (-0.3)	66.1 (+1.1)
5´-CAT CTG GT***K*** CTA CGA (**72**)	54.6 (+1.8)	62.2 (+0.3)	54.6 (+0.5)	65.3 (+0.3)
5´-CAT CTG GT***L*** CTA CGA (**73**)	57.9 (+5.1)	63.7 (+1.8)	54.2 (+0.1)	64.3 (-0.7)
5´-CAT C***L***G GTT C***L***A CGA (**78**)	62.0 (+9.2)	66.6 (+4.7)	56.7 (+2.6)	66.5 (+1.5)
5´- CAT C***M***G GTT C***M***A CGA (**79**)	61.0 (+8.2)	66.5 (+4.6)	57.3 (+3.2)	67.1 (+2.1)
5´- CAT CTG GT***N*** CTA CGA (**74**)	57.9 (+5.1)	62.2 (+0.3)	53.2 (-0.9)	64.8(-0.2)
5´-CAT CTG GT***O*** CTA CGA (**75**)	57.8 (+5.0)	63.5 (+1.6)	54.1 (±0.0)	65.1 (+0.1)
5´- CAT C***O***G GTT C***O***A CGA (**80**)	58.2 (+5.4)	62.8 (+0.9)	55.1 (+1.0)	65.2 (+0.2)
5´-CAT CTG GT***P*** CTA CGA (**76**)	56.1 (+3.3)	62.1 (+0.2)	52.5 (-1.6)	64.2 (-0.8)

[a]In 10 mmol L^{-1} potassium phosphate buffer (pH 7) containing 0.1 mol L^{-1} or 1.0 mol L^{-1} NaCl. The oligonucleotide conjugates and their cDNA or 2´-*O*-methyl RNA targets were used at a concentration of 2 μmol L^{-1}.

When one or three 4´-*C*-azidomethylthymidine monomers **B** were incorporated into an oligonucleotide (**58**, **59**), the melting temperature of the duplexes with complementary DNA and 2´-*O*-methyl RNA sequences dropped, but less with 2´-*O*-methyl RNA (ΔT_m/modification ≈ -0.5 ºC) than with DNA (ΔT_m/modification ≈ -1.5 ºC). On the contrary, the 4´-*C*-alkynyl modified monomers **H** and **I** were better accommodated into the duplexes and their oligonucleotides (**60**-**63**) formed more stable hybrids with DNA than with 2´-*O*-methyl RNA. One monomer **H** or **I** showed even a stabilizing effect with both complementary strands, but a slight destabilization took place with two such monomers.

Conjugates of mannose ligand

Conjugation of the 4´-*C*-azidomethylthymidine units with mannopyranoside (**D** in **66**, **69**) slightly increased the destabilization of the DNA-hybrid but, interestingly, hybridization with 2´-*O*-methyl RNA target was even slightly enhanced, in particular at high ionic strength.

With 4´-*C*-alkynyl derived mannose conjugates (**J** and **K** in **71**, **72**, **77**), the presence of a single monomer **J** (**71**) or **K** (**72**) in the DNA-hybrid increased the T_m, but two modified units in **77** were destabilizing. By contrast, on using a 2´-*O*-methyl RNA target, the conjugate containing two **J** monomers and, hence, four mannose residues hybridized almost as well as the corresponding unmodified 15-mer oligodeoxyribonucleotide. Actually, the destabilizing effect of two **H** units in the heteroduplex of sequence **61** was completely recovered with the conjugate **77** containing two **J** monomers (T_m increased -1.1 → -0.3 ºC) and the 2´-*O*-Me target became more favorable than the complementary DNA (compare T_m of -0.3 ºC to -1.5 ºC with cDNA). At high salt concentration, the mannose conjugates formed slightly more stable duplexes with 2´-*O*-methyl RNA than the unmodified sequence but in the case of DNA-hybrids the high ionic content lowered the melting temperatures compare to the low salt concentration and the presence of two **J** monomers was clearly destabilizing.

Conjugates of amino group bearing ligands

All conjugates bearing amino groups (**67**, **68**, **70**, **73-76**, **78-80**) stabilized the duplex with DNA target. This was especially marked with 4´-*C*-alkynyl derived monomers **L**, **M**, **N**, **O** and **P**. With the *p*-aminomethylbenzene conjugates, the DNA-hybrids incorporating one or two **L** (**73**, **78**) or **M** (**79**) monomers were stabilized by 4-5 ºC / modification. Towards 2´-*O*-methyl RNA, the stabilization was less prominent. The stabilization was more marked at a low ionic strength, but it still existed at a high ionic strength. Undoubtedly, major part of the stabilization results from reduced electrostatic repulsion between negatively charged sugar-phosphate backbones and positively charged amino groups present at neutral pH.

When one paromamine derived monomer, **N** (**74**) or **O** (**75**) was incorporated into the strand, the DNA-hybrid was stabilized by 5 ºC, but the second monomer (**80**) did not result in any extra stabilization. With 2´-*O*-Me RNA target, two monomers **O** were needed to achieve even a modest increase in T_m (ΔT_m = +1.0 ºC). Compared to the paromamine monomers, the neomycin group (monomer **P** in **76**) was less stabilizing than the paromamine group (monomer **O** in **75**) towards DNA, and towards 2´-*O*-Me-RNA, the effect was even destabilizing. Similarly to the *p*-aminomethylphenyl ligands, the duplex stabilizing effects of the aminoglycoside ligands were more marked at a low ionic strength.

With 4´-*C*-azido derived monomer **E** (**67**, **70**) and **F** (**68**) the stabilization of the DNA-hybrid was modest and T_m was in fact decreased at a high salt concentration. With complementary 2´-*O*-methyl RNA strand, the melting temperatures were decreased and in this case the drop was more profound at low than at high salt concentration.

Conclusion

The hybridization properties of the 4´-modified oligonucleotides were encouraging particularly with the conjugates of 4´-*C*-alkynyl monomers **2** and **3**. Evidently the 4´-position, facing the minor groove upon hybridization, can accommodate even rather large molecule clusters without appreciable destabilization of the duplex.

The results received with the mannose conjugated oligonucleotides lend some support for the feasibility of sugar-coated oligonucleotides as carriers of RNA-type oligonucleotides. It was demonstrated that the oligonucleotides containing one to four mannose ligands in the central part of the chain can form equally stable duplexes with complementary 2´-OMe RNA as the corresponding unmodified DNA sequence. The results with the space demanding aminoglycoside ligands further demonstrate the utility of 4´-modified nucleosides in glycoconjugations. In the case of 4´-*C*-alkynyl derived conjugates, all amino group bearing oligonucleotides stabilized the DNA·DNA duplex significantly. Among them, the most remarkable hybridization enhancement was obtained with *p*-aminomethylphenyl conjugates (**73**, **78**, **79**). Sterically more demanding aminoglycoside ligands (**74**-**76**, **80**) stabilized the DNA·DNA duplex less, but still notably. All conjugates bearing amino group preferred DNA over 2´-OMe RNA.

Compared to 4´-*C*-azido derived conjugates, oligonucleotides resulting from conjugation of 4´-*C*-alkynyl modified units exhibited better hybridization properties. This implies that the alkyl chain of the 4´-*C*-(4-pentyn-1-ylaminomethyl)thymidine monomers (**2**, **3**) allows a more flexible alignment of the triazole ring and conjugate groups upon hybridization. The tertiary amino group, which probably is protonated under physiological conditions, further stabilizes the duplex formation by diminishing the electrostatic repulsion between the complementary chains, as evidenced by the fact that the melting temperatures observed for the oligonucleotides containing 4´-*C*-(alkynylaminomethyl)thymidine units (**60**-**63**) are higher than those observed for their 4´-*C*-azidomethylthymidine counterparts (**58**, **59**).

3.1.4.2 Hybridization properties of 2´-*O*-conjugates

It has been shown previously that oligonucleotides bearing a *β*-D-ribofuranosyl group at an intrachain 2´-*O* form stable complexes with RNA (ΔT_m = 0 °C) and maintain A-type helical geometry with the additional 2′-*O*-ribose moiety located in the minor groove.[172,173] Consistent with these findings, the sugar ligands attached in the present study to 2´-*O* via a [2-(4-hydroxymethyl-1*H*-1,2,3-triazol-1-yl)ethoxy]methyl linker only slightly destabilized the duplex.[III] Table 4 records the melting temperatures (T_m) for the duplexes of oligonucleotide conjugates **81** and **82** with the fully complementary DNA and 2´-*O*-methyl RNA sequences.

Table 4. Melting temperatures for the duplexes of oligonucleotide conjugates **81** and **82** with their complementary DNA and 2´-*O*-Methyl-RNA Sequences[a]

	Compl. DNA T_m / °C and (ΔT_m / °C)		Compl. 2´-*O*-methyl RNA T_m / °C and (ΔT_m / °C)	
	0.1 mol L^{-1} NaCl	1.0 mol L^{-1} NaCl	0.1 mol L^{-1} NaCl	1.0 mol L^{-1} NaCl
5´-CAU CUG GUU CUA CGA	50.1	61.7	72.0	n.m.
5´-CAU ***X***UG GUU ***Y***UA CGA (**81**)	50.6 (+0.5)	60.6 (-1.1)	71.5 (-0.5)	n.m.
5´-CAU ***Y***UG GUU ***X***UA ***Y***GA (**82**)	47.0 (-3.1)	60.2 (-1.5)	68.2 (-3.8)	n.m.

[a] **X** = monomer **4** conjugated with **30**; **Y** = monomer **5** conjugated with **32**; n.m. = not measured (T_m was too high to be accurately determined). In 10 mmol L^{-1} potassium phosphate buffer (pH 7) containing 0.1 mol L^{-1} or 1.0 mol L^{-1} NaCl. The oligonucleotide conjugates and their cDNA or 2´-*O*-methyl RNA targets were used at a concentration of 2 μmol L^{-1}.

The sugar ligands accommodated quite well in the duplex structure. Oligonucleotide **81** bearing two sugar units in an intrachain position exhibited even a slight stabilization of the duplex with DNA target at a low ionic strength (ΔT_m = +0.5 °C) and a slight destabilization at a high ionic strength (ΔT_m = -1.1 °C). Addition of a third sugar ligand to obtain conjugate **82** resulted in a moderate destabilization even at a low ionic strength (ΔT_m = -3.1). At high ionic strength the destabilization was less prominent (ΔT_m = -1.5 °C). With 2´-*O*-Me RNA target, two sugar ligands within conjugate **81** were similarly well tolerated (ΔT_m = -0.5 °C), but with the **82**, containing three sugars, T_m again dropped significantly (ΔT_m = -3.8 °C). A tentative explanation for the marked destabilizing influence of the third sugar, especially at a low ionic strength, is that two of the sugars are rather close to each other within conjugate **82**, viz. in positions 10 and 13.

3.2 Characterization of RNA invasion by ^{19}F NMR spectroscopy

Invasion is a fundamental process of RNA, in which a weak stem region is denatured by an exterior single strand resulting in a reorganized secondary structure. This well-known process is applied e.g. in the antisense approach (Section 1.5),[136] but the means with which to follow its progress are rather limited. Methods employing thermal UV-denaturation profiles or fluorescence or CD spectra are more likely to fail in observation of invasion, since what happens is a conversion of double helix to another double helix. Gel shift assay in principle allows determination of the equilibrium constants for this kind of a chain invasion, but it may skew the equilibrium between weakly interacting species. Instead, ^{19}F NMR spectroscopy appears potential for such an analysis.[206,143-148] It has been previously utilized in several related studies, including identification of site-specific RNA binders,[145] detection of DNA duplex formation,[147] characterization of HIV-2 TAR RNA[146] and, finally, quantification of hairpin/hairpin[143,207] and duplex/hairpin[148] equilibria of self-complementary DNA/RNAs. The latter is an

excellent example of how a temperature-dependent shift of ^{19}F resonances can be used for the analysis of dynamic equilibria of co-existing intra- and intermolecular secondary structures. Compared to that, RNA invasion represents an even more complex reaction system and the present study offers the first example of the applicability of ^{19}F NMR spectroscopy for elucidation of the course of such a process.[IV] Accordingly, invasion of 2′-*O*-methyl oligoribonucleotides into a ^{19}F-labeled HIV-1 TAR RNA model and the temperature-dependent behavior of the complexes obtained were examined. Additionally, the influence of a known TAR ligand, *viz.* neomycin B,[208] on the invasion was demonstrated.

The fluorine atom has a single naturally occurring isotope (^{19}F) with a spin of ½ and its resonance is expected to give distinct signal in different molecular environments.[206] Compared to ^{1}H-NMR spectroscopy, which also is applicable for the purpose, the fluorine chemical shifts range is wider (~50-fold larger than that of ^{1}H) and the shifts are more sensitive to local environmental changes. In addition, the process may be monitored by user-friendly way without marked NMR specialization and without need of a high quality NMR-instrument. Finally, the nonexistence of fluorine atoms in RNA enables the measurements without background signal interference, but as a consequence, the method requires fluorine-labeling of the oligonucleotide.

Various fluorine probes incorporated into nucleic acids have been employed in ^{19}F-NMR spectroscopy including 2′-deoxy-2′-fluoronucleosides,[143,145] 5-[4,4,4,-trifluoro-3,3-bis(trifluoromethyl)but-1-ynyl]-2′-deoxyuridine,[147] 5-fluoropyrimidine nucleotides[144,146,207] and 2,4-difluorotoluene nucleosides[148] (Figure 36). An important requirement for the fluorine probe is that it should not cause any substantial deviations from the nativity of the biopolymer. As an alternative strategy, the potential of external probes has been proposed. Their applicability for the detection of RNA hairpin melting has been demonstrated with fluorinated 1,3-diaminocyclopentanes.[209]

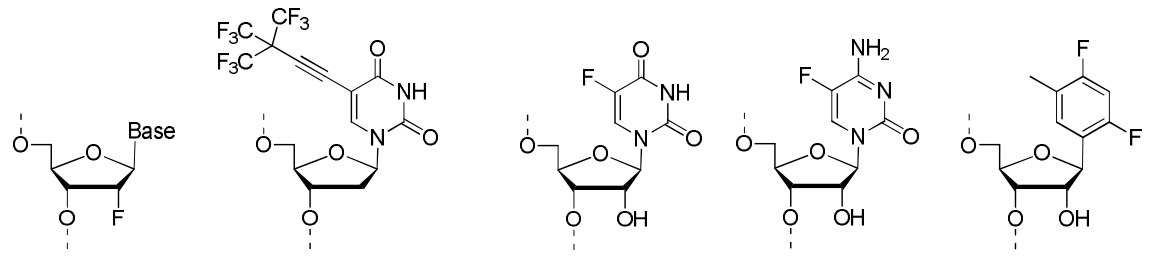

2′-Deoxy-2′-fluoronucleoside | 5-[4,4,4,-trifluoro-3,3-bis(trifluoromethyl)but-1-ynyl]-2′-deoxyuridine | 5-Fluorouridine | 5-Fluorocytidine | 2,4-difluorotoluene nucleoside

Figure 36. Nucleosidic fluorine probes applied in ^{19}F-NMR spectroscopy

3.2.1 Preparation of the ^{19}F-labeled RNA target

5-[4,4,4-Trifluoro-3,3-bis(trifluoromethyl)but-1-ynyl]-2′-deoxyuridine probe was selected as a fluorine-label and incorporated into the HIV-1 TAR RNA model in place of the uridine nucleoside within the tetranucleotide stem between the loop and the bulge of the native TAR structure (Figure 37).[IV] The selected probe bears nine magnetically equivalent fluorine atoms, which allows rapid measurements at a micromolar RNA concentration. Additionally, the fluorine atoms of this probe are not magnetically coupled to protons, which provides resonance signals as singlets without fluorine-proton decoupling. HIV-1 TAR element is a widely used target for the antisense oligonucleotides and it was introduced in Section 1.5.1.

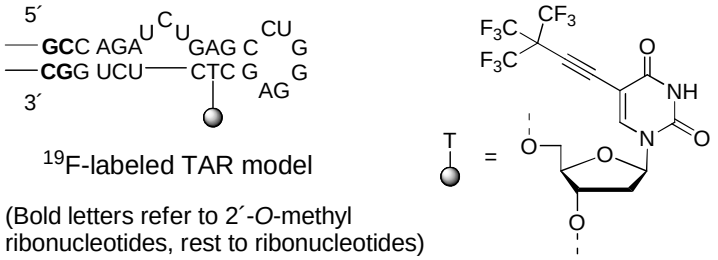

Figure 37. Sturcture of the prepared ^{19}F-labeled HIV-1 TAR RNA model.

5'-*O*-(4,4´-Dimethoxytrityl)-5-[4,4,4-trifluoro-3,3-bis(trifluoromethyl)but-1-ynyl]-2'-deoxyuridine phosphoramidite (**86**) monomer used in the oligonucleotide synthesis of ^{19}F-labeled TAR model was prepared as described earlier (Scheme 11).[147] Starting from 5-iodo-2'-deoxyuridine (**83**) the building block **86** was received with *Sonogashira* reaction, followed by tritylation and phosphitylation. The last step was performed here with 2-cyanoethyl *N*,*N*-diisopropylphosphoramidochloridite reagent.[IV]

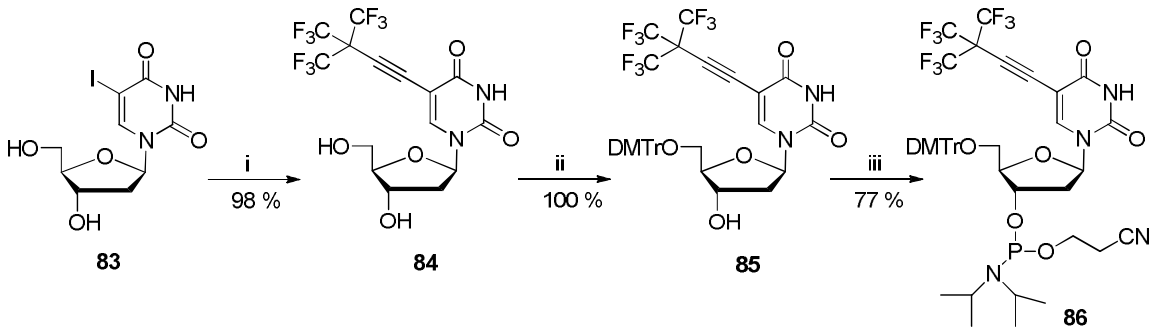

Scheme 11. Reagents: (i) 4,4,4-trifluoro-3,3-bis(trifluoromethyl)butyne, $Pd(PPh_3)_4$, DMF, CuI, diisopropylethylamine; (ii) DMTrCl, DMAP, pyridine; (iii) 2-cyanoethyl *N*,*N*-diisopropylphosphoramidochloridite, Et_3N, CH_2Cl_2.

The oligoribonucleotide assembly of the HIV-1 TAR model was performed on an automated synthesizer applying standard RNA coupling protocol (benzylthiotetratzole activator) for the commercially available 2´-*O*-TOM protected

and 2'-*O*-methyl ribonucleoside phosphoramidite monomers. Two 2′-*O*-methyl ribonucleotides were inserted to both ends of the chain to increase the stability of 3′/5′-stem region and to protect the model against degradation by exonucleases. As previously reported,[147] the fluorine label 5'-*O*-(4,4´-dimethoxytrityl)-5-[4,4,4-trifluoro-3,3-bis(trifluoromethyl)but-1-ynyl]-2'-deoxyuridine phosphoramidite (**86**) was coupled, however, manually since the automatic incorporation proved ineffective. Accordingly, the phosphoramidite (0.2 mol L^{-1}, 250 μL, 5.0 equiv) and the activator (0.25 mol L^{-1}, 250 μL) in MeCN were added to the solid-supported 5'-CUCUG**GC** resin (bold letters refer to protected 2'-*O*-methyl nucleotides and the rest to 2'-*O*-TOM-protected nucleotides) and the suspension was mixed for 15 min at 25°C under nitrogen. The coupling was carried out twice. After oxidation and capping steps which were also performed manually, the oligonucleotide synthesis with commercial monomers was continued on the synthesizer. On the basis of DMTr-cation assay, the manual coupling of **86** was quantitative. The oligoribonucleotide was released from the resin by the usual ammonolysis protocol and the 2'-*O*-TOM protections were removed by consecutive treatments with Et_3N•3HF (60:16, *v/v*, 65 °C, 1h) in DMSO and 0.1 mol L^{-1} aqueous NaOAc (65 °C, 1h). The crude TAR model was purified by RP HPLC and the authenticity of the product was verified by ESI-MS.

The influence of the ^{19}F-label to the native TAR structure was evaluated by UV-spectroscopy comparing T_m-values of the labeled HIV-1 TAR to that of the non-labeled (Figure 38, 25 mM NaH_2PO_4 buffer, pH 6.5).[IV] Respectively, T_m-values of 60.7 °C and 63.4 °C were received. As the label decreased melting temperature by 2.7 °C, it undoubtedly facilitated invasion to the TAR model. If the results are directly interpreted to the behavior of native TAR, this destabilization should be taken into account.

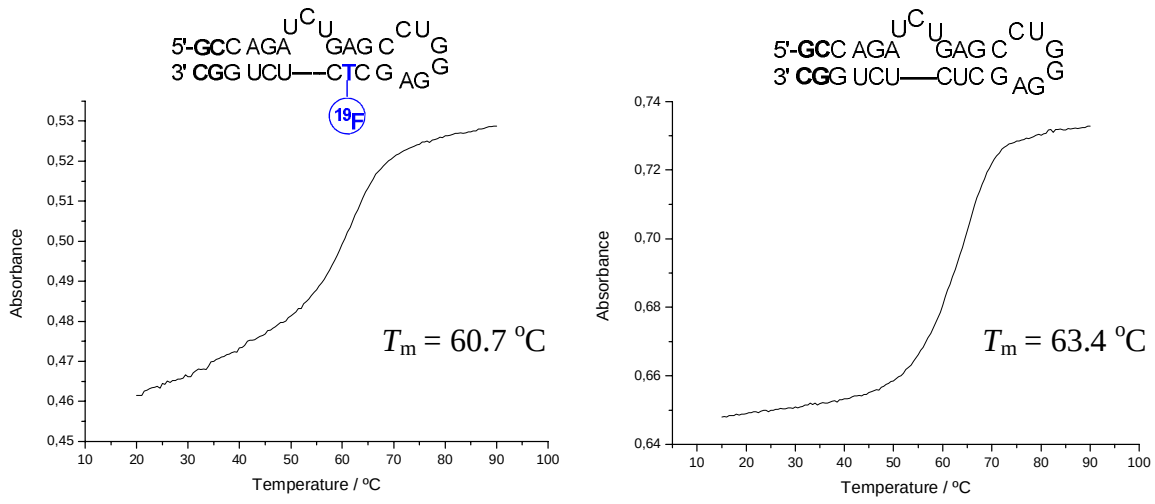

Figure 38. UV-melting curves of ^{19}F-labeled TAR model and native TAR.

3.2.2 ^{19}F NMR spectroscopy studies

The critical parameters for determining the effects on the spectrum upon ligand binding to target nucleic acid are the chemical shift differences resulting from changes in environment of the fluorine probe and the rate of transfer between free and complexed (RNA + ligand) states.[140] If the binding of a ligand is strong, the equilibrium between the complexed and the free state is slow in the NMR time scale and two distinct signals are obtained. Consequently, K_d may be determined by comparing relative peak areas. By contrast, when the binding of a ligand is relatively weak, the exchange between bound and free forms will be rapid. This leads to averaged signal and K_d may be accurately determined (if the well-behaved fast-exchange ligand-RNA interaction is obtained) by following the signal shift. Intermediate exchange case results in line broadening and this type of signal indicates the presence of dynamic processes.

Sample preparation for the ^{19}F-NMR measurements and the details of the instrumental and experimental protocols are presented in the Experimental part. The concentration used for TAR oligonucleotide was 20 μmol L^{-1} and the measurements were performed in 25 mmol L^{-1} NaH_2PO_4-buffer (pH 6.5) in D_2O-H_2O (1:5 *v*/*v*).

3.2.2.1 Melting temperature determination of TAR model

^{19}F-NMR spectroscopy was previously used in melting temperature determinations of hairpin and double helix structures incorporating 2,4-difluorotoluene nucleoside in the place of uridine.[148] Upon stepwise increase of temperature, the ^{19}F-NMR spectra reflected the melting behavior. In the case of monomolecular hairpin model, the melting process occurred in the fast exchange regime on the NMR time scale giving averaged signal. When the shifts in ^{19}F resonances were plotted against temperature, a sigmoidal curve was received and the obtained T_m was reported to correlate with that measured by UV-spectroscopy. In contrast, the melting behavior of a bimolecular duplex showed slow exchange regime on the NMR time scale and two sets of signals were observed. Plotting the fraction of single strand against temperature, afforded the T_m value.

Similarly, the applicability of the ^{19}F-probe used in the present study was evaluated for the melting temperature determination of TAR model (see **A**→**B** in Figure 39).[IV] At 25 °C, the probe gave one sharp ^{19}F resonance signal at −66.32 ppm, which upon heating underwent a linear temperature-dependent passive shift to downfield (traces i−iv in Figure 39a and slope 0.014 ppm K^{-1} in Figure 39b; note the reference signal with the same value). On approaching the T_m value (v−vii in Figure 39a), this signal was broadened and a new broad signal appeared 0.4 ppm upfield. The latter signal most likely referred to the denatured form **B** of the TAR model. As the two signals were observed simultaneously and no averaging occurred, it meant that the equilibration between the double-helical (**A**) and single-stranded (**B**) forms of the TAR model was slow on the NMR time scale below the melting temperature. Upon further heating, the signals shifted closer to each other,

being almost equal sized at 60 °C (~T_m, vii in Figure 39a). Coalescence to the broad signal at −66.32 ppm was observed at 66 °C (vi in Figure 39a). According to the shift, this signal referred to a mixture in which **B** predominated. After completion of the denaturation process (>70 °C), the signal was sharpened and a linear temperature-dependent passive shift downfield (vii in Figure 39a) was again observed. As seen in Figure 39b, a unique negative *S*-curve (^{19}F shift *vs* temperature) was obtained. The sharp inflection point of the curve referred to thermal denaturation, consistent with the profile obtained by UV spectroscopy (T_m = 60.7 °C).

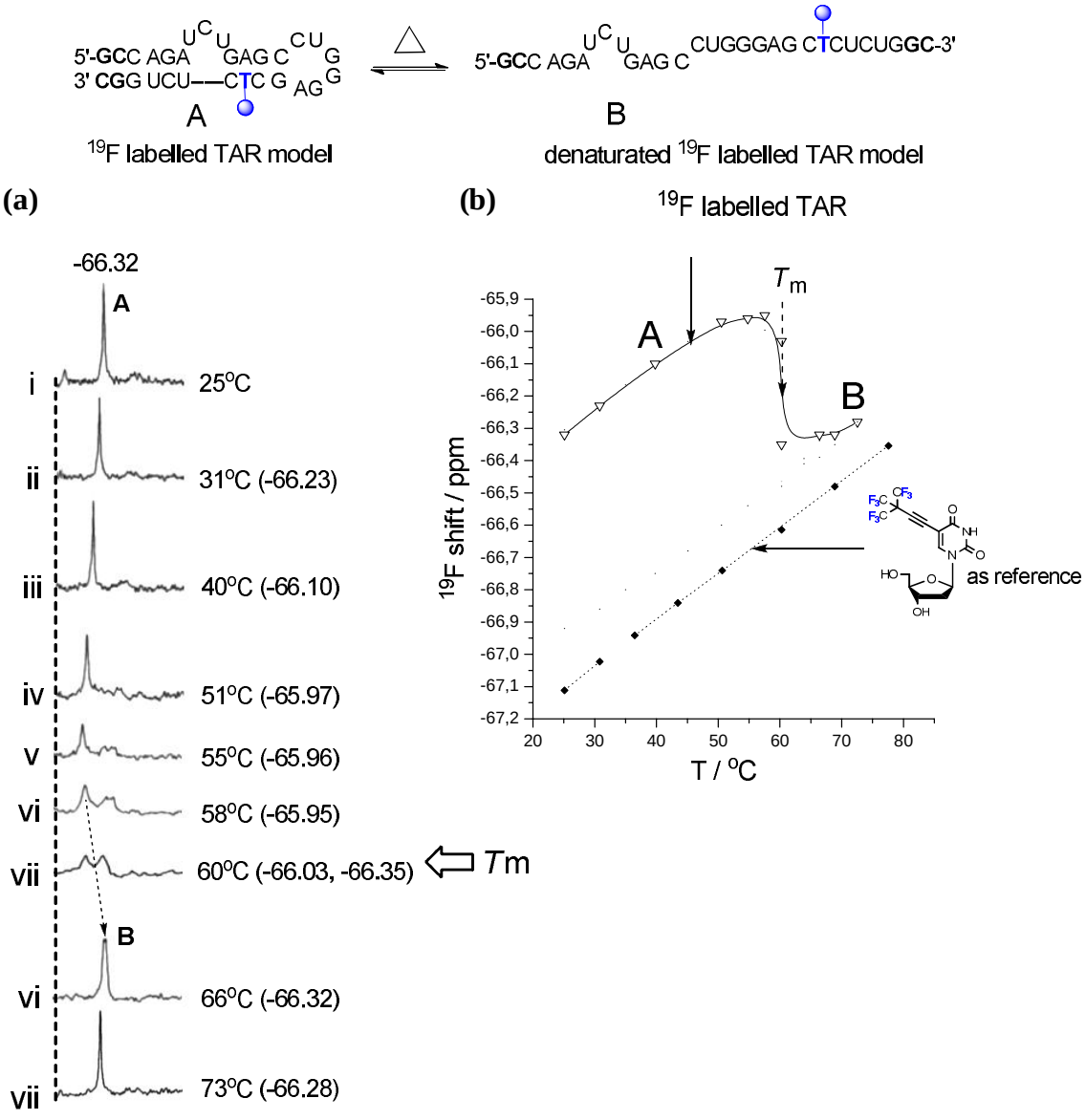

Figure 39. Thermal melting of the TAR model **A**. (a) Corresponding ^{19}F NMR spectra at different temperatures and (b) profile of the ^{19}F resonance shifts *versus* temperature of the TAR model (▽) and a reference 5-[4,4,4-trifluoro-3,3-bis(trifluoromethyl)but-1-ynyl]-2′-deoxyuridine (◆).

3.2.2.2 Invasion of short oligomers to TAR model

Two 2′-*O*-methyl oligoribonucleotide invaders, *viz*. 5′-CUC CCA GGC UCA-3′ (**ON^{12}**) and 5′-CA GGC UCA-3′ (**ON^{8}**), were chosen for invasion studies of the TAR model (Scheme 12). The selected 12-mer **ON^{12}** has been previously demonstrated to inhibit Tat-dependent *in vitro* transcription in HeLa cell nuclear extract.[51] Additionally, a pseudo-half-knotted TAR RNA complex has been reported to be formed with the two-nucleotide-shifted 12-mer 5′-CCC AGG CUC ACA-3′.[138] On the other hand, **ON^{8}** is of special interest, because a weak interaction is expected to occur between **ON^{8}** and TAR model **A** resulting in a dynamic equilibrium that is difficult to study by other methods. For the titration experiments the 2´-*O*-methyl invader oligomers **ON^{8}** and **ON^{12}** were gradually added as 1 and 5 mmol L^{-1} solutions, respectively, to the solution of **A**.[IV]

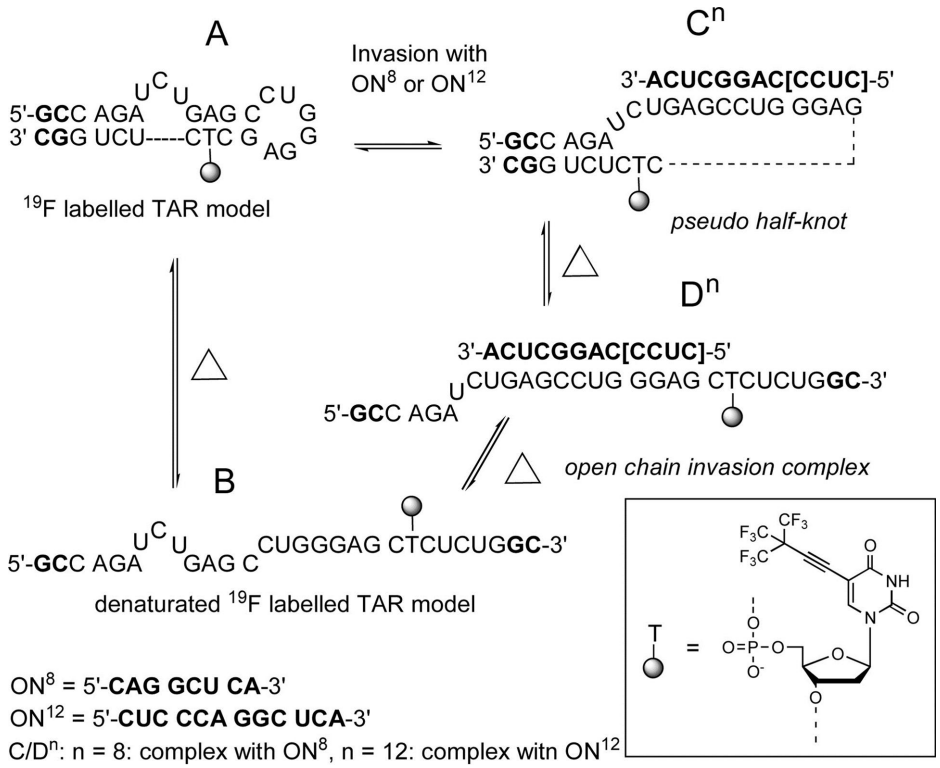

Scheme 12.

3.2.2.2.1 Invasion of ON^{12}

Upon titration of **A** with **ON^{12}** at 25 °C (see **A**→**C^{12}** and **D^{12}** in Scheme 12), the signal of **A** disappeared, and a novel signal at −66.89 ppm (Figure 40) appeared almost quantitatively (K_d = 0.11 ± 0.06 μmol L^{-1} at 25 °C), referring most likely to formation of **C^{12}** by chain invasion.

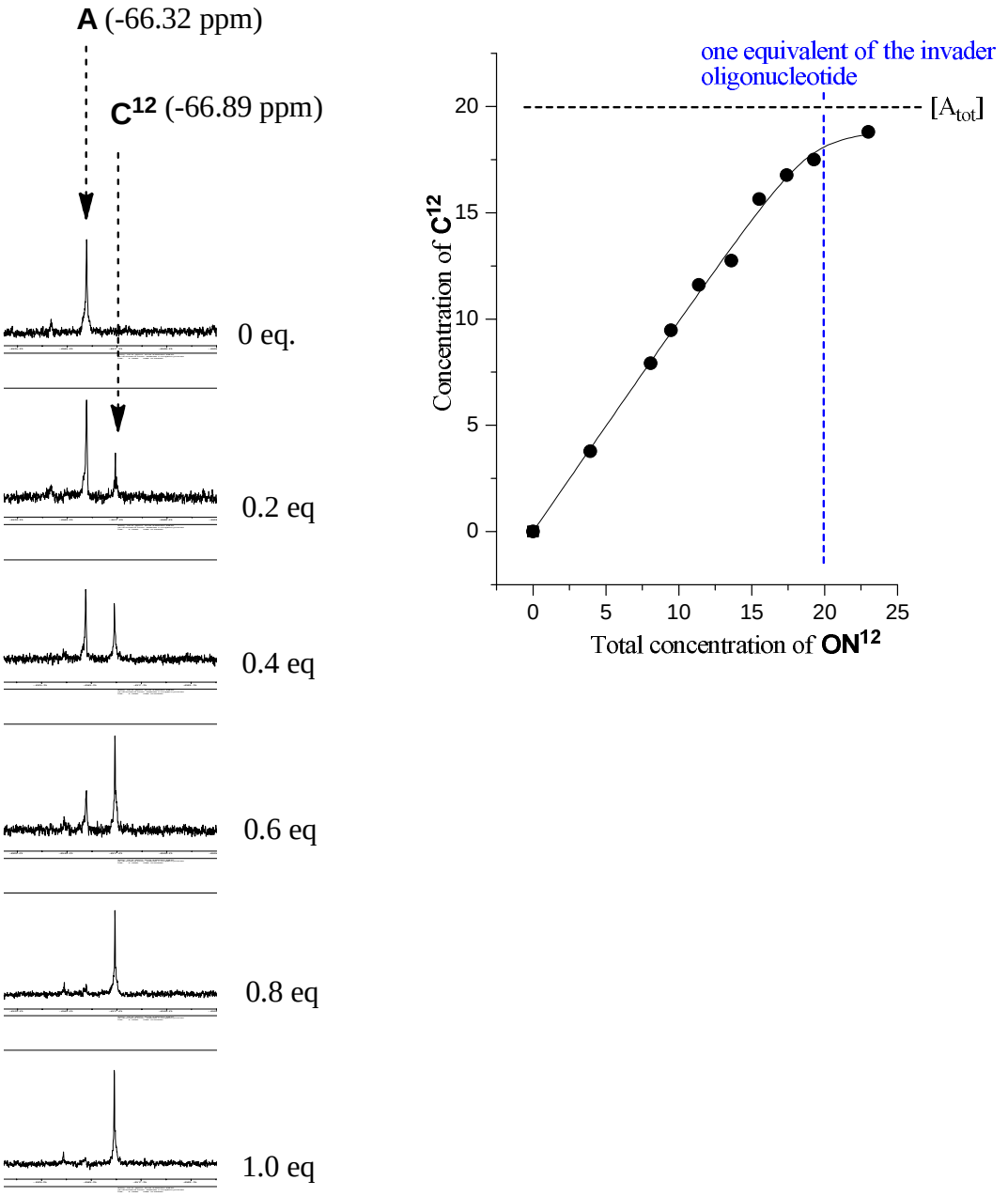

Figure 40. Titration of the TAR model **A** with $\mathbf{ON}^{12}$.

Dissociation constant K_d was calculated based on following equations (see Experimental):

$$K_d = \frac{[\mathbf{A}][\mathbf{ON}]}{[\mathbf{C}]} \qquad [\mathbf{A}] + [\mathbf{C}] = [\mathbf{A_{tot}}] \qquad [\mathbf{ON}] = [\mathbf{ON_{tot}}] - [\mathbf{C}]$$

where
[**C**] = concentration of the complex ($\mathbf{C}^8$ or $\mathbf{C}^{12}$)
[$\mathbf{ON_{tot}}$] = total concentration of the 2'-*O*-methyl oligoribonucleotide ($\mathbf{ON}^8$ or $\mathbf{ON}^{12}$)
[**ON**] = concentration of the free $\mathbf{ON}^8$ or $\mathbf{ON}^{12}$
[**A**] = concentration of the free ^{19}F labelled TAR model **A**.
[$\mathbf{A_{tot}}$] = initial concentration of **A**

Interestingly, on increasing the temperature, gradual conversion of this signal to another one 0.05 ppm upfield took place (i−vi in Figure 41), the two signals being equal at 45 °C (v in Figure 41). At 51 °C, they were merged to a single broad signal (vi in Figure 41). As mentioned above, a pseudo-half-knotted TAR RNA complex has previously been characterized.[138] Most likely, the first observed signal referred to a macro-looped complex that resembles the half-knot $\mathbf{C}^{12}$ (Scheme 12) and the latter signal to a stable open-chain invasion complex $\mathbf{D}^{12}$. When the temperature was further increased, the signal of $\mathbf{D}^{12}$ was almost linearly shifted downfield, and eventually it merged with the signal of the single-stranded form **B** of the TAR model (vii in Figure 39). Thermal denaturation of $\mathbf{D}^{12}$, hence, took place at a higher temperature than the conversion of the hairpin TAR (**A**) to an open-chain form (**B**), consistent with the T_m value of 65.7 °C obtained by thermal UV profile. The signals of $\mathbf{D}^{12}$ and **B** overlap as expected, since the melting of $\mathbf{D}^{12}$ was not accompanied by any marked change in the immediate vicinity of the ^{19}F probe. The temperature-dependent behavior of the $\mathbf{C}^{12}\rightarrow\mathbf{D}^{12}$ complex was additionally characterized by ^{1}H NMR spectroscopy of the imino region involved in Watson-Crick base pairing. ^{1}H NMR spectroscopy supported qualitatively the ^{19}F NMR spectroscopic data, but suffered from signal overlapping and complexity.

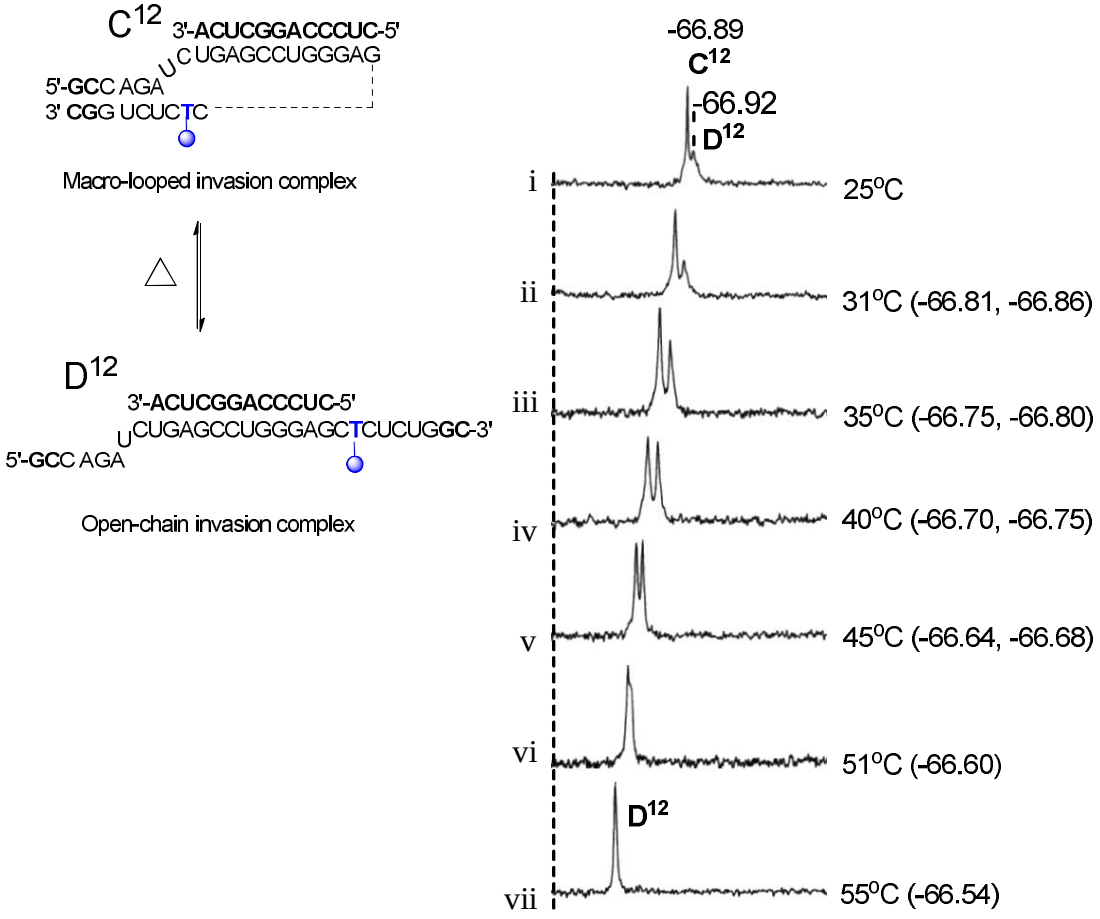

Figure 41. Thermal melting of the complex $\mathbf{C}^{12}$.

3.2.2.2.2 Invasion of ON^{8}

Titration with an 8-mer oligonucleotide, **ON^{8}**, could also be successfully monitored. As expected, the affinity was weak, but a 1:1 complex was formed (K_d = 18.5 ± 1.1 μmol L^{-1} at 25 °C, Figure 42). At 25 °C and in an excess (15 equiv) of **ON^{8}**, the ^{19}F signal referring to the macro-looped invasion complex **C^{8}** (−66.90 ppm, Figure 42) predominated.

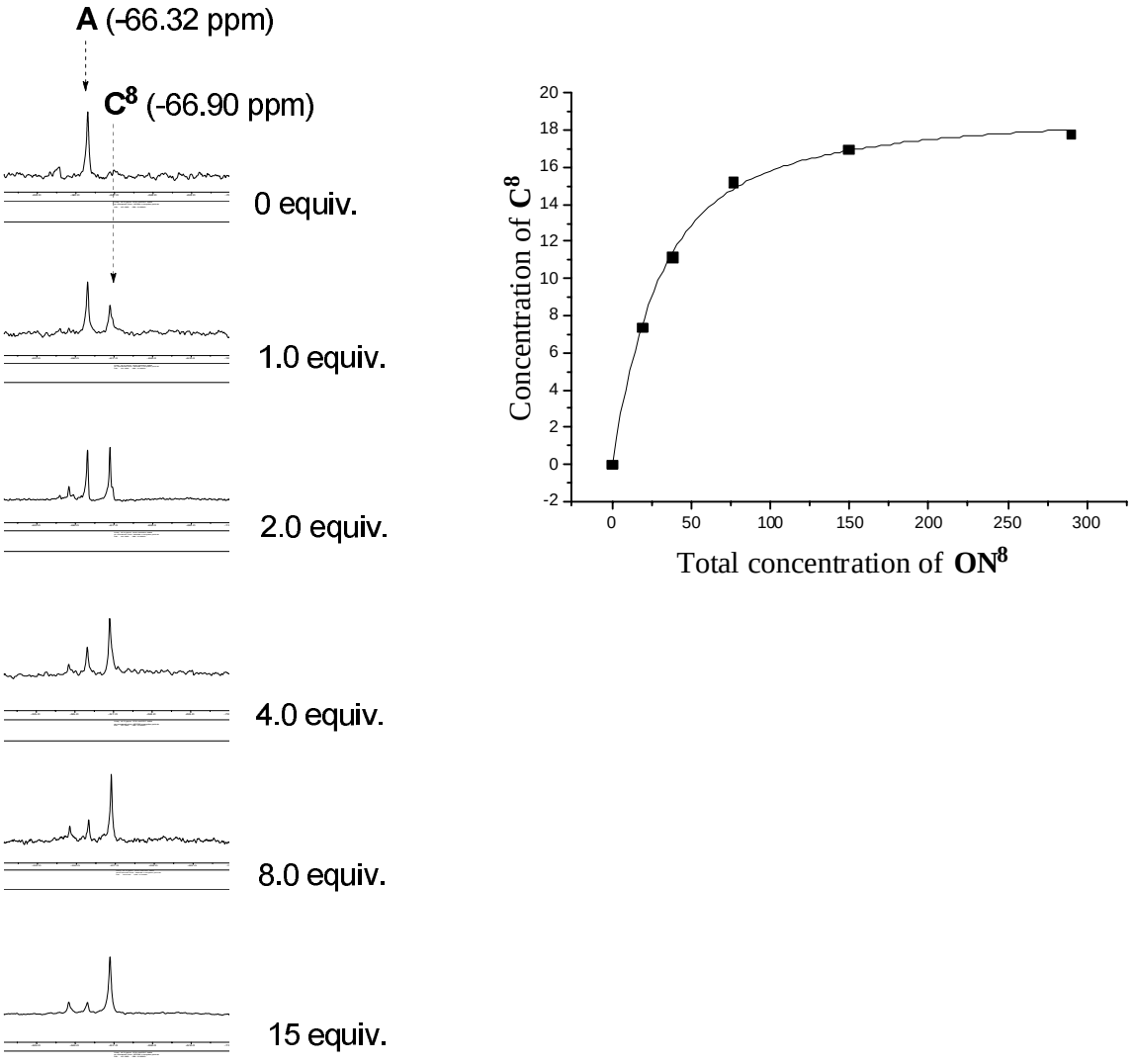

Figure 42. Titration of the TAR model **A** with **ON^{8}**.

As with **ON^{12}**, the complex exhibited two, albeit broader and partially overlapped, signals at a higher temperature (**C^{8}**/**D^{8}**). In addition, the signal of the hairpin form **A** of the uncomplexed TAR model was increased upon heating (from 25 to 45 °C, viii−x in Figure 43a). Owing to this dynamic equilibrium, a clear thermal denaturation temperature for the complex could not be determined. However, compared to the signal of **A** the relative peak area of the complex signal suddenly started to increase on passing 45 °C (xi−xiv in Figure 43a). This phenomenon occurred clearly prior to thermal unwinding of **A**. The relative peak areas of the ^{19}F

resonance signals at various temperatures are seen in Figure 43b. It is worth noting that the composition of the structures cannot be reliably determined, since signals may be sums of overlapped coalescent and scattered signals. In spite of the potential integration errors, the profile in Figure 43b illustrates competition of intramolecular (**A**⇄**B**) and intermolecular (**D**⇄**B**) hybridization prior to thermal unwinding of **A**, and the invasion clearly took over on passing 45 °C. In other words, at a temperature higher than 45 °C, the predominant complex was $\mathbf{D}^{8}$ and the efficiency of $\mathbf{ON}^{8}$ (present in excess) to work as a denaturant increased upon heating. At a temperature lower than 45 °C, the predominant invasion complex was $\mathbf{C}^{8}$, and its proportion decreased upon heating.

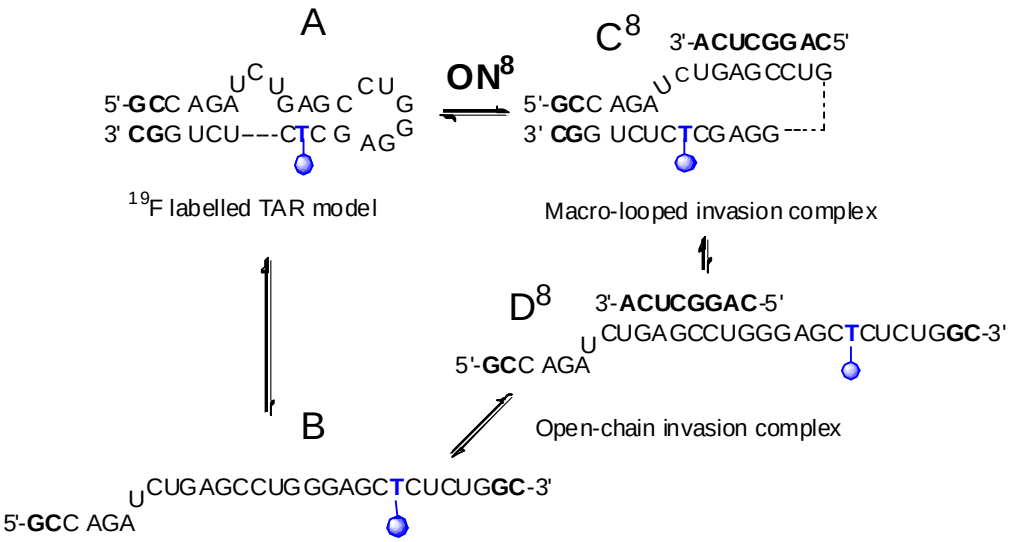

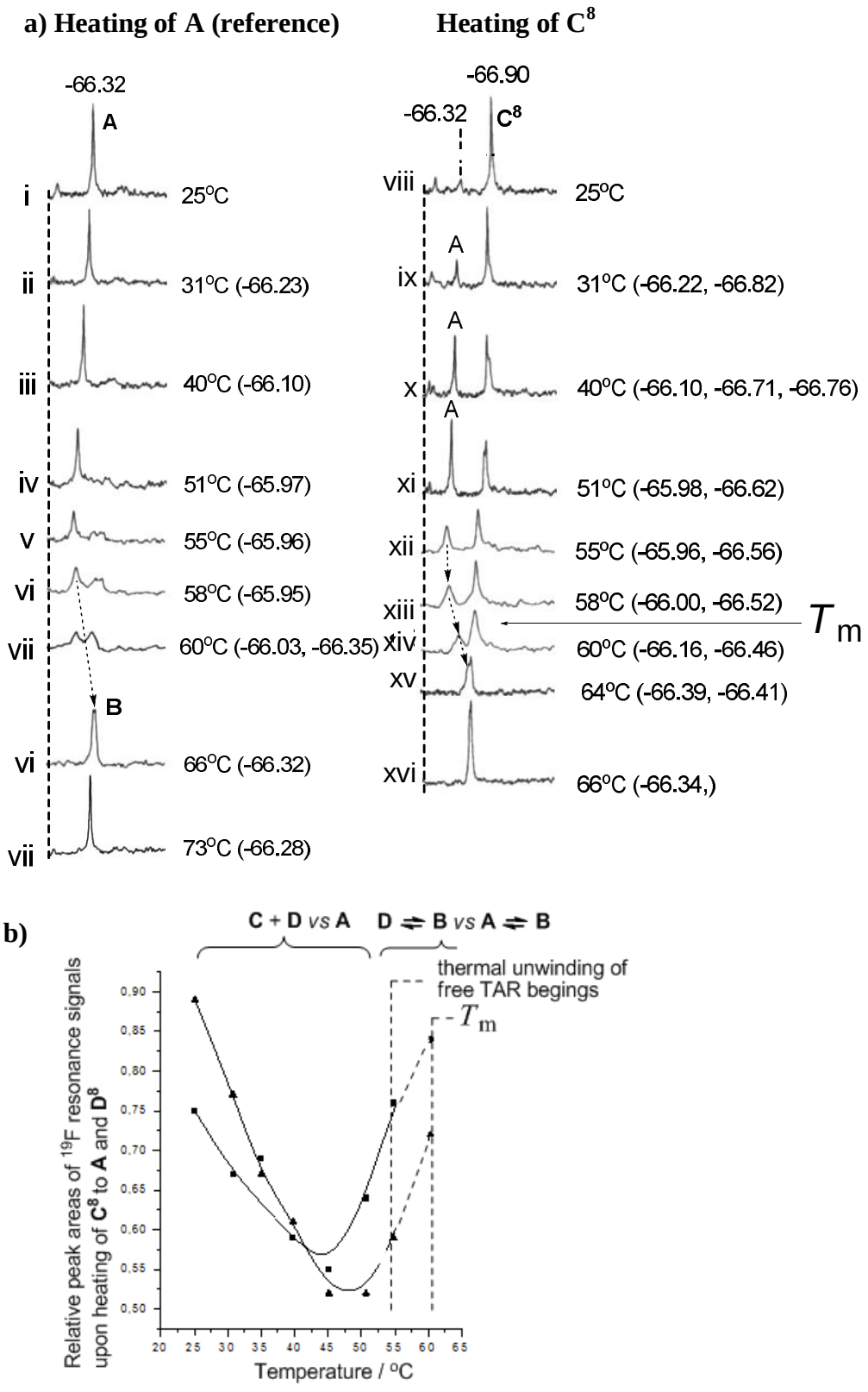

Figure 43. (a) Thermal melting of the complex $\mathbf{C}^{8}$, (b) relative peak areas of the ^{19}F resonance signals upon heating of the invasion complex $\mathbf{C}^{8}$ (to **A** and $\mathbf{D}^{8}$) in the presence (■) and absence (▲) of neomycin B (see Section 3.2.2.2.3).

Thermal ^{19}F profiles (^{19}F shift *vs* temperature) obtained by heating **C**^{8} and **C**^{12} complexes are shown in Figure 44. The UV melting profile of the mixture **A** + **ON**^{8} (15 equiv) exhibited T_m = 58.9 °C, which was lower than that of the thermal denaturation of the TAR model **A** to an open-chain form **B** (60.7 °C) without **ON**^{8}. Noteworthy, since the UV-studies were performed in a diluted 2 μmol L^{-1} solution of **A**, the weak complexes are more dissociated.

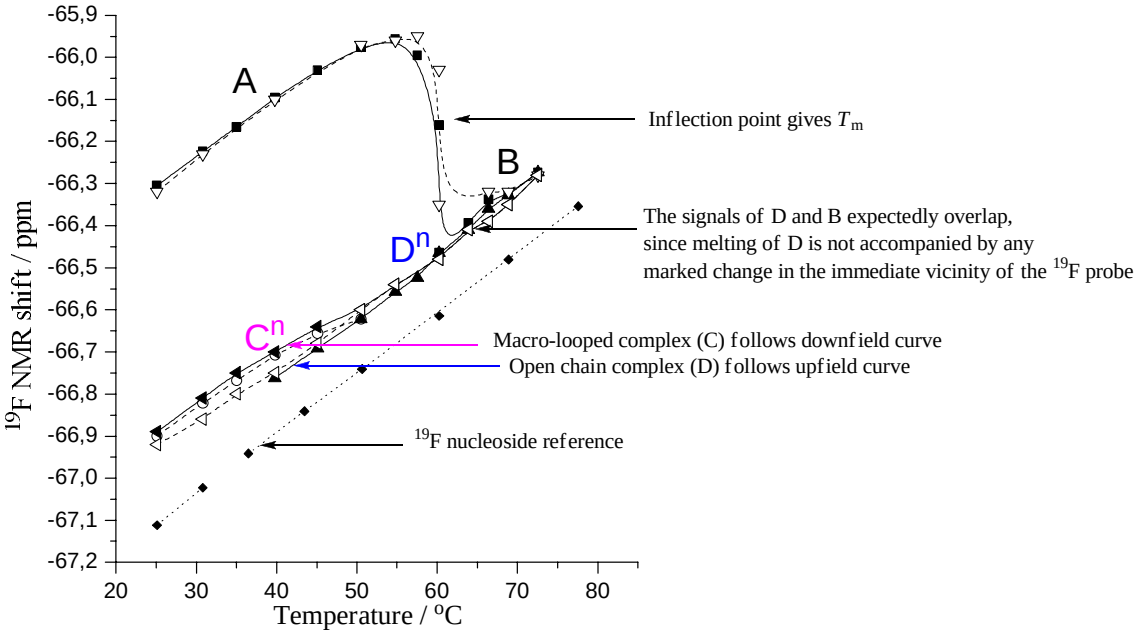

Figure 44. Profiles of the ^{19}F NMR resonance shifts *versus* temperature. Shifts obtained by heating **C**^{8} (■,▲,◀), **A** (▽), **C**^{12} (○,◁) and 5-[4,4,4-trifluoro-3,3-bis(trifluoromethyl)but-1-ynyl]-2′-deoxyuridine (◆) as a reference.

3.2.2.2.3 Invasion of ON^{8} in the presence of neomycin B

Titration of **A** with **ON**^{8} was additionally performed in the presence of a known TAR ligand, neomycin B, which was used 1.0 equiv compared to **A**. Binding of neomycin itself led to formation of two additional broad ^{19}F signals (peaks with asterisks, vii in Figure 45), which skewed integration of relative peak areas at low **ON**^{8} concentrations (viii in Figure 45). Upon further titration, the signal of the complex was sharpened (ix−xi), and a ballpark estimate of the K_d value (11 ± 7 μmol L^{-1} at 25 °C) could be determined. As a result, the presence of neomycin B ligand somewhat enhanced the invasion (compare to K_d = 18.5 ± 1.1 μmol L^{-1}).

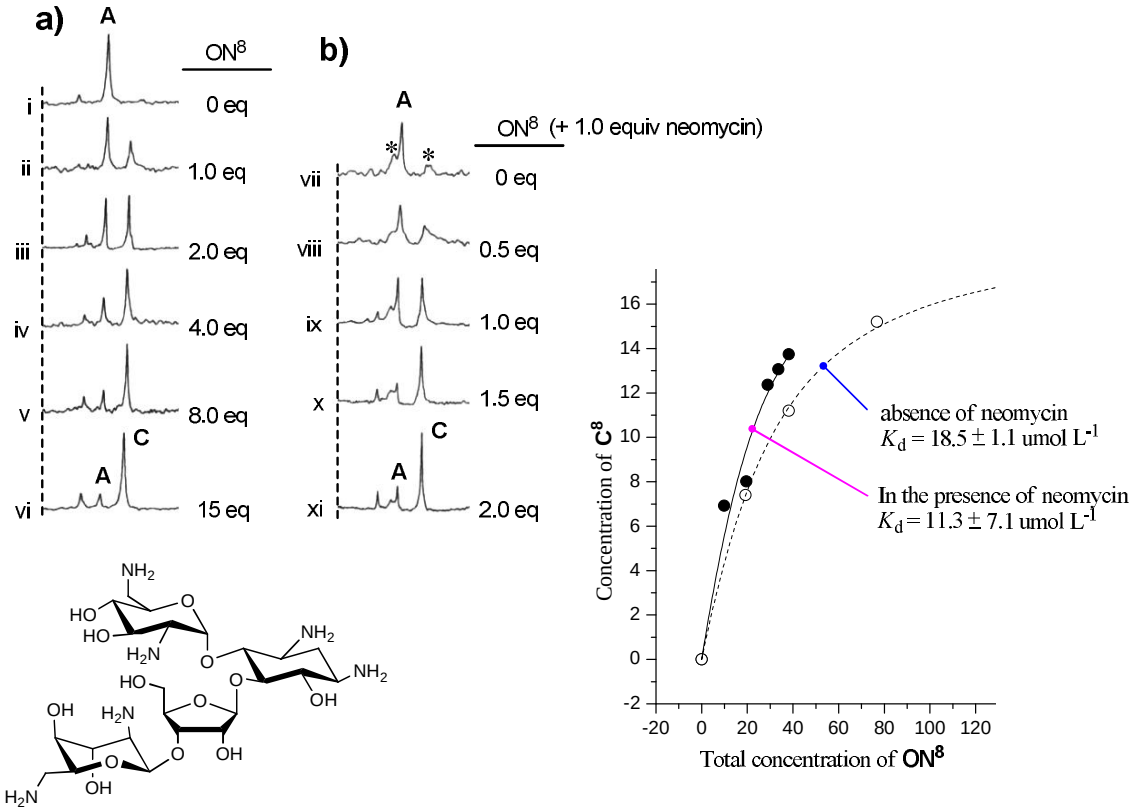

Figure 45. ^{19}F NMR spectra upon titration of **A** with **ON^8** in the absence (a, ii−vi) and in the presence (b, viii−xi) of neomycin.

The site-specific binding of neomycin is known to occur below the bulged nucleotides of native TAR region through the minor groove.[23,210] Therefore, it was expected that any change in the invasion efficiency is related to this specific binding and is confined to low temperatures. Upon heating of the mixture of **A**, **ON^8**, and neomycin (1:2:1 n/n/n), the equilibrium inconsistently behaved like the mixture without neomycin, and the ^{19}F shift *vs* temperature followed the profile of **C^8** (Figure 43b, 44).[IV] Although the temperature-dependent behavior did not show mechanistic details, neomycin clearly enhanced the invasion. For example, in these experiments, a 1:2 mixture of **A** and **ON^8** in the presence of neomycin resulted in approximately the same conversion as obtained by the corresponding 1:8 mixture without neomycin (xi compared to v in Figure 45). The UV melting profile of the mixture gave T_m = 62.5 °C, which was higher than that of the mixture without neomycin (**A**:**ON^8**, 1:15 n/n).

4. SUMMARY

Altogether five different nucleosidic building blocks that allow the development of post-synthetic click-conjugation strategies were synthesized in high yield: 4´-*C*-azidomethylthymidine 3´-(*H*-phosphonate) (**1**), 4´-*C*-[*N*,*N*-di(4-pentyn-1-yl)aminomethyl]thymidine 3´-phosphoramidite (**2**), 4´-*C*-[*N*-methyl-*N*-(4-pentyn-1-yl)aminomethyl]thymidine 3´-phosphoramidite (**3**), 2´-*O*-[(2-azidoethoxy)methyl]cytidine 3´-(*H*-phosphonate) (**4**) and 2´-*O*-[(2-bromoethoxy)methyl]cytidine 3´-phosphoramidite (**5**). Click chemistry, referring here to the Cu(I)-catalyzed Huisgen 1,3-dipolar cycloaddition between azide and alkyne, was proven to be highly efficient and orthogonal conjugation method for oligonucleotides incorporating monomers **1**-**4**. Ligands included azido or alkynyl functionalized derivatives of neutral carbohydrates, aminoglycosides and *p*-aminomethylbenzene. Nucleoside **2** bearing two 4-pentyn-1-yl groups enables high density functionalization of oligonucleotides whereas nucleosides **1**, **3** and **4** allow one-armed conjugations. Click reactions were performed mostly on a solid support, but they can also be carried out in solution. The parallel use of monomers **1**-**4** with monomer **5** having 2´-*O*-[(2-bromoethoxy)methyl]-branch enables double click conjugation strategy. That is, two different ligands can be attached to the oligonucleotide when after first click reaction of monomers **1**-**4**, the same reaction is utilized to conjugate the second ligand after conversion of the bromo substituent in monomer **5** to azido group on solid support. This was demonstrated with oligonucleotides containing building blocks **4** and **5**.

In oligonucleotide assembly on an automated DNA/RNA synthesizer, the azido-bearing monomers **1** and **4** were introduced to the chain applying *H*-phosphonate coupling instead of the conventional phosphoramidite approach, because of the intramolecular Staudinger reaction between azido and phosphoramidite groups. However, the presence of an azido group in the growing solid-supported oligonucleotide chain did not disturb the phosphoramidite coupling of subsequent monomers and thus, the Staudinger reaction seems to interfere with only genuinely intramolecular reactions. This observation is of practical value, since phosphoramidite method is applied in majority of synthesizers and with commercially available building blocks. Therefore, *H*-phosphonate coupling was used only for monomers **1** and **4** and otherwise phosphoramidite method was applied for oligonucleotide synthesis.

Importantly, monomers **1**-**4** were shown to allow intrachain conjugations of the oligonucleotides as they were well accommodated to the duplexes formed with complementary DNA and 2´-*O*-Me RNA targets. The melting temperature studies demonstrated the utility of 2´- and 4´-modified nucleosides **1**-**4** in glycoconjugations. The 4´-modified oligonucleotides containing one to four mannose ligands in the central part of the chain formed equally stable duplexes with complementary 2´-OMe RNA as the corresponding unmodified DNA sequence. At high salt content, the mannose-conjugation was even stabilizing. Especially the conjugates of 4´-*C*-alkynyl monomers **2** and **3** showed encouraging

hybridization properties and all amino group bearing conjugates stabilized the DNA·DNA duplex significantly and the DNA·2´-*O*-methyl RNA duplex notably.

In the second part of the Results and Discussion, the applicability of ^{19}F NMR spectroscopy for the characterization of RNA invasion was demonstrated. 5-[4,4,4-Trifluoro-3,3-bis(trifluoromethyl)but-1-ynyl]-2′-deoxyuridine fluorine probe was incorporated into the HIV-1 TAR RNA model, which was then targeted with two 2′-*O*-methyl oligoribonucleotide invaders, *viz*. 5′-CUC CCA GGC UCA-3′ (**ON^{12}**) and 5′-CA GGC UCA-3′ (**ON^{8}**). The K_d values for RNA-ligand interaction were determined with titration studies and the methodology allowed the detection of temperature-dependent behavior of the complexes. Additionally, the invasion of **ON^{8}** to the TAR model was shown to be enhanced in the presence of a known TAR ligand neomycin B. ^{19}F NMR provided a novel approach for detailed monitoring of equilibrium dynamics, which is hardly achieved by any other method.

5. EXPERIMENTAL

5.1 General

The synthetic methods discussed in the thesis are reported in the original publications except for the synthesis of 3´-*O*-(4,4´-dimethoxytrityl)-4´-*C*-hydroxymethylthymidine (**11**), which has been previously reported[168] but with undetailed description and with different transient protecting group in 5´-OH (See below). Also the formation of compounds **23** and **26** bearing an oxetane-ring structure are descripted here. The oligonucleotides were synthesized on an Applied Biosystems 392 DNA synthesizer and the protocol details for oligonucleotide assembly as also for click-conjugations are described in the Results and Discussion and in original publications.

For the characterization of compounds obtained by solution synthesis ^{1}H NMR, ^{13}C NMR, ^{31}P NMR and HRMS methods have been employed when applicable. RP HPLC analysis of oligonucleotide conjugates were performed using either Supelco Ascentis C18 (150 × 4.6 mm, 5 µm) analytical column (for ONs **58**, **59**, **66**-**70**) or Thermo ODS Hypersil C18 (250 × 4.6 mm, 5 μm) column (for ONs **60**-**65**, **71**-**82**). UV detection at 260 nm was used. Detailed chromatographic conditions are given in the Results and Discussion. Electropherograms were obtained by capillary zone electrophoresis using a fused silica capillary (75 μm, 50 cm), inverted polarity, citrate buffer (0.2 mol L^{-1}, pH 3.1), -30 kV voltage and detection wavelength of 254 nm.

Synthesis of 3´-O-(4,4´-dimethoxytrityl)-4´-C-hydroxymethylthymidine:

3´-*O*-(4,4´-Dimethoxytrityl)thymidine (10). To a solution of thymidine **9** (5.16 g, 21.3 mmol) in 80 mL of dry pyridine, benzoyl chloride (2.5 mL, 21.5 mmol) was added on an ice bath. The mixture was stirred overnight at room temperature and evaporated. The residue was dissolved in dichloromethane and extracted with water. The organic fraction was dried with Na_2SO_4, evaporated and subjected to the next step without further purification. The crude 5´-*O*-benzoylthymidine was dissolved in dry pyridine (60 mL) and 4,4´-dimethoxytrityl chloride (6.65 g, 19.6 mmol) was added. The reaction was heated at 50 ºC overnight and after evaporation, the residue was partitioned between dichloromethane and water. The organic fraction was dried with Na_2SO_4 and evaporated. The crude 5´-*O*-benzoyl-3´-*O*-(4,4´-dimethoxytrityl)thymidine was dissolved in MeOH (120 mL) and to remove the benzoyl protection, sodium methoxide [sodium (1.00 g, 43.0 mmol) in MeOH (50 mL)] was added. After stirring the reaction at room temperature for 2 h, the mixture was evaporated and purified by silica gel chromatography (60-100 % ethyl acetate in petroleum ether + 0.1 % triethylamine). This afforded compound **10** (8.36 g, 78%) as a white solid foam. The given yield is calculated from the restrictive compound DMTrCl, but since the first benzoylation step goes quantitatively (isolation data not shown here) the given yield can be considered as an overall yield of the three steps. ^{1}H NMR (500 MHz, $CDCl_3$) δ_{ppm} 8.56 (br s, 1H), 7.46-7.42 (m, 2H), 7.36-7.27 (m, 6H), 7.25-7.20 (m, 2H), 6.86-6.81 (m, 4H), 6.13

(dd, 1H, *J* = 8.8 Hz, 5.8 Hz), 4.36 (m, 1H), 3.97 (m, 1H), 3.79 (s, 6H), 3.66 (m, 1H), 3.32 (m, 1H), 2.46 (m, 1H), 1.93 (m, 1H), 1.85 (s, 3H), 1.70 (m, 1H); ^{13}C NMR (125 MHz, $CDCl_3$) δ_{ppm} 163.5, 158.8, 150.3, 145.1, 137.2, 136.3, 136.2, 130.3, 130.2, 128.3, 128.0, 127.1, 113.4, 113.3, 111.0, 87.5, 87.2, 86.6, 74.3, 62.6, 55.3, 38.7, 12.5.

3´-*O*-(4,4´-Dimethoxytrityl)-4´-*C*-hydroxymethylthymidine (11). To the suspension of compound **10** (3.35g, 6.2 mmol) and DCC (3.79g, 18.4 mmol) in DMSO (23 mL), a solution of trifluoroacetic acid (0.24 mL, 3.1 mmol) and pyridine (0.73 mL, 9.1 mmol) in DMSO (20 mL) was added on an ice bath and the reaction proceeded at room temperature overnight. Ethyl acetate was added to the reaction mixture and prior to the extraction with water and brine, the precipitated DCU (*N*,*N'*-dicyclohexylurea) was removed by filtration. The organic phase was separated, dried with Na_2SO_4 and evaporated to dryness. The received aldehyde product was then subjected to the aldol condensation followed by Cannizzaro reduction. The crude product was dissolved in 1,4-dioxane (170 mL) and formaldehyde (47 mL of 37% solution) and aq NaOH (93 mL of 2.0 mol L^{-1} solution) was added. After stirring overnight at room temperature and evaporation, the reaction mixture was extracted with dichloromethane and water. The organic fraction was dried with Na_2SO_4, evaporated and purified by silica gel chromatography (3-10% MeOH in dichloromethane + 0.1 % triethylamine). The product (**11**, 3.37 g) was isolated in 95% yield. ^{1}H NMR (500 MHz, $CDCl_3$) δ_{ppm} 9.40 (br, 1H), 7.45-7.42 (m, 2H), 7.37-7.27 (m, 6H), 7.23 (m, 1H), 6.86-6.79 (m, 5H), 6.30 (dd, 1H, *J* = 8.3 Hz, 4.3 Hz), 4.54 (dd, 1H, *J* = 8.0 Hz, 8.0 Hz), 4.09 (d, 1H, *J* = 12.5 Hz), 3.97 (d, 1H, *J* = 11.5 Hz), 3.82-3.74 (m, 7H), 3.43 (d, 1H, *J* = 11.0 Hz), 1.98 (m, 1H), 1.71 (s, 3H), 1.16 (m, 1H); ^{13}C NMR (125 MHz, $CDCl_3$) δ_{ppm} 163.7, 158.9, 158.9, 150.7, 145.1, 136.6, 136.1, 135.9, 130.4, 128.3, 128.0, 127.3, 113.3, 113.3, 111.2, 89.2, 87.2, 82.8, 72.5, 62.7, 61.7, 55.3, 38.7, 12.3.

*The formation of oxetane compounds **23** and **26**:*

5´-*O*-(4,4´-Dimethoxytrityl)-*O*$^{3´}$,4´-methylenethymidine (23). 5´-*O*-(4,4´-Dimethoxytrityl)-4´-*C*-tosyloxymethylthymidine (**22**, 0.80 g, 1.1 mmol) was dissolved in DMF (7 mL) and pyridine (1.8 mL) and sodium azide (0.36 g, 5.5 mmol) was added. The reaction mixture was heated at 140 °C for 8 h and evaporated. The residue was partitioned between dichloromethane and water. The organic fraction was dried with Na_2SO_4, evaporated and purified by silica gel chromatography (50-100% ethyl acetate in petroleum ether). The compound **23** (0.35g) was isolated as white foam in 57% yield. The desired product 4´-*C*-azidomethyl-5´-*O*-(4,4´-dimethoxytrityl)thymidine (**15**) was not detected. ^{1}H NMR (500 MHz, $CDCl_3$) δ_{ppm} 8.57 (br, 1H), 7.48 (d, 1H, *J* = 1.0 Hz), 7.40-7.37 (m, 2H), 7.32-7.24 (m, 7H), 6.89 (dd, 1H, *J* = 8.8 Hz, 5.8 Hz), 6.86-6.82 (m, 4H), 5.37 (d, 1H, *J* = 4.5 Hz), 4.54 (d, 1H, *J* = 7.5 Hz), 4.42 (d, 1H, *J* = 8.0 Hz), 3.80 (s, 3H), 3.80 (s, 3H), 3.55-3.50 (m, 2H), 2.69 (dd, 1H, *J* = 14.0 Hz, 5.8 Hz), 1.90 (m, 1H), 1.45 (d, 3H, *J* = 1.0 Hz); ^{13}C NMR (125 MHz, $CDCl_3$) δ_{ppm} 163.5, 158.8, 150.1,

144.3, 135.3, 135.2, 130.0, 128.1, 128.0, 127.2, 113.3, 112.0, 87.5, 86.7, 86.6, 85.4, 78.3, 63.2, 55.3, 39.4, 11.8; HRMS (FAB$^-$): [M-H] calcd 555.2131, obsd 555.2149.

3´-*O*-(4,4´-Dimethoxytrityl)-*O*$^{5´}$,4´-methylenethymidine (26). 3′-*O*-(4,4′-Dimethoxytrityl)-4′-*C*-propargyloxymethyl-*O*^{2},5′-anhydrothymidine (**24**, 0.57 g, 1.0 mmol) and 3′-*O*-(4,4′-dimethoxytrityl)-4′-*C*-pentynyloxymethyl-*O*^{2},5′-anhydrothymidine (**25**, 0.64 g, 1.0 mmol) were dissolved in 1,4-dioxane (15 mL) and aqueous NaOH (4.5 mL, 2 mol L^{-1}, 9.0 mmol) was added. The mixtures were stirred overnight at room temperature and partitioned between ethyl acetate (150 mL) and water (20 mL). The organic phases were separated, dried with Na_2SO_4, and evaporated to dryness. In both cases, the compound **26** was isolated in >90% yield and, hence, the desired products 3´-*O*-(4,4´-dimethoxytrityl)-4´-*C*-propargyloxymethylthymidine and 3´-*O*-(4,4´-dimethoxytrityl)-4´-*C*-pentynyloxymethylthymidine were not detected . ^{1}H NMR (500 MHz, $CDCl_3$) δ_{ppm} 8.50 (br, 1H), 7.58-7.54 (m, 2H), 7.50-7.41 (m, 4H), 7.36-7.31 (m, 2H), 7.27 (m, 1H), 6.91-6.85 (m, 4H), 6.69 (s, 1H), 5.78 (dd, 1H, *J* = 7.3 Hz, 4.8 Hz), 5.43 (d, 1H, *J* = 6.5 Hz), 4.82 (d, 1H, *J* = 7.0 Hz), 4.78 (d, 1H, *J* = 7.5 Hz), 4.60 (d, 1H, *J* = 7.0 Hz), 4.39 (dd, 1H, *J* = 7.0 Hz, 6.5 Hz), 3.82 (s, 6H), 1.88 (s, 3H), 1.64 (m, 1H), 1.28 (m, 1H); ^{13}C NMR (125 MHz, $CDCl_3$) δ_{ppm} 163.6, 158.9, 149.8, 145.1, 136.2, 136.1, 135.9, 130.4, 130.3, 128.3, 128.1, 127.3, 113.4, 113.4, 111.0, 87.3, 86.2, 86.0, 80.9, 79.1, 75.2, 55.3, 38.0, 12.5; ESI-MS: [M+Na] calcd 579.2, obsd 579.4.

5.2 Melting temperature studies

The melting curves (absorbance versus temperature) were measured at 260 nm on a Perkin-Elmer Lambda 35 UV-vis spectrometer equipped with a Peltier temperature-controller except for ONs **58**, **59**, **66**-**70**, which were measured using an older instrument Perkin-Elmer Lambda 2 UV-vis spectrometer. The results obtained by these instruments differ from each other because the temperature is measured differently. While the newer machine detects the temperature from reference cuvette directly, the old one can measure only the temperature of the peltier element that rounds the cuvette. As a consequence, the obtained T_m values are not directly comparable with each other. The temperature was changed at a rate of 0.5 ºC / min (from 20 to 90 ºC). The measurements were performed in 10 mmol L^{-1} potassium phosphate buffer (pH 7) containing 0.1 mol L^{-1} or 1.0 mol L^{-1} NaCl except in the studies with HIV-1 TAR RNA, in which case 25 mM NaH_2PO_4 buffer (pH 6.5) was used. The oligonucleotides and their targets were used at a concentration of 2 μmol L^{-1}. Only in measurements of HIV-1 TAR RNA with invader **ON^8**, the invader was used in larger quantities (See supporting information of the original publication IV). T_m values were determined as the maximum of the first derivate of the melting curve.

5.3 Invasion studies of HIV-1 TAR RNA using NMR

Oligonucleotides (triethylammonium salts) used in the ^{19}F NMR studies were lyophilized to dryness and dissolved in 25 mmol L^{-1} NaH_2PO_4-buffer (pH 6.5) in D_2O-H_2O (1:5 *v/v*). For the titration experiments, **ON^8** and **ON^{12}** were added as 1

and 5 mmol L^{-1} solutions to a 20 μmol L^{-1} solution of ^{19}F labelled TAR model **A**. For studies with ^{1}H NMR, the fluorine-labeled TAR model **A** and unmodified native TAR sequence **A´** (both 100 μmol L^{-1}) were measured in 25 mmol L^{-1} NaH_2PO_4-buffered (pH 6.5) D_2O-H_2O (1:9, *v/v*) and 1.0 equiv of **ON^{12}** (100 μmol L^{-1}) was added to NMR tubes. Prior to each spectroscopic detection, the mixtures were heated to 90°C for 1 minute and then allowed to cool down to room temperature.

^{19}F NMR spectra were recorded at a frequency of 376.1 MHz on a Bruker Avance 400 MHz spectrometer. Typical experimental parameters were chosen as follows: ^{19}F excitation pulse 12.6 μs, acquisition time 0.675 s, relaxation delay 1.0 s and usual number of scans were 2400 or 4800. ^{19}F resonances were referenced relative to external CCl_3F. ^{1}H NMR spectra were recorded at a frequency of 500.1 MHz on a Bruker Avance 500 MHz spectrometer. Water was suppressed by excitation sculpting technique.[211] Sample temperature was calibrated by using known shifts of ethylene glycol in different temperatures.

K_d values were calculated from relative peak areas of ^{19}F resonance signals of the free TAR model **A** and of the complexes (**C^{8}** and **C^{12}**), according to following equations:

$$K_d[\mathbf{C}] = [\mathbf{A}][\mathbf{ON}]$$

$$[\mathbf{A}] + [\mathbf{C}] = [\mathbf{A_{tot}}]$$

$$[\mathbf{ON}] = [\mathbf{ON_{tot}}] - [\mathbf{C}]$$

$$[\mathbf{C}]^2 - ([\mathbf{A_{tot}}] + [\mathbf{ON_{tot}}] + K_d)[\mathbf{C}] + [\mathbf{ON_{tot}}][\mathbf{A_{tot}}] = 0$$

where:

[**C**] = concentration of the complex (**C^{8}** or **C^{12}**)
[**ON$_{tot}$**] = total concentration of the 2'-*O*-methyl oligoribonucleotide (**ON^{8}** or **ON^{12}**)
[**ON**] = concentration of the free **ON^{8}** or **ON^{12}**
[**A**] = concentration of the free ^{19}F labelled TAR model **A**.
[**A$_{tot}$**] = initial concentration of **A**

$$[C] = \frac{C}{A + C}[A_{tot}] \qquad [A_{tot}] = 20 \times 10^{-6}\ \text{mol}\ L^{-1}$$

↑ a relative ^{19}F peak area of C

6. REFERENCES

[1] Cech, T. R., Zaug, A. J., Grabowski, P. J. *Cell* **1981**, *27*, 487-496.
[2] Guerrier-Takada, C., Gardiner, K., Marsh, T., Pace, N., Altman, S. *Cell* **1983**, *35*, 849-857.
[3] Groβhans, H., Filipowicz, W. *Nature* **2008**, *451*, 414-416.
[4] Serganov, A., Dinshaw, P. J. *Nat. Rev. Genetics* **2007**, *8*, 776-790.
[5] Cheng, J., Kapranov, P., Drenkow, J., Dike, S., Brubaker, S., Patel, S., Long, J., Stern, D., Tammana, H., Helt, G., Sementchenko, V., Piccolboni, A., Bekiranov, S., Bailey, D. K., Ganesh, M., Ghosh, S., Bell, I., Gerhard, D. S., Gingeras, T. R. *Science* **2005**, *308*, 1149-1154.
[6] Uhlmann, E., Peyman, A. *Chem. Rev*. **1990**, *90*, 543-584.
[7] Crooke, S. T. *Annu. Rev. Med*. **2004**, *55*, 61-95.
[8] Aboul-Fadl, T. *Curr. Med. Chem*. **2005**, *12*, 2193-2214.
[9] Chan, J. HP, Lim, S., Wong, WS F. *Clin. Exp. Pharmacol. Physiol*. **2006**, *33*, 533-540.
[10] Dean, N. M., Bennett, C. F. *Oncogene* **2003**, *22*, 9087-9096.
[11] Coppelli, F. M., Grandis, J. R. *Curr. Pharm. Des.* **2005**, *11*, 2825-2840.
[12] Kota, S. K., Balasubramanian, S. *Drug Discovery Today* **2010**, *15*, 733-740.
[13] Fabani, M. M., Turner, J. J., Gait, M. J. *Curr. Opin. Mol. Ther*. **2006**, *8*, 108-114.
[14] Scherr, M., Morgan, M. A., Eder, M. *Curr. Med. Chem*. **2003**, *10*, 245-256.
[15] Sen, G. L., Blau, H. M. *FASEB* **2006**, *20*, 1293-1299.
[16] Kim, D. H., Rossi, J. J. *Nat. Rev. Genetics* **2007**, *8*, 173-184.
[17] Castanotto, D., Rossi, J. J. *Nature* **2009**, *457*, 426-433.
[18] Carthew, R. W., Sontheimer, E. J. *Cell* **2009**, *136*, 642-655.
[19] Kurreck, J. *Angew. Chem. Int. Ed*. **2009**, *48*, 1378-1398.
[20] Fire, A., Xu, S., Montgomery, M. K., Kostas, S. A., Driver, S. E., Mello, C. C. *Nature* **1998**, *391*, 806-811.
[21] Zamecnik, P. C., Stephenson, M. L. *Proc. Natl. Acad. Sci. USA* **1978**, *75*, 280-284.
[22] Stephenson, M. L., Zamecnik, P. C. *Proc. Natl. Acad. Sci. USA* **1978**, *75*, 285-288.
[23] Thomas, J. R., Hergenrother, P. J. *Chem. Rev*. **2008**, *108*, 1171-1224.
[24] Krishnamurthy, M., Simon, K., Orendt, A. M., Beal, P. A. *Angew. Chem. Int. Ed*. **2007**, *46*, 7044-7047.
[25] Gareiss, P. C., Sobczak, K., McNaughton, B. R., Palde, P. B., Thornton, C. A., Miller, B. L. *J. Am. Chem. Soc*. **2008**, *130*, 16254-16261.
[26] Manoharan, M. *Antisense Nucleic Acid Drug Dev*. **2002**, *12*, 103-128.
[27] Behlke, M. A. *Oligonucleotides* **2008**, *18*, 305-320.
[28] Watts, J. K., Deleavey, G. F., Damha, M. J. *Drug Discovery Today* **2008**, *13*, 842-855.
[29] Juliano, R., Bauman, J., Kang, H., Ming, X. *Mol. Pharmaceutics* **2009**, *6*, 686-695.
[30] Jeong, J. H., Mok, H., Oh, Y.-K., Park, T. G., *Bioconjugate Chem*. **2009**, *20*, 5-14.
[31] Bennett, C. F., Swayze, E. E., *Annu. Rev. Pharmacol. Toxicol*. **2010**, *50*, 259-293.
[32] Gaglione, M., Messere, A. *Mini Rev. Med. Chem.* **2010**, *10*, 578-595.
[33] Crooke, S. T. *Biochim. Biophys. Acta* **1999**, *1489*, 31-44.
[34] Zamaratski, E., Pradeepkumar, P. I., Chattopadhyaya, J. *J. Biochem. Biophys. Methods* **2001**, *48*, 189-208.
[35] Corey, D. R. *Nat. Chem. Biol*. **2007**, *3*, 8-11.
[36] Shi, F., Hoekstra, D. *J. Control. Rel*. **2004**, *97*, 189-209.
[37] Khalil, I. A., Kogure, K. Akita, H. Harashima, H. *Pharmacol. Rev.* **2006**, *58*, 32-45.
[38] Monia, B. P., Lesnik, E. A., Gonzalez, C., Lima, W. F., McGee, D., Guinosso, C. J., Kawasaki, A. M., Cook, P. D., Freier, S. M. *J. Biol. Chem.* **1993**, *268*, 14514-14522.
[39] Manoharan, M. *Biochim. Biophys. Acta* **1999**, *1489*, 117-130.
[40] Bramsen, J. B., Laursen, M. B., Damgaard, C. K., Lena, S. W., Babu, B. R.,

Wengel, J., Kjems, J. *Nucleic Acids Res*. **2007**, *35*, 5886-5897.
[41] Hall, A. H. S., Wan, J., Shaughnessy, E. E., Shaw, B. R., Alexander, K. A. *Nucleic Acids Res*. **2004**, *32*, 5991-6000.
[42] Gryaznov, S. M. *Chem. Biodiversity* **2010**, *7*, 477-493.
[43] Prakash, T. P., Kawasaki, A. M., Wancewicz, E. V., Shen, L., Monia B. P., Ross, B. S., Bhat, B., Manoharan, M. *J. Med. Chem*. **2008**, *51*, 2766-2776.
[44] Yu, R. Z., Geary, R. S., Monteith, D. K., Matson, J., Truong, L., Fitchett, J., Levin, A. A. *J. Pharm. Sci.* **2004**, *93*, 48-59.
[45] Chiu, Y.-L., Rana, T. M. *RNA* **2003**, *9*, 1034-1048.
[46] Cekaite, L., Furset, G., Hovig, E., Sioud, M. *J. Mol. Biol*. **2007**, *365*, 90-108.
[47] Judge, A., MacLachlan, I. *Hum. Gene Ther*. **2008**, *19*, 111-124.
[48] Hoshika, S., Minakawa, N., Shionoya, A., Imada, K., Ogawa, N., Matsuda, A. *ChemBioChem* **2007**, *8*, 2133-2138.
[49] Wengel, J. *Acc. Chem. Res.* **1999**, *32*, 301-310.
[50] Koizumi, M. *Biol. Pharm. Bull*. **2004**, *27*, 453-456.
[51] Arzumanov, A., Stetsenko, D. A., Malakhov, A. D., Reichelt, S., SØrensen, M. D., Babu, B. R., Wengel, J., Gait, M. J. *Oligonucleotides* **2003**, *13*, 435-453.
[52] Swayze, E. E., Siwkowski, A. M., Wancewicz, E. V., Migawa, M. T., Wyrzykiewicz, T. K., Hung, G., Monia, B. P., Bennett, C. F. *Nucleic Acids Res.* **2007**, *35*, 687-700.
[53] Seth, P. P., Siwkowski, A., Allerson, C. R.,Vasquez, G., Lee, S., Prakash, T. P., Wancewicz, E. V., Witchell, D., Swayze, E. E. *J. Med. Chem*. **2009**, *52*, 10-13.
[54] Mitsuoka, Y., Kodama, T., Ohnishi, R., Hari, Y., Imanishi, T., Obika, S. *Nucleic Acids Res*. **2009**, *37*, 1225-1238.
[55] Prakash, T. P., Siwkowski, A., Allerson, C. R., Migawa, M. T., Lee, S., Gaus, H. J., Black, C., Seth, P. P., Swayze, E. E., Bhat, B. *J. Med. Chem*. **2010**, *53*, 1636-1650.
[56] Nielsen, P. E. *Chem. Biodiversity* **2010**, *7*, 786-804.
[57] Summerton, J. *Biochim. Biophys. Acta* **1999**, *1489*, 141-158.
[58] Herdewijn, P. *Chem. Biodiversity* **2010**, *7*, 1-59.
[59] Verbeure, B., Lescrinier, E., Wang, J., Herdewijn, P. *Nucleic Acids Res*. **2001**, *29*, 4941-4947.
[60] Juliano, R., Alam, M. R., Dixit, V., Kang, H. *Nucleic Acids Res*. **2008**, *36*, 4158-4171.
[61] Trabulo, S., Cardoso, A. L., Mano, M., Pedroso de Lima, M. C. *Pharmaceuticals* **2010**, *3*, 961-993.
[62] Moulton, J. D., Jiang, S. *Molecules*, **2009**, *14*, 1304-1323.
[63] Zhang, N., Tan, C., Cai, P., Zhang, P., Zhao, Y., Jiang, Y. *Bioorg. Med. Chem*. **2009**, *17*, 2441-2446.
[64] Kang, H., Fisher, M. H., Xu, D., Miyamoto, Y. J., Marchand, A., Van Aerschot, A., Herdewijn, P., Juliano, R. L. *Nucleic Acids Res*. **2004**, *32*, 4411-4419.
[65] Fisher, M., Abramov, M., Van Aerschot, A., Rozenski, J., Dixit, V., Juliano, R. L., Herdewijn, P. *Eur. J. Pharmacol*. **2009**, *606*, 38-44.
[66] Fisher, M., Abramov, M., Van Aerschot, A., Xu, D., Juliano, R. L., Herdewijn, P. *Nucleic Acids Res*. **2007**, *35*, 1064-1074.
[67] Nauwelaerts, K., Fisher, M., Froeyen, M., Lescrinier, E., Van Aerschot, A., Xu, D., DeLong, R., Kang, H., Juliano, R. L., Herdewijn, P. *J. Am. Chem. Soc*. **2007**, *129*, 9340-9348.
[68] Ittig, D., Luisier, S., Weiler, J., Schümperli, D., Leumann, C. J. *Artificial DNA: PNA & XNA* **2010**, *1*, 9-16.
[69] Bramsen, J. B., Pakula, M. M., Hansen, T. B., Bus, C., Langkjær, N., Odadzic, D., Smicius, R., Wengel, S. L., Chattopadhyaya, J., Engels, J. W., Herdewijn, P., Wengel, J., Kjems, J. *Nucleic Acids Res*. **2010**, *38*, 5761-5773.

[70] Vaish, N., Chen, F., Seth, S., Fosnaugh, K., Liu, Y., Adami, R., Brown, T., Chen, Y., Harvie, P., Johns, R., Severson, G., Granger, B., Charmley, P., Houston, M., Templin, M. V., Polisky, B. *Nucleic Acids Res*. **2011**, *39*, 1823-1832.
[71] Pasternak, A., Wengel, J. *Org. Biomol. Chem*. **2011**, *9*, 3591-3597.
[72] Karikó, K., Buckstein, M., Ni, H., Weissman, D. *Immunity* **2005**, *23*, 165-175.
[73] Herdewijn, P. *Antisense Nucleic Acid Drug Dev*. **2000**, *10*, 297-310.
[74] Shen, L., Siwkowski, A., Wancewicz, E. V., Lesnik, E., Butler, M., Witchell, D., Vasquez, G., Ross, B., Acevedo, O., Inamati, G., Sasmor, H., Manoharan, M., Monia, B. P. *Antisense Nucleic Acid Drug Dev*. **2003**, *13*, 129-142.
[75] Sipa, K., Sochacka, E., Kazmierczak-Baranska, J., Maszewska, M., Janicka, M., Nowak, G., Nawrot, B. *RNA* **2007**, *13*, 1301-1316.
[76] Xia, J., Noronha, A., Toudjarska, I., Li, F., Akinc, A., Braich, R., Frank-Kamenetsky, M., Rajeev, K. G., Egli, M., Manoharan, M. *ACS Chem. Biol*. **2006**, *1*, 176-183.
[77] Debart, F., Abes, S., Deglane, G., Moulton, H. M., Clair, P., Gait, M. J., Vasseur, J., Lebleu, B. *Curr. Top. Med. Chem*. **2007**, *7*, 727-737.
[78] Burke, R. S., Pun, S. H. *Bioconjugate Chem*. **2008**, *19*, 693-704.
[79] Lönnberg, H. *Bioconjugate Chem*. **2009**, *20*, 1065-1094.
[80] Soutschek, J., Akinc, A., Bramlage, B., Charisse, K., Constien, R., Donoghue, M., Elbashir, S., Geick, A., Hadwiger, P., Harborth, J., John, M., Kesavan, V., Lavine, G., Pandey, R. K., Racie, T., Rajeev, K. G., Röhl, I., Toudjarska, I., Wang, G., Wuschko, S., Bumcrot, D., Koteliansky, V., Limmer, S., Manoharan, M., Vornlocher, H.-P. *Nature* **2004**, *432*, 173-178.
[81] Wolfrum, C., Shi, S., Jayaprakash, K. N., Jayaraman, M., Wang, G., Pandey, R. K., Rajeev, K. G., Nakayama, T., Charrise, K., Ndungo, E. M., Zimmermann, T., Koteliansky, V., Manoharan, M., Stoffel, M. *Nat. Biotechnol*. **2007**, *25*, 1149-1157.
[82] Lorenz, C., Hadwiger, P., John, M., Vornlocher, H.-P., Unverzagt, C. *Bioorg. Med. Chem. Lett*. **2004**, *14*, 4975-4977.
[83] Moschos, S. A., Jones, S. W., Perry, M. M., Williams, A. E., Erjefalt, J. S., Turner, J. J., Barnes, P. J., Sproat, B. S., Gait, M. J., Lindsay, M. A. *Bioconjugate Chem*. **2007**, *18*, 1450-1459.
[84] Nishina, K., Unno, T., Uno, Y., Kubodera, T., Kanouchi, T., Mizusawa, H., Yokota, T. *Mol. Ther*. **2008**, *16*, 734-740.
[85] Marlin, F., Simon, P., Saison-Behmoaras, T., Giovannangeli, C. *ChemBioChem* **2010**, *11*, 1493-1500.
[86] Ikeda, Y., Taira, K. *Pharm. Res*. **2006**, *23*, 1631-1640.
[87] Sato, Y., Murase, K., Kato, J., Kobune, M., Sato, T., Kawano, Y., Takimoto, R., Takada, K., Miyanishi, K., Matsunaga, T., Takayama, T., Niitsu, Y. *Nat. Biotechnol*. **2008**, *26*, 431-442.
[88] Thomas, M., Kularatne, S. A., Qi, L., Kleindl, P., Leamon, C. P., Hansen, M. J., Low, P. S. *Oligonucleotide Ther*. **2009**, *1175*, 32-39.
[89] Hassane, F. S., Saleh, A. F., Abes, R., Gait, M. J., Lebleu, B. *Cell. Mol. Life Sci*. **2010**, *67*, 715-726.
[90] Astriab-Fisher, A., Sergueev, D., Fisher, M., Shaw, B. R., Juliano, R. L. *Pharm. Res*. **2002**, *19*, 744-754.
[91] Turner, J. J., Arzumanov, A. A., Gait, M. J. *Nucleic Acids Res*. **2005**, *33*, 27-42.
[92] Wu, B., Moulton, H. M., Iversen, P. L., Jiang, J., Li, J., Li, J., Spurney, C. F., Sali, A., Guerron, A. D., Nagaraju, K., Doran, T., Lu, P., Xiao, X., Lu, Q. L. *Proc. Natl. Acad. Sci. USA* **2008**, *105*, 14814-14819.
[93] Amantana, A., Moulton, H. M., Cate, M. L., Reddy, M. T., Whitehead, T., Hassinger, J. N., Youngblood, D. S., Iversen, P. L. *Bioconjugate Chem*. **2007**, *18*, 1325-1331.

[94] Wu, R. P., Youngblood, D. S., Hassinger, J. N., Lovejoy, C. E., Nelson, M. H., Iversen, P. L., Moulton, H. M. *Nucleic Acids Res*. **2007**, *35*, 5182-5191.
[95] Ivanova, G. D., Arzumanov, A., Abes, R., Yin, H., Wood, M. J. A., Lebleu, B., Gait, M. J. *Nucleic Acids Res*. **2007**, *35*, 6418-6428.
[96] Chiu, Y.-L., Ali, A., Chu, C.-Y., Cao, H., Rana, T. M. *Chem. Biol*. **2004**, *11*, 1165-1175.
[97] Davidson, T. J., Harel, S., Arboleda, V. A., Prunell, G. F., Shelanski, M. L., Greene, L. A., Troy, C. M. *J. Neurosci*. **2004**, *24*, 10040-10046.
[98] Jeong, J. H., Kim, S. H., Kim, S. W., Park, T. G. *J. Biomater. Sci. Polymer Edn*. **2005**, *16*, 1409-1419.
[99] Kim, S. H., Jeong, J. H., Lee, S. H., Kim, S. W., Park, T. G. *Bioconjugate Chem*. **2008**, *19*, 2156-2162.
[100] Meyer, M., Dohmen, C., Philipp, A., Kiener, D., Maiwald, G., Scheu, C., Ogris, M., Wagner, E. *Mol. Pharm.* **2009**, *6*, 752-762.
[101] Zhou, P., Wang, M. M., Du, L., Fisher, G. W., Waggoner, A., Ly, D. H. *J. Am. Chem. Soc*. **2003**, *125*, 6878-6879.
[102] Dragulescu-Andrasi, A., Zhou, P., He, G. F., Ly, D. H. *Chem. Commun*. **2005**, *2*, 244-246.
[103] Ohmichi, T., Kuwahara, M., Sasaki, N., Hasegawa, M., Nishikata, T., Sawai, H., Sugimoto, N. *Angew. Chem. Int. Ed*. **2005**, *44*, 6682-6685.
[104] Deglane, G., Abes, S., Michel, T., Prévot, P., Vives, E, Debart, F., Barvik, I., Lebleu, B., Vasseur, J.-J. *ChemBioChem* **2006**, *7*, 684-692.
[105] Li, Y.-F., Morcos, P. A. *Bioconjugate Chem*. **2008**, *19*, 1464-1470.
[106] Nothisen, M., Kotera, M., Voirin, E., Remy, J.-S., Behr, J. P. *J. Am. Chem. Soc*. **2009**, *131*, 17730-17731.
[107] Winkler, J., Gilbert, M., Kocourková, A., Stessi, M., Noe, C. R. *ChemMedChem* **2008**, *3*, 102-110.
[108] Winkler, J., Saadat, K., Díaz-Gavilán, M., Urban, E., Noe, C. R. *Eur. J. Med. Chem*. **2009**, *44*, 670-677.
[109] Houghton , J. L., Green, K. D., Chen, W., Garneau-Tsodikova, S. *ChemBioChem* **2010**, *11*, 880-902.
[110] Riguet, E., Tripathi, S., Chaubey, B., Désiré, J., Pandey, V. N., Décout, J.-L. *J. Med. Chem*. **2004**, *47*, 4806-4809.
[111] Charles, I., Xi, H., Arya, D. P. *Bioconjugate Chem*. **2007**, *18*, 160-169.
[112] Ketomäki, K., Virta, P. *Bioconjugate Chem*. **2008**, *19*, 766-777.
[113] Napoli, S., Carbone, G. M., Catapano, C. V., Shaw, N., Arya, D. P. *Bioorg. Med. Chem. Lett*. **2005**, *15*, 3467-3469.
[114] Bucior, I., Burger, M. M. *Curr. Opin. Struct. Biol*. **2004**, *14*, 631-637.
[115] Gabius, H.-J., Siebert, H.-C., André, S., Jiménez-Barbero, J., Rüdiger, H. *ChemBioChem* **2004**, *5*, 740–764.
[116] Ernst, B., Magnani, J. L. *Nat. Rev. Drug Discovery* **2009**, *8*, 661– 677.
[117] Ambrosi, M., Cameron, N. R., Davis, B. G. *Org. Biomol. Chem*. **2005**, *3*, 1593-1608.
[118] Yan, H., Tram, K. *Glycoconj. J*. **2007**, *24*, 107-123.
[119] Lundquist, J. J., Toone, E. J. *Chem. Rev*. **2002**, *102*, 555-578.
[120] Biessen, E. A. L., Beuting, D. M., Roelen, H. C. P. F., van de Marel, G. A., van Boom, J. H., van Berkel, T. J. C. *J. Med. Chem*. **1995**, *38*, 1538-1546.
[121] Hangeland, J. J., Flesher, J. E., Deamond, S. F., Lee, Y. C., Ts´O, P. O. P., Frost, J. J. *Antisense Nucleic Acid Drug Dev*. **1997**, *7*, 141-149.
[122] Duff, R. J., Deamond, S. F., Roby, C., Zhou, Y., Ts´O, P. O. P. *Methods Enzymol*. **1999**, *313*, 297-321.

[123] Biessen, E. A. L., Vietsch, H., Rump, E. T., Fluiter, K., Kuiper, J., Bijsterbosch, M. K., van Berkel, T. J. C. *Biochem. J.* **1999**, *340*, 783-792.
[124] Zhu, L., Ye, Z., Cheng, K., Miller, D. D., Mahato, R. I. *Bioconjugate Chem*. **2008**, *19*, 290-298.
[125] Oishi, M., Nagasaki,Y., Itaka, K., Nishiyama, N., Kataoka, K. *J. Am. Chem. Soc.* **2005**, *127*, 1624-1625.
[126] Oishi, M., Nagasaki,Y., Nishiyama, N., Itaka, K., Takagi, M., Shimamoto, A., Furuichi, Y., Kataoka, K. *ChemMedChem* **2007**, *2*, 1290-1297.
[127] Zhu, L., Mahato, R. I. *Bioconjugate Chem*. **2010**, *21*, 2119-2127.
[128] Ohta, T., Miura, N., Fujitani, N., Nakajima, F., Niikura, K., Sadamoto, R., Guo, C.-T., Suzuki, Y., Monde, K., Nishimura, S.-I. *Angew. Chem. Int. Ed*. **2003**, *42*, 5186-5189.
[129] Matsuura, K., Hibino, M., Ikeda, T., Yamada, Y., Kobayashi, K. *Chem. Eur. J*. **2004**, *10*, 352-359.
[130] Moni, L., Pourceau, G., Zhang, J., Meyer, A., Vidal, S., Souteyrand, E., Dondoni, A., Morvan, F., Chevolot, Y., Vasseur, J.-J., Marra, A. *ChemBioChem* **2009**, *10*, 1369-1378.
[131] Ugarte-Uribe, B., Pérez-Rentero, S., Lucas, R., Aviñó, A., Reina, J. J., Alkorta, I., Eritja, R., Morales, J. C. *Bioconjugate Chem*. **2010**, *21*, 1280-1287.
[132] Virta, P., Katajisto, J., Niittymäki, T., Lönnberg, H. *Tetrahedron* **2003**, *59*, 5137-5174.
[133] Singh, Y., Spinelli, N., Defrancq, E. *Curr. Org. Chem*. **2008**, *12*, 263-290.
[134] Singh, Y., Murat, P., Defrancq, E. *Chem. Soc. Rev*. **2010**, *39*, 2054-2070.
[135] Kolb, H. C., Finn, M. G., Sharpless, K. B. *Angew. Chem. Int. Ed*. **2001**, *40*, 2004-2021.
[136] Eguchi, Y., Itoh, T., Tomizawa, J. *Annu. Rev. Biochem*. **1991**, *60*, 631-652.
[137] Chastain, M., Tinoco, I. *Prog. Nucleic Acid Res. Mol. Biol*. **1991**, *41*, 131-177.
[138] Ecker, D. J., Vickers, T. A., Bruice, T. W., Freier, S. M., Jenison, R. D., Manoharan, M., Zounes, M. *Science* **1992**, *257*, 958-961.
[139] Kretschmer-Kazemi Far, R., Sczakiel, G. *Nucleic Acids Res*. **2003**, *31*, 4417-4424.
[140] Wemmer, D. E., Williams, P. G. *Methods Enzymol*. **1994**, *239*, 739-767.
[141] Fürtig, B., Richter, C., Wöhnert, J., Schwalbe, H. *ChemBioChem* **2003**, *4*, 936-962.
[142] Mayer, M., James, T. L. *Methods Enzymol*. **2005**, *394*, 571-587.
[143] Kreutz, C., Kählig, H., Konrat, R., Micura, R. *J. Am. Chem. Soc*. **2005**, *127*, 11558-11559.
[144] Hennig, M., Munzarová, M. L., Bermel, W., Scott, L. G., Sklenář, V., Williamson, J. R. *J. Am. Chem. Soc*. **2006**, *128*, 5851-5858.
[145] Kreutz, C., Kählig, H., Konrat, R., Micura, R. *Angew. Chem. Int. Ed*. **2006**, *45*, 3450-3453.
[146] Hennig, M., Scott, L. G., Sperling, E., Bermel, W., Williamson, J. R. *J. Am. Chem. Soc*. **2007**, *129*, 14911-14921.
[147] Barhate, N. B., Barhate, R. N., Cekan, P., Drobny, G., Sigurdsson, S. *Org. Lett*. **2008**, *10*, 2745-2747.
[148] Graber, D., Moroder, H., Micura, R. *J. Am. Chem. Soc*. **2008**, *130*, 17230-17231.
[149] Leonard, J. N., Shah, P. S., Burnett, J. C., Schaffer, D. V. *Cell Host Microbe* **2008**, *4*, 484-494.
[150] Turner, J. J., Fabani, M., Arzumanov, A. A., Ivanova, G., Gait, M. J. *Biochim. Biophys. Acta* **2006**, *1758*, 290-300.
[151] Boulmé, F., Freund, F., Moreau, S., Nielsen, P. E., Gryaznov, S., Toulmé, J.-J., Litvak, S. *Nucleic Acids Res*. **1998**, *26*, 5492-5500.
[152] Arzumanov, A., Walsh, A. P., Liu, X., Rajwanshi, V. K., Wengel, J., Gait, M. J. *Nucleosides, Nucleotides & Nucleic Acids* **2001**, *20*, 471-480.

[153] Kaushik, N., Basu, A., Palumbo, P., Myers, R. L., Pandey, V. N. *J. Virol.* **2002**, *76*, 3881-3891.
[154] Tripathi, S., Chaubey, B., Ganguly, S., Harris, D., Casale, R. A., Pandey, V. N. *Nucleic Acids Res.* **2005**, *33*, 4345-4356.
[155] Turner, J. J., Ivanova, G. D., Verbeure, B., Williams, D., Arzumanov, A. A., Abes, S., Lebleu, B., Gait, M. J. *Nucleic Acids Res.* **2005**, *33*, 6837-6849.
[156] Jacque, J.-M., Triques, K., Stevenson, M. *Nature* **2002**, *418*, 435-438.
[157] Yoshinari, K., Miyagishi, M., Taira, K. *Nucleic Acids Res.* **2004**, *32*, 691-699.
[158] Grimm, D. Kay, M. A. *Mol. Ther.* **2007**, *15*, 878-888.
[159] Dutta, S., Bhaduri, N., Rastogi, N., Chandel, S. G., Vandavasi, J. K., Upadhayaya, R. S., Chattopadhyaya, J. *MedChemComm* **2011**, *2*, 206-216.
[160] El-Sagheer, A. H., Brown, T. *Chem. Soc. Rev.* **2010**, *39*, 1388-1405.
[161] Rostovtsev, V. V., Green, L. G., Fokin, V. V., Sharpless, K. B. *Angew. Chem. Int. Ed.* **2002**, *41*, 2596-2599.
[162] Tornoe, C. W., Christensen, C., Meldal, M. *J. Org. Chem.* **2002**, *67*, 3057-3064.
[163] Gramlich, P. M. E., Wirges, C. T., Manetto, A., Carell, T. *Angew. Chem. Int. Ed.* **2008**, *47*, 8350 – 8358.
[164] Chan, T. R., Hilgraf, R., Sharpless, K. B., Fokin, V. V. *Org. Lett.* **2004**, *6*, 2853-2855.
[165] Maag, H., Schmidt, B., Rose, S. J. *Tetrahedron Lett.* **1994**, *35*, 6449-6452.
[166] Fensholdt, J., Thrane, H., Wengel, J. *Tetrahedron Lett.* **1995**, *36*, 2535-2538.
[167] Thrane, H., Fensholdt, J., Regner, M., Wengel, J. *Tetrahedron* **1995**, *51*, 10389-10402.
[168] Wang, G., Seifert, W. E. *Tetrahedron Lett.* **1996**, *37*, 6515-6518.
[169] Ueno, Y., Nagasawa, Y., Sugimoto, I., Kojima, N., Kanazaki, M., Shuto, S., Matsuda, A. *J. Org. Chem.* **1998**, *63*, 1660-1667.
[170] Pfundheller, H. M., Bryld, T., Olsen, C. E., Wengel, J. *Helv. Chim. Acta* **2000**, *83*, 128-151.
[171] Raunkjær, M., Bryld, T., Wengel, J. *Chem. Commun.* **2003**, 1604-1605.
[172] Luyten, I., Esnouf, R. M., Mikhailov, S. N., Efimtseva, E. V., Michiels, P., Heus, H. A., Hilbers, C. W., Herdewijn, P. *Helv. Chim. Acta* **2000**, *83*, 1278-1289.
[173] Efimtseva, E. V., Bobkov, G. V., Mikhailov, S. N., Van Aerschot, A., Schepers, G., Busson, R., Rozenski, J., Herdewijn, P. *Helv. Chim. Acta* **2001**, *84*, 2387-2397.
[174] Fluiter, K., Mook, O. R. F., Vreijling, J., Langkjær, N., Højland, T., Wengel, J., Baas, F. *Mol. BioSyst.* **2009**, *5*, 838-843.
[175] Wada, T., Mochizuki, A., Higashiya, S., Tsuruoka, H., Kawahara, S., Ishikawa, M., Sekine, M. *Tetrahedron Lett.* **2001**, *42*, 9215-9219.
[176] Stawinski, J., Strömberg, R., In *Oligonucleotide synthesis: methods and applications, 288* (Methods in Molecular Biology, Ed. Herdewijn, P.), Humana Press, U.S.A **2005**, p. 81-100.
[177] Pourceau, G., Meyer, A., Vasseur, J.-J., Morvan, F. *J. Org. Chem.* **2009**, *74*, 1218-1222.
[178] Pourceau, G., Meyer, A., Chevolot, Y., Souteyrand, E., Vasseur, J.-J., Morvan, F. *Bioconjugate Chem.* **2010**, *21*, 1520-1529.
[179] Jones, G. H., Taniguchi, M., Tegg, D., Moffatt, J. G. *J. Org. Chem.* **1979**, *44*, 1309-1317.
[180] Jung, K.-H., Marx, A. *Curr. Org. Chem.* **2008**, *12*, 343-354.
[181] O-Yang, C., Kurz, W., Eugui, E. M., McRoberts, M. J., Verheyden, J. P. H., Kurz, L. J., Walker, K. A. M. *Tetrahedron Lett.* **1992**, *33*, 41-44.
[182] Wu, T., Nauwelaerts, K., Van Aerschot, A., Froeyen, M., Lescrinier, E., Herdewijn, P. *J. Org. Chem.* **2006**, *71*, 5423-5431.
[183] Bobkov, G. V., Mikhailov, S. N., Van Aerschot, A., Herdewijn, P. *Tetrahedron* **2008**,

64, 6238-6251.
[184] Markiewicz, W. T., Wiewiorowski, M., *In Nucleic Acid Chemistry. Improved and New Synthetic Procedures and Techniques*. Part 3, (Ed. Townsend, L. B. and Tipson, R. S.), John Wiley&Sons, **1986**, p. 229-231.
[185] Bobkov, G. V., Brilliantov, K. V., Mikhailov, S. N., Rozenski, J., Van Aerschot, A., Herdewijn, P. *Coll. Czech. Chem. Commun*. **2006**, *71*, 804-819.
[186] Efimtseva, E. V., Kulikova, I. V., Mikhailov S. N. *Molecular Biology (Russia)* **2009**, *43*, 301-312.
[187] Mereyala, H. B., Gurrala, S. R. *Carbohydr. Res.* **1998**, *307*, 351-354.
[188] Schmidt, M., Chatterjee, S. K., Dobner, B., Nuhn, P. *Chem. Phys. Lip.* **2002**, *114*, 139-147.
[189] Park, W. K. C., Auer, M., Jaksche, H., Wong, C.-H. *J. Am. Chem. Soc.* **1996**, *118*, 10150–10155.
[190] Cottaz, S., Brimacombe, J. S., Ferguson, M. A. J. *Carbohydrate Res.* **1993**, *247*, 341-345.
[191] Alper, P. B., Hung, S.-C., Wong, C.-H. *Tetrahedron Lett.* **1996**, *37*, 6029-6032.
[192] Simonsen, K. B., Ayida, B. K., Vourloumis, D., Takahashi, M., Winters, G. C., Barluenga, S., Qamar, S., Shandrick, S., Zhao, Q., Hermann, T. *ChemBioChem* **2002**, *3*, 1223-1228.
[193] Garegg, P. J., Lindh, I., Regberg, T., Stawinski, J., Strömberg, R. *Tetrahedron Lett.* **1986**, *27*, 4051-4054.
[194] Garegg, P. J., Lindh, I., Regberg, T., Stawinski, J., Strömberg, R. *Tetrahedron Lett.* **1986**, *27*, 4055-4058.
[195] Gierlich, J., Burley, G. A., Gramlich, P. M. E., Hammond, D. M., Carell, T. *Org. Lett.* **2006**, *8*, 3639-3642.
[196] Seela, F., Sirivolu, V. R. *Helv. Chim. Acta* **2007**, *90*, 535-552.
[197] Brown, T., Pritchard, C. E., Turner, G., Salisbury, S. A. *J. Chem. Soc., Chem. Commun.***1989**, 891-893.
[198] Pon, R. T., Yu, S. *Nucleic acids Res.* **1997**, *25*, 3629-3635.
[199] Papa, A. J. *J. Org. Chem.* **1966**, *31*, 1426-1430.
[200] Mergny, J.-L., Lacroix, L. *Oligonucleotides* **2003**, *13*, 515-537.
[201] Karskela, M., Helkearo, M., Virta, P., Lönnberg, H. *Bioconjugate Chem.* **2010**, *21*, 748-755.
[202] Bouillon, C., Meyer, A., Vidal, S., Jochum, A., Chevolot, Y., Cloarec, J.-P., Praly, J.-P., Vasseur, J.-J., Morvan, F. *J. Org. Chem.* **2006**, *71*, 4700-4702.
[203] Singh, Y., Renaudet, O., Defrancq, E., Dumy, P. *Org. Lett.* **2005**, *7*, 1359-1362.
[204] Dubber, M., Fréchet, J. M. J. *Bioconjugate Chem.* **2003**, *14*, 239-246.
[205] Marx, A., Erdmann, P., Senn, M., Körner, S., Jungo, T., Petretta, M., Imwinkelried, P., Dussy, A., Kulicke, K. J., Macko, L., Zehnder, M., Giese, B. *Helv. Chim. Acta* **1996**, *79*, 1980-1994.
[206] Rastinejad, F., Evilia, C., Lu, P. *Methods Enzymol.* **1995**, *261*, 560-575.
[207] Puffer, B., Kreutz, C., Rieder, U., Ebert, M.-O., Konrat, R., Micura, R. *Nucleic acids Res.* **2009**, *37*, 7728-7740.
[208] Mei, H.-Y., Galan, A. A., Halim, N. S., Mack, D. P., Moreland, D. W., Sanders, K. B., Truong, H. N., Czarnik, A. W. *Bioorg. Med. Chem. Lett.* **1995**, *5*, 2755-2760.
[209] Moumné, R., Pasco, M., Prost, E., Lecourt, T., Micouin, L., Tisné, C. *J. Am. Chem. Soc.* **2010**, *132*, 13111-13113.
[210] Wang, S., Huber, P. W., Cui, M., Czarnik, A. W., Mei, H.-Y. *Biochemistry* **1998**, *37*, 5549-5557.
[211] Hwang, T.-L.; Shaka, A. J. *J. Magn. Reson. Ser. A* **1995**, *112*, 275-279.